



THE HONG KONG
POLYTECHNIC UNIVERSITY

香港理工大學

Pao Yue-kong Library

包玉剛圖書館

Copyright Undertaking

This thesis is protected by copyright, with all rights reserved.

By reading and using the thesis, the reader understands and agrees to the following terms:

1. The reader will abide by the rules and legal ordinances governing copyright regarding the use of the thesis.
2. The reader will use the thesis for the purpose of research or private study only and not for distribution or further reproduction or any other purpose.
3. The reader agrees to indemnify and hold the University harmless from and against any loss, damage, cost, liability or expenses arising from copyright infringement or unauthorized usage.

IMPORTANT

If you have reasons to believe that any materials in this thesis are deemed not suitable to be distributed in this form, or a copyright owner having difficulty with the material being included in our database, please contact lbsys@polyu.edu.hk providing details. The Library will look into your claim and consider taking remedial action upon receipt of the written requests.

REMOVAL OF DYESTUFFS AND HEAVY METAL
FROM EFFLUENT VIA ENCAPSULATION
TECHNOLOGY

LUK CHI HIM JIM

Ph.D

The Hong Kong Polytechnic University

2017

The Hong Kong Polytechnic University
Institute of Textiles and Clothing

Removal of Dyestuffs and Heavy Metal from Effluent
Via Encapsulation Technology

Luk Chi Him Jim

A thesis submitted in partial fulfilment of the
requirements for the degree of Doctor of Philosophy

September 2016

CERTIFICATE OF ORIGINALITY

I hereby declare that this thesis is my own work and that, to the best of my knowledge and belief, it reproduces no material previously published or written, nor material that has been accepted for the award of any other degree or diploma, except where due acknowledgement had been made in the text.

_____(Signed)

LUK CHI HIM JIM _____(Name of student)

Abstract

Pollution problems instigated by human activities and economic development have been threatening the environment for decades. Water pollution, one of the most serious problems, is attributed to contamination from biochemical substances and chemicals. Synthetic dyes and heavy metal ions are common pollutants from the effluents of dyeing industries, electrochemical plants, tannery industries, etc. Both synthetic dyes and heavy metal ions, even in a part-per-million scale, give rise to serious environmental damage. Although conventional methods such as precipitation, ion exchange, filtration, etc. are being used to treat polluted water, these methods have their own shortcomings or implementation is costly for satisfactory results. As an alternative, adsorption has been introduced into water treatment and this method is still being extensively explored by researchers. Adsorption is well known for its excellent removal ability of a number of pollutants, and not limited to the major targets in this study. Biosorption is a kind of adsorption making use of biological adsorbents to physically or chemically remove the target adsorbates. Biosorbents have been explored in-depth in terms of utilizing their removal ability with physical and chemical treatments. Besides biosorption, biological functions from live cultures have also been one of the promising way to treat synthetic dyes and heavy metals. In this study, encapsulation was used to prepare chitosan-based and alginate-based biosorbents. The encapsulation of microorganisms and subsequent evaluation of the scavenger of the pollutants is the main objective of the present study. Although biosorption that incorporates cultures are effective, the practical separation issues in treatment plants are a concern. The rationale of the

encapsulation is to minimize the separation problems as well as keep the original biological and chemical characteristics of the combined biosorbents, which includes possible biodegradation of synthetic dyes and biological reactions with heavy metal ions. After the encapsulation of microorganisms and evaluation of the biosorption performance, a further mechanistic study was also performed to understand the biosorption.

The research methods of this study are as follows: (1) synthesis of biosorbents and preparation of microorganisms, (2) characterisation by using various instrumentations, (3) removal of synthetic dyes and heavy metal ions, as well as (4) kinetics and isotherm model fitting. A number of bacteria and yeast were screened to observe for possible biodegradation of synthetic dyes. Afterward, suitable encapsulating materials were chosen for the synthesis of biosorbents. The biosorbents were characterized by using Fourier transform infrared (FTIR) spectroscopy, zeta potential measurement and scanning electron microscopy (SEM). The viability of the encapsulated culture was also examined to determine whether live culture encapsulation is successfully carried out. Biosorption and mechanistic studies were subsequently conducted to evaluate the biosorption performance of the synthesized biosorbents.

Lactobacillus casei (*L. casei*) was encapsulated into chitosan hydrogel beads synthesized through a coacervation process with alkali neutralization and ionotropic crosslinking. Further chemical crosslinking of the chitosan beads was also conducted to strengthen their chemical stability. Direct Red 80, Reactive Yellow 25 and Acid Blue 25 are used to evaluate the biosorption performance. The effects of pH, temperature, crosslinking and encapsulating *L. casei* were

examined to evaluate the biosorption of the combined biosorbents. No biodegradation was observed as the encapsulated *L. casei* were not live culture. Nevertheless, *L. casei* had positive effects on the biosorption of Direct Red 80 with satisfactory enhancement. Further kinetic and isotherm modelling revealed that the biosorption of all three dyes followed a pseudo-second-order kinetic and also the Freundlich isotherm. Another synthetic dye, Reactive Blue 19, was also biosorbed by *L. casei*-encapsulated chitosan beads in which its viability was maintained. Freeze-drying can improve the physical and chemical stabilities of the beads. It is found that plain beads could remove Reactive blue 19 with a high removal efficiency in both acidic and alkaline environments. A kinetic study revealed that encapsulating *L. casei* in a chitosan matrix could bring about minor enhancement to biosorption. A yeast strain, *Candida krusei* (*C. krusei*), was encapsulated into alginate-based hydrogel beads and the viability of the culture was also maintained. The biosorption of heavy metal ions was carried out by using free and encapsulated *C. krusei* with calcium alginate. However, the biosorption of chromium(VI) and nickel(II) is not as expected while copper(II) and lead(II) were well biosorbed. Furthermore, biosorption of copper(II) was conducted and the pH and temperature effects were also evaluated. A kinetic study revealed that all three biosorbents follow pseudo-second-order kinetics. The isotherm modelling shows good fit to Temkin isotherm with *C. krusei*. Calcium alginate and encapsulated *C. krusei*-calcium alginate both followed Langmuir isotherm.

LIST OF PUBLICATIONS

Journal papers

1. **Luk C. H. J.**, Yip J., Yuen C. W. M., Lam K. H., Kan C. W. (2015) “Study of Freeze-dried Chitosan Beads Encapsulating Live Lactic Acid Bacteria for Removal of Reactive Dyes”, *Journal of Fiber Bioengineering and Informatics*, 8(1):13-23.
2. **Luk C. H. J.**, Yip J., Yuen C. W. M., Kan C. W., Lam K. H. (2014) “A Comprehensive Study on Adsorption Behaviour of Direct, Reactive and Acid Dyes on Crosslinked and Non-crosslinked Chitosan Beads”, *Journal of Fiber Bioengineering and Informatics*, 7(1):35-52.
3. **Luk, C. H. J.**, Yip, J., Yuen, C. W. M., Lam, K. H., Kan, C. W., Pang, S. K. “Biosorption performance of encapsulated *Candida krusei* for the removal of copper(II)”, *Scientific Reports* (Accepted).

Conference paper

1. **Luk C.H.J.**, Yip J., Yuen C.W.M, Lam K.H. (2014). Removal of reactive blue 19 by Encapsulating *Lactobacillus Casei* into Freeze-dried chitosan beads. The 7th Textile Bioengineering and Informatics Symposium, Hong Kong, China, 6-8 August, 2014, p.101-107.

ACKNOWLEDGEMENT

I would like to express my sincere appreciation to Dr. Joanne YIP, for her constant guidance, invaluable advice and sustained interest throughout my preparation of the project work. I would once again express my deepest gratitude for her guidance, patience and enthusiasm throughout my study.

In addition, I would also like to thank two of my co-supervisors, Prof. Chun-Wah Marcus YUEN at ITC, The Hong Kong Polytechnic University and Dr. Kim-Hung LAM at Department of Applied Biology and Chemical Technology, The Hong Kong Polytechnic University, for their valuable guidance and unconditional support for my study.

I must send special gratitude to Mr. Siu-Kwong PANG at ITC for the professional advice and stimulating discussion on the current research aspect. I would also like to express my thanks to my research colleagues for their support during my research period.

Table of content

	Page
ABSTRACT.....	i
LIST OF PUBLICATION.....	iv
ACKNOWLEDGEMENT.....	v
TABLE OF CONTENT.....	vi
LIST OF FIGURES.....	xi
LIST OF TABLES.....	xv
LIST OF ABBREVIATIONS.....	xvii
CHAPTER 1 INTRODUCTION.....	1
1.1 Research Background.....	1
1.2 Research Gap.....	3
1.3 Aim and Research Objectives.....	4
1.4 Project Originality and Significance	5
1.5 Outline of Thesis.....	6
CHAPTER 2 LITERATURE REVIEW.....	7
2.1 Introduction.....	7
2.2 Impact of Synthetic Dyes and Heavy Metals on Environment	7
2.2.1 Synthetic Dyes.....	8
2.2.2 Heavy Metals	11
2.3 Removal of Dyestuffs and Heavy Metal s from Water.....	13
2.3.1 Conventional methods.....	13
2.3.1.1 Chemical Processing.....	14
2.3.1.2 Physical Processing.....	16
2.3.1.3 Biological Treatment.....	18

2.3.2	Non-Conventional Methods	21
2.3.2.1	Adsorption	21
2.3.2.2	Biosorption	22
2.3.2.3	Factors that Affect Adsorption and Biosorption Efficiency	41
2.4	Encapsulation Technique for Removal of Dyestuffs and Heavy Metals from Water	43
2.4.1	Encapsulation Materials	43
2.4.2	Encapsulation Methods	45
2.5	Removal of Synthetic Dyes and Heavy Metals	47
2.5.1	Adsorption Kinetics	48
2.5.2	Adsorption Isotherm Modelling	50
2.5.3	Metabolic-Dependent Removal of Synthetic Dyes and Heavy Metals	53
2.5.3.1	Bioremediation of Synthetic Dyes	53
2.5.3.2	Biotransformation of Heavy Metals	56
2.6	Chapter Summary	57
CHAPTER 3 RESEARCH METHODOLOGY		61
3.1	Introduction	61
3.2	Experimental Design	61
3.3	Materials and Reagents	63
3.4	Instrumentation and Characterisation	66
3.4.1	Biosorption Experiment	66
3.5	Culturing and Inoculation of Microorganisms	67
3.6	Screening of Non-Encapsulated Microorganisms on Biodegradation of Synthetic Dyes	68

3.6.1	Trials of Aerobic and Anaerobic Biodegradation with agar	68
3.6.2	Trials of Aerobic and Anaerobic Biodegradation with solution	69
3.7	Synthesis of Biosorbents	70
3.7.1	Chitosan Hydrogel Beads	70
3.7.1.1	Chitosan Beads Synthesized by Coacervation	70
3.7.1.2	Chemically Crosslinked Chitosan Beads	71
3.7.1.3	Ionotropically Crosslinked Chitosan Beads	71
3.7.2	Alginate Hydrogel Beads	72
3.7.3	Encapsulation of Microorganisms	72
3.8	Characterisation of Biosorbents	73
3.8.1	Fourier Transform Infrared Spectroscopy	73
3.8.2	Zeta Potential Measurement	73
3.8.3	Viability of Microorganisms	74
3.8.4	Surface Morphology	74
3.9	Batch Biosorption Experiments	74
3.9.1	Removal of Synthetic Dyes/ Heavy Metal Ions	74
3.9.2	pH Effects	76
3.9.3	Temperature Effects	76
3.9.4	Biosorption Kinetics	76
3.9.5	Biosorption Isotherms	77
3.10	Chapter Summary	78
CHAPTER 4 SYNTHESIS OF BIOSORBENTS		79
4.1	Introduction	79
4.2	Synthesis of Chitosan-Based Hydrogel Beads	79

4.2.1	Chitosan Hydrogel Beads – Coacervation through Neutralization.....	81
4.2.2	Crosslinked Chitosan Hydrogel Beads.....	84
4.2.3	Iontropic Crosslinked Chitosan Hydrogel Beads.....	85
4.3	Synthesis of Alginate-Based Hydrogel Beads.....	87
4.4	Selection and Encapsulation of Microorganisms.....	90
4.4.1	Screening of Microorganisms for Removal of Synthetic Dyes And Heavy Metal Ions.....	90
4.4.2	Encapsulation of Microorganisms	94
4.5	Characterisation of Biosorbents.....	96
4.5.1	Fourier Transform Infrared Spectroscopy Analysis.....	96
4.5.2	Zeta Potential Measurement.....	102
4.5.3	Scanning Electron Microscopy Analysis.....	104
4.6	Chapter Summary.....	107
CHAPTER 5 BIOSORPTION OF SYNTHETIC DYES		109
5.1	Introduction.....	109
5.2	Biosorption of Synthetic Dyes by Chitosan-Based Biosorbents...	109
5.2.1	Removal of DR80, RY25 and AB25 by Chitosan Hydrogel Beads.....	109
5.2.1.1	Effect of pH.....	110
5.2.1.2	Effect of Temperature.....	112
5.2.1.3	Effect of Crosslinking.....	115
5.2.1.4	Effect from Encapsulated <i>L. casei</i>	117
5.2.1.5	Kinetics Study and Isotherm Modelling.....	120
5.2.2	Removal of RB19 by Freeze-Dried Chitosan Hydrogel Beads.....	124

5.2.2.1	Effect of pH.....	125
5.2.2.2	Kinetics Study.....	127
5.3	Chapter Summary.....	131
CHAPTER 6	BIOSORPTION OF HEAVY METAL IONS.....	133
6.1	Introduction.....	133
6.2	Biosorption of Heavy Metal Ions by Alginate-Based Biosorbents	133
6.2.1	Preliminary Studies on Heavy Metal Ions Removal.....	133
6.3	Biosorption of copper (II): alginate-type hydrogel beads.....	138
6.3.1	Effect of pH.....	140
6.3.2	Effect of Temperature.....	141
6.3.3	Kinetics Study and Isotherm Modelling.....	143
6.4	Chapter Summary.....	154
CHAPTER 7	CONCLUSION AND RECOMMENDATIONS.....	155
7.1	Conclusion.....	155
7.2	Recommendations.....	159
REFERENCE	161

LIST OF FIGURES

	Page
Figure 2.1 Molecular structures of synthetic dyes.....	10
Figure 2.2 Dipropyl dithiophosphate, a lead-, cadmium-, copper- and mercury-chelating agent synthesised and studied by Ying and Fang.....	15
Figure 3.1 Experimental designs for the study of removal of synthetic dyes and heavy metal ions.....	62
Figure 3.2 Chemical structures of synthetic dyes used in this study.....	65
Figure 3.3 Biosorption experiments conducted in OLS 200 orbital shaking water bath (Grant Instruments).....	66
Figure 3.4 Agar plates mixed with synthetic dyes.....	69
Figure 3.5 Schematic diagram of the streaking of culture material on agar plates for aerobic/ anaerobic biodegradations of synthetic dyes.....	70
Figure 4.1 Chemical structure of chitosan	80
Figure 4.2 Flow diagram of synthesis of chitosan hydrogel beads (CB).....	83
Figure 4.3 Reaction scheme of the formation of an imide bond - the crosslink between chitosan and glutaraldehyde.....	85
Figure 4.4 Flow diagram of synthesis of ionotropic crosslinked chitosan hydrogel beads (TPPCB).....	86
Figure 4.5 Chemical structure of alginate.....	88
Figure 4.6 Flow diagram of the synthesis of calcium alginate hydrogel Beads.....	89
Figure 4.7 10^6 CFU cm^{-1} loop inoculation of <i>L. casei</i> on MRS agar plates. Left: <i>L. casei</i> -chitosan solution mixture; middle: <i>L. casei</i> -encapsulated CB (MCB); right: <i>L. casei</i> -encapsulated TPPCB (MTPPCB).....	95

Figure 4.8	FTIR spectra of (a) CB and (b) GCB	96
Figure 4.9	FTIR spectra of (a) MTPPCB and (b) TPPCB and (c) <i>L. casei</i>	97
Figure 4.10	FTIR spectra of (a) <i>C. krusei</i> , (b) CaAlg and (c) MCaAlg. (d-f) spectra of the region of 1200-1700 cm ⁻¹ for <i>C. krusei</i> , CaAlg and MCaAlg respectively.....	98
Figure 4.11	Zeta potential plot of CB and GCB as a function of pH	102
Figure 4.12	Zeta potential of TPPCB, MTPPCB and <i>L. casei</i> as a function of pH.....	103
Figure 4.13	SEM images of: (a) and (b) TPPCB; (c) to (h) MTPPCB.....	107
Figure 5.1	Effect of pH on removal of DR80, AB25 and RY25	111
Figure 5.2(a)	Effect of temperature on removal of DR80.....	113
Figure 5.2(b)	Effect of temperature on removal of AB25.....	114
Figure 5.2(c)	Effect of temperature on removal of RY25.....	114
Figure 5.3(a)	Effect of crosslink on the biosorption of DR80.....	116
Figure 5.3(b)	Effect of crosslink on the biosorption of AB25.....	116
Figure 5.3(c)	Effect of crosslink on the biosorption of RY25.....	117
Figure 5.4(a)	Effect of encapsulating <i>L. casei</i> on the biosorption of DR80 (GCB).....	118
Figure 5.4(b)	Effect of encapsulating <i>L. casei</i> on the biosorption of AB25 (GCB).....	119
Figure 5.4(c)	Effect of encapsulating <i>L. casei</i> on the biosorption of RY25 (GCB).....	119
Figure 5.4(d)	Effect of encapsulating <i>L. casei</i> on the biosorption of DR80 (CB).....	120

Figure 5.5	Freeze-dried TPPCB (left) and MTPPCB (right)	125
Figure 5.6	Effect of pH on removal of RB19 by TPPCB	127
Figure 5.7(a)	Removal of RB19 by MTB and TPPCB	128
Figure 5.7(b)	Pseudo-first order modelling of the removal of RB19	128
Figure 5.7(c)	Pseudo-second order modelling of the removal of RB19	129
Figure 5.7(d)	Intraparticle diffusion modelling of the removal of RB19	129
Figure 6.1	Biosorption of copper (II) by plain <i>C. krusei</i> as a function of culture concentration	139
Figure 6.2	Effect of pH on <i>C. krusei</i> , CaAlg and MCaAlg on the biosorption of copper(II)	141
Figure 6.3	Effect of temperature on <i>C. krusei</i> , CaAlg and MCaAlg on the biosorption of copper(II)	142
Figure 6.4(a)	Removal kinetics of copper(II) by <i>C. krusei</i> , CaAlg and MCaAlg	144
Figure 6.4(b)	Intraparticle diffusion fitting of <i>C. krusei</i> , CaAlg and MCaAlg	145
Figure 6.4(c)	Pseudo-first order fitting of <i>C. krusei</i> , CaAlg and MCaAlg	145
Figure 6.4(d)	Pseudo-second order fitting of <i>C. krusei</i> , CaAlg and MCaAlg	146
Figure 6.5(a)	Equilibrium removal efficiency of <i>C. krusei</i> , CaAlg and MCaAlg	149
Figure 6.5(b)	Langmuir isotherm fitting of <i>C. krusei</i> , CaAlg and MCaAlg	150
Figure 6.5(c)	Freundlich isotherm fitting of <i>C. krusei</i> , CaAlg and MCaAlg	150

Figure 6.5(d) Temkin isotherm fitting of *C. krusei*, CaAlg and MCaAlg

.....151

LIST OF TABLES

	Page
Table 2.1 Different classes of synthetic dyes.....	9
Table 2.2 Acute and chronic health effects resultant of exposure to heavy metals.....	12
Table 2.3. Summary of non-living biomass as biosorbent on synthetic dyes.....	23
Table 2.4. Summary of algal or fungal biomass used as biosorbent on synthetic Dyes.....	24
Table 2.5. Summary of bacterial biomass used as biosorbent on synthetic dyes.....	26
Table 2.6. Summary of yeast biomass used as biosorbent on synthetic dyes.....	28
Table 2.7 Summary of non-living biomass used as biosorbent on heavy metals.....	29
Table 2.8 Summary of algal biomass used as biosorbent on heavy metals.....	31
Table 2.9 Summary of fungal biomass used as biosorbent on heavy metals.....	32
Table 2.10 Summary of bacterial biomass used as biosorbent on heavy metals.....	33
Table 2.11 Summary of yeast biomass used as biosorbent on heavy metals.....	35
Table 2.12 Kinetics models adopted in biosorption evaluation.....	49
Table 2.13 Isotherm models adopted in biosorption evaluation.....	51

Table 4.1	Summary of optimized synthesis conditions of different kinds of chitosan beads in this study.....	87
Table 4.2	Summary of aerobic degradation results on agar streaking and dye solutions on <i>B. cereus</i> , <i>E. aerogenes</i> , <i>L. casei</i> and <i>P. putida</i>	91
Table 4.3	Summary of anaerobic degradation results on agar streaking and dye solutions on <i>B. cereus</i> , <i>E. aerogenes</i> , <i>L. casei</i> and <i>P. putida</i>	92
Table 5.1	Kinetics parameters for the biosorption of DR80, RY25 and AB25 with chitosan beads.....	121
Table 5.2	Biosorption isotherm parameters of DR80, RY25 and AB25 by using crosslinked chitosan beads.....	124
Table 5.3	Kinetics parameters of the biosorption of RB19 by MTPPCB and TPPCB.....	130
Table 6.1	Biosorption of chromium(VI) by alginate-based hydrogel beads.....	135
Table 6.2	Biosorption of copper(II), nickel(II) and lead(II) by alginate-based hydrogel beads.....	137
Table 6.3	Summary of linear mathematical expressions of three kinetics models. k_1 , k_2 , and k_i are the rate constants of the corresponding kinetic models, respectively; q_e is the amount of adsorbed copper (II) at equilibrium and q_t is the amount of copper (II) adsorbed at time t (mmol g^{-1}).....	144
Table 6.4	Summary of kinetics parameters of biosorption of copper(II) by using <i>C. krusei</i> , CaAlg and MCaAlg.....	147
Table 6.5	Isotherm modelling constants of <i>C. krusei</i> , CaAlg and MCaAlg for removal of copper(II).....	152

LIST OF ABBREVIATIONS

FTIR	Fourier Transform Infrared
SEM	Scanning Electron Microscope
UV-VIS	Ultraviolet-visible
GFAAS	Graphite Furnace Atomic Absorption Spectrometer
CB	Chitosan Beads
GCB	Glutaraldehyde-crosslink-Chitosan beads
MCB	Microorganism-Encapsulated-Chitosan beads
TPPCB	Tripolyphosphate-crosslinked-Chitosan beads
MTPPCB	Microorganisms-encapsulated-Tripolyphosphate-crosslinked-Chitosan beads
CaAlg	Calcium Alginate beads
MCaAlg	Microorganisms-encapsulated- Calcium Alginate beads
<i>B. cereus</i>	<i>Bacillus cereus</i>
<i>C. krusei</i>	<i>Candida krusei</i>
<i>E. aerogenes</i>	<i>Enterobacter aerogenes</i>
<i>L. casei</i>	<i>Lactobacillus casei</i>
<i>P. putida</i>	<i>Pseudomonas putida</i>

CHAPTER 1 INTRODUCTION

1.1 Research background

For many decades, human activities and economic development have increased rapidly and inevitably brought about pollution problems. Water pollution is one of the related issues that seriously affects various parties. Among the pollutants in water, synthetic dyes and heavy metals both have significant impacts on aquatic systems and the water quality (Li, X. et al., 2012). The high color intensities of dye concentration have already changed light penetration in water and hence negatively affected the photosynthesis of water plants (Robinson, T. et al., 2002b). Some of the synthetic dyes are carcinogenic and also impose other health problems to living organisms. If bacteria present in the water environment metabolize synthetic dyes into smaller molecules, they consume extra oxygen which might eventually lead to algal bloom, a serious water pollution problem potentially initiated by dye because they are toxic and kill other plants and animals. On the other hand, heavy metal ions dissolved in water can accumulate in water plants and animals which cannot be easily metabolized and excreted. Therefore, along the food chain, heavy metal concentration accumulates and finally reaches the highest consumers on the food chain (human beings). Even at low concentrations, some heavy metal species have hazardous effects and may even be carcinogenic (Singh, K. & Arora, S., 2011). Therefore, proper waste water treatment methods are vital in industries where residual levels of pollutants are highest in concentration.

There are conventional methods used to remove pollutants, such as through precipitation, ion exchange, electro-coagulation, reverse osmosis, filtration, etc. (Ejder-Korucu, M. et al., 2015). However, some of these methods are either ineffective or expensive, e.g. precipitation is ineffective toward low target concentration values. Reverse osmosis and ion exchange are rather expensive procedures in which ion exchange requires specific control of the operating environments. In order to further explore removal processes, the use of many kinds of different biomasses have been examined, which is an inexpensive and more environmentally friendly alternative (Gupta, V. K. & Suhas, 2009; Wang, H. et al., 2009). Living and non-living biomasses, as well as single and mixed strains have been explored in dye biodegradation, physical adsorption as well as heavy metal ion removal.

A good number of research work on chemisorption and physisorption by using biomasses has been carried out. The processes are based on chemical or physical interactions between non-living biomass and corresponding dyes (Ejder-Korucu, M. et al., 2015). To remove heavy metal ions, non-living biomasses act as ligands that chelate to the ions, thus giving effective removal (Fu, Fenglian & Wang, Qi, 2011). On the other hand, the use of living biomasses, either single or mixed strains, have been also extensively explored (El-Sheekh, M. M. et al., 2009; Hai, F. I. et al., 2006; Ola, I. O. et al., 2010b; Silva-Stenico, M. E. et al., 2012). Dyes are biodegraded by enzymes secreted from living biomasses while metal ions are assimilated by them (Robinson, T. et al., 2002a). The advantages of biomass removal over conventional methods include the low cost of implementation, biodegradable properties as well as the potential of different combinations of biomasses to optimize waste water treatment.

1.2 Research gap

This study aims to encapsulate microorganisms with polymeric wall materials to remove synthetic dyes and heavy metal ions. Although the use of microorganisms has already been studied by a number of researchers for their use in pollutant removal or biodegradation, there are still several issues in the use of biosorption to remove target pollutants as follows.

1. Separation is inevitably an issue associated with the use of microorganisms. Although the use of microbes is exceptional for removing and biodegrading target pollutants, separating the microbes from the treated water results in clogging of pipes and filter beds. The recovery of the separated components is a dilemma when applying biosorbents.
2. Both living and dead microorganisms have their own advantages in pollutant removal, but there is no approach that can incorporate both of their merits. Living microbes can be used to biologically treat pollutants but the conditioning procedures of the bulk environment in a reaction tank might be too limited to use on certain microorganisms, and the substrate concentrations also affect the biological processes. On the other hand, dead microorganisms eliminate all nutrient conditioning problems and work only with biosorption, but biological treatment cannot be carried out with dead cells.
3. Encapsulating microbes into polymeric supports has been extensively studied in the biochemistry field as well as the medical and pharmaceutical fields. The technique has potential to solve the above mentioned problems, but when

applied to the removal of water pollutants, removal efficiencies are similar to plain polymeric material or even result in reduced removal efficiency after encapsulation. Further studies on the encapsulation in the removal of synthetic dyes and heavy metal ions are important in order to develop a biosorbent combining merits from the two candidates in water pollution treatment.

1.3 Aim and Research Objectives

This research aims to study the synthesis of environmentally safe polymeric capsules with microorganisms through encapsulation for the removal of synthetic dyes and toxic heavy metals. The conditions of the removal process, such as type of microorganism encapsulated, variation in pH, initial dye concentration and temperature, will be evaluated. The removal mechanism will be studied by using mathematical models such as equilibrium sorption isotherms and kinetic models. This study will explore the feasibility of using combined biosorbents that contain microorganisms being encapsulated to remove dyes and toxic heavy metals from wastewater.

The primary objectives of this thesis are:

1. to develop biosorbents with encapsulated microorganisms and investigate the performance of these microcapsules in their ability to remove synthetic dyes and toxic heavy metals,
2. to establish systematic characterisations methods for biosorbents,
3. to evaluate the effectiveness and sorption capacities of biosorbents toward synthetic dyes and heavy metal ions, and
4. to study the mechanism of bioaccumulation and biosorption by using isotherm models and kinetics models upon the removal of dyes and heavy metal ions.

1.4 Project originality and significance

The textile industry is one of the most influential industries and affects human beings yet produces tremendous amounts of pollutants. Although a number of conventional measures to address this issue have been examined, some are expensive, have limited conditioning procedures, and insufficient for large volume and wide variety of dyes and toxic metal ions. The use of economical and environmentally friendly polymeric capsules as well as the incorporation of microorganisms will be a breakthrough among pollutant removal research studies. While there have been numerous reports on the implementation of polymeric capsules in the pharmaceutical and medical areas, the use of polymeric capsules embedded with microorganisms in pollutant removal is still novel. The development of a encapsulation system, which is inexpensive, stable, biodegradable and non-toxic, will be beneficial to the environment.

1.5 Outline of thesis

There are 7 chapters in this thesis. Chapter 1 provides the background information, concept, rationale and objectives of the study. Chapter 2 is the literature review, which includes a review of the effects of synthetic dyes and heavy metal ions on the environment, types of adsorbents applied in pollutant removal, their advantages and disadvantages, and removal performance, and the methods used in a mechanistic study. Chapter 3 describes the methods. Chapter 4 presents a discussion on the synthesis of biosorbents. Chapter 5 contains the results and a discussion on the use of the synthesized biosorbents for the removal of synthetic dyes. Chapter 6 presents the results of the removal of heavy metal ions. The last chapter is a general conclusion on the thesis work and provides recommendations for future work.

CHAPTER 2 LITERATURE REVIEW

2.1 Introduction

The project aims to study the synthesis of environmentally safe encapsulation systems, such as chitosan-based and alginate-based encapsulation matrixes that contain microorganisms, for the removal of synthetic dyes and toxic heavy metals. In this chapter, an overview of the impacts of synthetic dyes and heavy metals on the environment is provided. The removal of dyestuffs and heavy metals from water by using conventional and non-conventional methods are also reviewed. In addition, the removal mechanism of synthetic dyes and heavy metals with the integration of commonly adopted kinetics and isotherm models is presented, which can be useful for understanding the mechanistic information of removal systems.

2.2 Impact of synthetic dyes and heavy metals on environment

Nowadays, many industries, such as paper and pulp, textiles, electroplating, mining, tanneries, etc. are developing rapidly which involve the application of large amounts of synthetic dyes and heavy metals(Fu, Fenglian & Wang, Qi, 2011). Improper treatment of the water effluents give rise to pollution after their discharge. At particular concentrations, synthetic dyes and heavy metals bring about adverse effects which can threaten human lives and the environment.

2.2.1 Synthetic dyes

The first synthetic dye was discovered by William Henry Perkin (Hunger, Klaus et al., 2003) and then after that, research work on dye synthesis developed at a fast pace and still continues today. Synthetic dyes are made of non-living precursors, for example, organic substances like aromatics, while natural dyes are commonly extracted from plants, microorganisms that produce various colours when grown on substrates. (Hunger, Klaus et al., 2003) The ability of synthetic dyes to show colour is due to the extensive electron delocalisation of the dye molecules. The chromophore components of the dye molecules absorb different wavelengths which provides their corresponding colours. Synthetic dyes can be synthesised into many more varieties in comparison to natural dyes and classified by their chemical properties and dye usage. Table 2.1 summarises some of the different classes of dyes that are commonly used in the dye industry and Figure 2.1 shows molecular structures of some synthetic dyes.

Table 2.1 Different classes of synthetic dyes.(Hunger, Klaus et al., 2003)

Class	Substrate	Chemical type
Acid	nylon, wool, silk, paper, inks, and leather	azo (including premetallised), anthraquinone, triphenylmethane, azine, xanthene, nitro and nitroso
Basic	paper, polyacrylonitrile, modified nylon, polyester, inks	cyanine, hemicyanine, diazahemicyanine, diphenylmethane, triarylmethane, azo, azine, xanthene, acridine, oxazine, and anthraquinone
Direct	cotton, rayon, paper, leather, nylon	azo, phthalocyanine, stilbene, and oxazine
Disperse	polyester, polyamide, acetate, acrylic plastics	azo, anthraquinone, styryl, nitro, and benzodifuranone
Reactive	cotton, wool, silk, nylon	azo, anthraquinone, phthalocyanine, formazan, oxazine
Mordant	wool, leather	azo and anthraquinone
Vat	cotton, rayon, wool	anthraquinone (including polycyclic quinones) and indigoids

Nevertheless, the environmental impacts that are associated with synthetic dyes are detrimental. Over 0.7 million tons of synthetic dyes for dyeing and printing purposes are produced worldwide annually, and about 5 - 10% are discharged with wastewater(Chen, Gang et al., 2011) into aquatic bodies like rivers and lakes. Synthetic dyes are highly visible even at a concentration of a part-per-million (ppm) scale. This affects solar penetration and gaseous exchange in aqueous environments which greatly deteriorate the eco-system(Chen, Gang et al., 2011). Aside from physical problems, the chemistry of synthetic dyes is also problematic. Commonly adopted synthetic dyes, such as heterocyclic dyes, usually have constituents like sulphate, as well as nitro, chloro, hydroxo ether and alkyl components.(Hunger, Klaus et al., 2003) Although synthetic dyes basically have recalcitrant molecules, which are relatively stable toward chemical reactions, the biological breakdown of synthetic dyes is still possible which

subsequently generate aromatic fragments with the above mentioned constituents. These fragments can be toxic organic compounds which bring about adverse effects to the environmental surroundings where the effluents are discharged. As a result, proper treatment of effluents is vital with the use of synthetic dyes. Figure 2.1 shows some molecular structures of synthetic dyes.

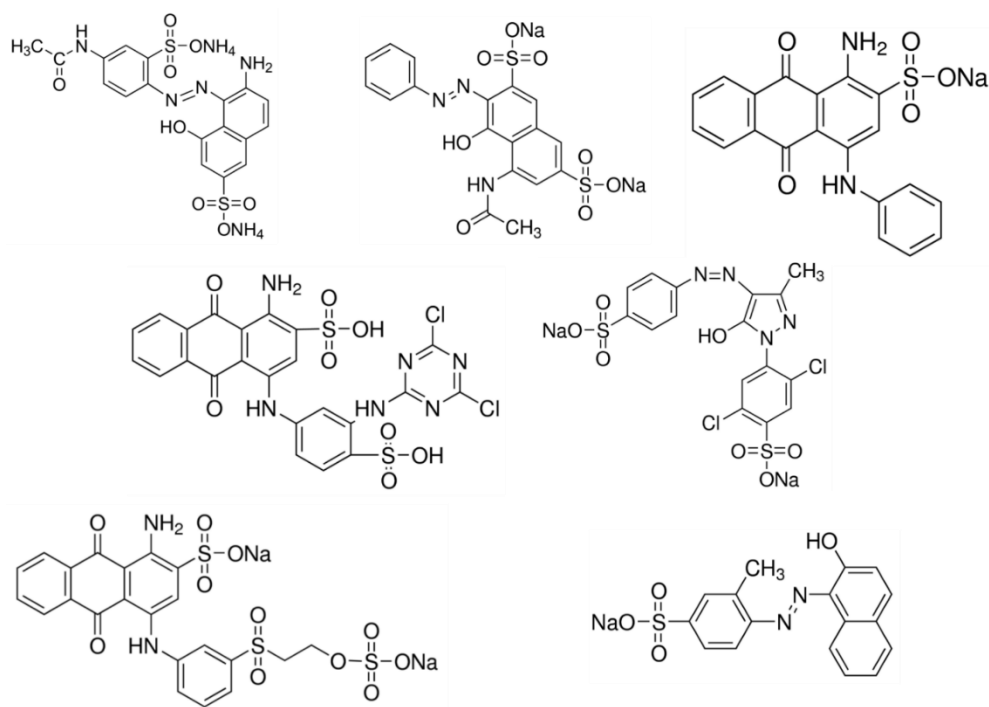


Figure 2.1 Molecular structures of synthetic dyes.

2.2.2 Heavy metals

Heavy metals are naturally found on earth and toxic to humans at particular concentrations. The general definition of heavy metals is that they are metallic elements that have an atomic weight higher than 40.04 with a specific gravity at least 5 times higher than that of water (Yu, Ming-Ho, 2005). With rapid technological development in many industries which lead to anthropogenic activities, for example, electroplating, mining, smelting, and metal finishing to name a few, the exposure of heavy metals to humans, the environment and animal life has drastically increased in the last few decades. Although some heavy metals are essential for the normal metabolism and function of humans and wildlife, excessive intake could bring about adverse health effects. Moreover, once ingested, heavy metals are not easily excreted through normal metabolism, but instead accumulate inside the body. These heavy metals will subsequently bind to biomolecules inside the body, thus impairing their functions (Yu, Z. & Wen, X., 2005a). Besides, low level organisms like plants will pass the accumulated heavy metals to higher levels of consumers along the food chain and finally concentrated levels of hazardous heavy metals will reach the top level consumers which then brings about adverse effects.

Different heavy metals have different acute and chronic effects on human beings with excessive intake, and most are carcinogenic along with high or long term exposure. The adverse health effects of heavy metals are summarised in Table 2.2.

Table 2.2 Acute and chronic health effects resultant of exposure to heavy metals(Järup, Lars, 2003; Mahiya, Suresh et al., 2014).

Heavy metal	Acute effects	Chronic effects
Arsenic	Vomiting, nausea, diarrhoea, painful neuropathy, encephalopathy	Diabetes, hyperkeratosis, hypopigmentation
Cadmium	Lung inflammation	Kidney damage, skeletal damage
Copper	Vomiting, nausea, diarrhoea	Gastrointestinal problems , kidney damage, anaemia
Chromium (hexavalent)	Gastrointestinal haemorrhage, haemolysis, renal failure	Pulmonary fibrosis
Lead	Vomiting, nausea, abdominal pain, diarrhoea	Anaemia, encephalopathy, memory deterioration, kidney damage
Mercury	Lung damage, vomiting, nausea, diarrhoea	Adverse neurological and psychological effects, kidney damage
Nickel	Vomiting, nausea, dizziness, dermatitis	Pharyngitis, sinusitis

Exposure to heavy metals can be through air, direct contact, and food and drink contamination, which are hence assimilated by the body. The present study mainly focuses on the contamination of water by heavy metal ions. Unlike synthetic dyes and other organic contaminants, heavy metals at toxic concentrations can be odourless, colourless and tasteless in water which means that they are difficult to detect. The World Health Organization (WHO) and US Environment Protection Agency (US EPA) have determined and suggested different tolerable concentrations of particular kinds of heavy metals in drinking water. The permissible limit of arsenic (AS) in drinking water is 10 µg/L; cadmium (Cd) is 0.01 mg/L; copper (Cu) is 2 mg/L; chromium (Cr) is 0.05 mg/L; lead (Pb) is 0.05 mg/L; mercury (Hg) is 0.1 µg/kg body weight per day and nickel (Ni) is 0.02 mg/ L(Mahiya, Suresh et al., 2014). Since the permitted concentration of hazardous heavy metals is at a very low level of ppm or even

part-per-billion (ppb), proper water treatment is critical prior to the distribution of water into water bodies and household areas.

2.3 Removal of dyestuffs and heavy metals from water

As mentioned in Section 2.2, proper water treatment is important to ensure suitable water/effluent quality. In general, conventional methods are primarily the removal of hazardous targets since some of the other methods are not effective or efficient enough when there is a low concentration of contaminants, or otherwise very expensive to satisfactorily remove the contaminants. Therefore, researchers have started to put in efforts towards the use of biosorption which is one of the most efficient methods to address low concentrations of contaminants. In this section, conventional methods for the removal of dyestuffs and heavy metals in general will be reviewed and biosorption of water contaminants will be discussed in detail.

2.3.1 Conventional methods

Both synthetic dyes and heavy metals are conventionally treated with different physical and chemical processes. Although many of these processes are effective enough to remove water pollutants in particular conditions and reduce substrate concentration, each has its own limitations. Therefore, research work has now shifted to examining biosorption, which is a more versatile method and can also overcome the major shortcomings of conventional methods.

2.3.1.1 Chemical processing

The chemical processes to remove dye and heavy metals include coagulation, flocculation, precipitation, electrokinetic coagulation, electrochemical processes, irradiation and also oxidation(Ejder-Korucu, M. et al., 2015). Heavy metal ions are typically removed through the processes of precipitation and chelation(Ku, Y. & Jung, I. L., 2001). Conventionally, hydroxide and sulphur precipitation are used to remove heavy metals, such as Zn^{2+} , Cr^{3+} , Cu^{2+} , Pb^{2+} , Hg^{2+} , Cd^{2+} , Mn^{7+} , etc. The precipitating agents can reduce high substrate concentrations and subsequently, the residual concentration is low enough to meet wastewater standards accordingly(Alvarez, M. T. et al., 2007; Chen, Q. Y. et al., 2009; Kousi, P. et al., 2007; Ku, Y. & Jung, I. L., 2001; Mirbagheri, S. A. & Hosseini, S. N., 2005; Özverdi, A. & Erdem, M., 2006). Hydroxide precipitation is carried out when hydroxide is added to the waste water to form precipitates; that is, the metal ions are precipitated into metal hydroxides. Heavy metal hydroxides can be amphoteric. When the pH is adjusted to a suitable range, metal hydroxides will have minimum solubility or are insoluble, so that they precipitate as a result. Sulphide precipitation is used with a wide range of pH levels because metal sulphides are not amphoteric with particular pH environment. (Kongsricharoern, N. & Polprasert, C., 1995). However, during the sulphide precipitation process, hydrogen sulphide is produced, which is toxic. As well, the resultant product are colloidal metal sulphides, which cause severe separation problems. Therefore, as an alternative option, chelating agents are used to remove heavy metal ions. The use of chelating agents is done so through chelation, which can remove large concentrations of heavy metals with satisfactory removal efficiency(Bhakta, J. N. et al., 2012; Fu, F. et al., 2006; Fu, F. et al., 2007; Ying, X. & Fang, Z., 2006). The chelating agents are also more versatile in their use as opposed to

conventional precipitating reagents Figure 2.2 shows an example of chelating agents, dipropyl dithiophosphate from Ying and Fang's research work, in removing heavy metals.

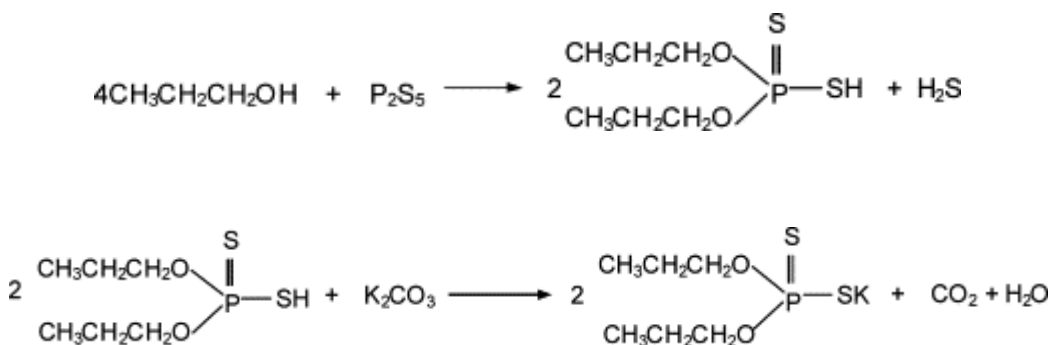


Figure 2.2 Dipropyl dithiophosphate, a lead-, cadmium-, copper- and mercury-chelating agent synthesised and studied by Ying and Fang (Ying, X. & Fang, Z., 2006).

Chemical treatments can also remove synthetic dyes. However, many of the processes involve the excessive use of chemical reagents and thus there is the generation of sludge and high costs are incurred due the consumption of reagents. However, some are effective in removing dyes of particular dye classes. Synthetic dyes that are highly soluble in water, such as acid, direct and reactive dyes, have low coagulation efficiency and hence show low removal efficiency (Singh, K. & Arora, S., 2011). Recent developments and research on chemically removing dye effluents as well as organic pollutants have indicated that advanced oxidation processes (AOPs) and ozonation work well. These two methods have high removal efficiency and also greatly reduce the by-products compared to the conventional methods mentioned above. Nevertheless, they are still costly which limits their applications in industrial plants.

2.3.1.2 Physical processing

Conventional techniques that physically remove dye and heavy metals used by industrial plants include ion exchange, filtration, reverse osmosis, nanofiltration, and adsorption. These methods are mostly effective, especially adsorption and reverse osmosis. However, some of them involve equipment that have high operating costs and short life time, thus requiring periodic maintenance.

The ion exchange process is generally known as the cationic and anionic processes(Ejder-Korucu, M. et al., 2015). Since synthetic dyes are mostly in ionic forms, ion exchange resins can be used to physically attract the corresponding substrates until saturation of the column. Although ion exchange has its advantages in that there is no loss of adsorbent upon regeneration and collection of solvents is possible after separation, its substrate scope is narrow compared to the wide variety of synthetic dyes available. On the other hand, the ion exchange process is quite effective for the removal of heavy metal ions. Cationic exchangers work well with the influx that contain positively charged metal ions. The ion exchange process is highly efficient and has a high removal capacity as well as fast exchange kinetics(Abo-Farha, S. A. et al., 2009; Doula, M. K., 2009; Gode, F. & Pehlivan, E., 2006; Kang, S. Y. et al., 2004; Motsi, T. et al., 2009; Ostroski, I. C. et al., 2009; Taffarel, S. R. & Rubio, J., 2009). Yet despite these advantages, the high regeneration cost of the exchangers and ineffectiveness with disperse dyes reduce the applicability of the ion exchange process in removing pollutants(Ejder-Korucu, M. et al., 2015; Fu, Fenglian & Wang, Qi, 2011). Membrane filtration is another well known physical separation process that is adopted in wastewater treatment plants. Similar to the ion exchange process, membrane filtration also clarifies, concentrates and separates

the target substrates from the effluents(Ejder-Korucu, M. et al., 2015; Fu, Fenglian & Wang, Qi, 2011). The types of membrane filtration processes include ultrafiltration, nanofiltration and reverse osmosis. Membrane filtration can be combined with other biological or chemical processes such as membrane bioreactors, ozonation, and activated sludge oxidation(Ciardelli, G. et al., 2000; Hai, F. I. et al., 2006; Joshi, M. & Purwar, r., 2008; Petrinić, I. et al., 2007; Vishnu, G. & Joseph, K., 2007; Wu, J. et al., 1998; Zheng, X. & Liu, J., 2006). Although membrane filtration is excellent in reducing chemical oxygen demand (COD), biochemical oxygen demand (BOD) and turbidity, colour removal is not always guaranteed with conventional membrane filtration processing(Singh, K. & Arora, S., 2011; Zheng, X. & Liu, J., 2006). The more advanced techniques, such as nanofiltration and reverse osmosis, can be used to treat highly soluble reactive dyes(Petrinić, I. et al., 2007; Vishnu, G. & Joseph, K., 2007). Membrane filtration processing for the removal of heavy metals has been extensively studied and developed into numerous other approaches that demonstrate high removal efficiency(Fu, Fenglian & Wang, Qi, 2011). For example, micellar enhanced ultrafiltration (MEUF) and polymer enhanced ultrafiltration (PEUF) show excellent removal efficiency of positively charged divalent and trivalent metal ions(Barakat, M. A. & Schmidt, E., 2010; Camarillo, R. et al., 2010; Danisa, U. & Aydiner, C., 2009; Ennigrou, D. J. et al., 2009; Ferella, F. et al., 2007; Korus, I. & Loska, K., 2009; Landaburu-Aguirre, J. et al., 2010). The techniques involve the entrapment of metal ions into micelle or the use of polymer for metal ion complexation followed by filtration. Although these filtration techniques appear to be effective and efficient, they still require further modifications of the membrane and other techniques are required to be used so as to optimise the overall removal performance(Hai, F. I. et al., 2006). Moreover,

chemical incompatibility in pre-treatment, reduced temperatures and pH conditions which cause fouling of the membrane are problems associated with conventional membrane filtration. The maintenance of the membrane is also relatively costly if the aim is to remove a multitude of pollutants.

2.3.1.3 Biological treatment

Biological treatment involves the use of bacteria, fungus and algae to carry out biodegradation, bioaccumulation or bioremediation of synthetic dyes and heavy metals. Microorganisms are used in biological treatments, such as *Cunninghamella elegans*(Ambrósio, S. T. et al., 2012), *Aspergillus niger*(Karthikeyan, K. et al., 2010), *taphylococcus epidermidis*(Lamia, A. et al., 2010), *Cosmarium sp.*(Daneshvar, N. et al., 2007), *Pseudomonas desmolyticum*(Kalme, S. D. et al., 2007), *Phormidium sp.*(Silva-Stenico, M. E. et al., 2012) and *Citrobacter sp.*(Hui, W. et al., 2010) Although biological treatment is relatively more economical than physical and chemical processing, the efficiency of the decolouration and metal removal varies with different substrates and microbes used.

Since synthetic dyes possess numerous functional groups and have a wide variety as mentioned in Section 2.1.1, it is difficult in reality to establish a general biological environment that would treat the various synthetic dyes in the target wastewater. Although researchers have reported a high efficiency of decolourisation and biosorption by using biological treatment, they usually worked with a single synthetic dye and not mixed substrates, which is much more simple than real life complex cases (Alhassani, H. A. et al., 2007; Anjaneya, O. et al., 2011; Balapure, K. H. et al., 2014; Haq, I. et al., 2016; Jain, K. et al., 2012; Jin, X. & Ning, Y., 2013; Kalme, S. D. et al., 2007). Moreover, conventional biological treatment usually uses live biomass. The toxicity of wastewater is therefore a challenge in terms of the maintenance of the biomass as the toxicity may reduce the biomass population hence decreasing the decolourisation efficiency. Biological treatment processes require a good nutrition supply and the removal process is usually time consuming (Ola, I. O. et al., 2010b).

The biological processes for dye removal mainly comprise aerobic and anaerobic treatments. In the former, the microbes require an oxygen supply for bioremediation and the end products are generally carbon dioxide, water and biodegraded organic fragments. In contrast, the latter does not require oxygen to carry out bioremediation and methane instead of water is generated as the end product as well as other end products also found in aerobic treatment (Ejder-Korucu, M. et al., 2015). A number of research works have revealed that anaerobic bioremediation is usually carried out with microbes in which enzymatic decolourisation involves azoreductase enzymes. These enzymes cleave the azo bonds of the target colourants in the process of decolourisation

and mineralisation of the dye molecules. Toxic aromatic amines are usually generated after the cleavage of synthetic dyes which is a disadvantage of using a biological process for decolourisation, as these toxins threaten human health and also aquatic life. Moreover, the toxins might be harmful to the microbes themselves which then reduce the population for the biological process. The toxicity of the metabolites after bioremediation depends on the chemical structure of the original dye molecules. In fact, a number of researchers have reported the results of their phytotoxicity tests which show that the metabolites generated from bioremediation have less toxicity than the original dye molecules (Balapure, K. H. et al., 2014; Chaudhari, A. U. et al., 2013; Kalme, S. D. et al., 2007).

The biological treatment of heavy metals involves the oxidation state changes of heavy metals which will then require treatment with chemical or physical processes. Biosorption occurs between the heavy metal ions and the biomasses adopted which will be discussed in more detail. Overall, the efficiency and effectiveness of using biological treatment to remove dye strongly depend on the microbe and substrate. A general means of decolourisation is difficult with the use of biological treatment.

2.3.2 Non-conventional methods

2.3.2.1 Adsorption

Adsorption is a well known technique to remove dye and heavy metals, which involves the application of a solid bed absorbent or suspension of solids into solutions that contain the target substrates. Chemisorption, physisorption, electrostatic interactions, could occur between the adsorbents and adsorbates. Chemisorption refers to chemical bonds formation between the adsorbent and adsorbate, such as covalent bonds, while physisorption is the formation of weakly reversible bonds, such van der Waals forces, hydrogen bonds, and dipole-dipole interactions. Electrostatic interaction refers to columbic attractions between opposite charges possessed on the adsorbent and adsorbate(Ruthven, D. M., 1984). Adsorption is economical, and has flexibility in chemical and physical modifications. Its primary advantages are: simple and practical to use, high resistance towards various physical conditions and toxic compounds, low sludge generation, and reversible by desorption to collect adsorbed compounds(Gupta, V. K. & Suhas, 2009; Pereira, L. & Alves, M., 2012). Commonly used adsorbents include, but are not limited to: activated carbon, carbon nanotubes, alumina, silica gel, zeolites, agricultural and industrial wastes, and living or non-living biomasses that have plant origins(Ejder-Korucu, M. et al., 2015; Gupta, V. K. & Suhas, 2009; Pereira, L. & Alves, M., 2012).

Activated carbon has been used for a long period of time as an absorbent and available in a variety of products, such as coal, coconut shells, lignite, wood, etc.(Gupta, V. K. & Suhas, 2009) The activation of carbon can be through physical or chemical means, and the preparation and final surface chemistry after activation have significant influence on the removal capacity of the activated

carbon (Forgacs, E. et al., 2004; Pereira, M. F. R. et al., 2003). In general, activated carbon is advantageous due to its highly porous structure (thus a high total surface area), versatile adsorption performance with various chemical and physical processes, and high levels of stability in various surrounding environments (Pereira, L. & Alves, M., 2012). Nevertheless, the versatility of activated carbon means that it is not as economical as biosorbents which are lower in cost, and the complex manufacturing processes to produce activated carbon are high in cost and energy consumption. The advantages of activated carbon at the same time limit its general application worldwide (Forgacs, E. et al., 2004). On the other hand, silica gel and zeolites and also many other physical adsorbents do well to remove dye with respect to particular groups of dyes; however, they cannot be used to satisfactorily remove all dyes in general and the cost limits their broad applications.

2.3.2.2 Biosorption

Biosorption is a type of adsorption mechanism that uses biomass as the adsorbent and has been extensively studied for a long period of time. Compared to inorganic adsorbents and activated carbon, biosorbents are inexpensive and abundantly found in nature. More importantly, they are effective in sequestering low concentrations of dyes and heavy metal ions (Fu, Fenglian & Wang, Qi, 2011). There are mainly three types of biosorbents: (a) non-living; (b) algal; and (c) microbial biomasses, which include fungi, bacteria and yeast, to name a few (Apiratikul, R. & Pavasant, P., 2008). Tables 2.3 – 2.6 summarise the research work on the biosorption of synthetic dyes while Tables 2.7 – 2.11 summarise the research work on the biosorption of heavy metal ions.

Table 2.3. Summary of non-living biomass used as biosorbent on synthetic dyes

Biosorbent(s)	Synthetic dye(s)	Biosorption capacity (mg g ⁻¹)	Source
Apple pomace	Mixed reactive dyes	2.79	Robinson et al.(Robinson, T. et al., 2002a)
Rice husk	Brilliant green	26.20	Mane et al.(Mane, V. S. et al., 2007)
	Congo red	14.00	Han et al.(Han, R. et al., 2008)
	Indigo carmine	65.90	Lakshmi et al.(Lakshmi, U. R. et al., 2009)
Sugarcane bagasse	Basic violet 3	3.79	Khattari and Singh(Khattari, S. & Singh, M. K., 2000)
	Methyl red	54.60	Azhar et al.(Azhar, S. S. et al., 2005)
	Methylene blue	34.20	Filho et al.(Filho, N. C. et al., 2007)
Silkworm pupa	Basic blue 4	6.33 ^a	Noroozi et al.(Noroozi, B. et al., 2008)
	Basic red 18	0.42 ^a	
Carbonaceous adsorbent	Ethyl orange	198.40	Jain et al.(Jain, A. K. et al., 2003)
	Methylene yellow	211.90	
	Acid blue 13	221.20	
Banana pith	Rhodamine B	206.60	Kadirvelu et al.(Kadirvelu, K. et al., 2003)
	Congo Red	191.40	
	Methylene blue	233.40	
	Methyl violet	93.60	
	Malachite green	120.50	
Wheat straw	Methylene blue	312.50	Gong et al.(Gong, R. et al., 2008b)

Brazilian pine fruit shell	Methylene blue	413.00	Royer et al.(Royer, B et al., 2009)
Chitosan (powder form)	Acid Green 25	645.10	Wong et al.(Wong, Y. C. et al., 2004)
	Acid orange 10 / 12	922.90 / 973.30	
	Acid red 18 / 73	693.20 / 728.20	
Chitosan nanoparticle	Acid orange 10 / 12	1.77 ^a / 4.33 ^a	Cheung et al.(Cheung, W. H. et al., 2009)
	Acid red 18 / 72	1.37 ^a /2.13 ^a	
Chitin Chitosan	Tartrazine	30.00	Dotto et al.(Dotto, G. L. et al., 2012)
		350.00	
Chitosan (Glutaldehyde-cross-linked magnetic beads)	Direct red 23	1250.00	Sanlier et al.(Sanlier, S. H. et al., 2013)
Chitosan (hollow fibre)	Reactive blue 19	454.50	Mirmohseni et al.(Mirmohseni, A. et al., 2012)
Chitosan (graft-copolymerized with PMMA)	Reactive blue 19	1498.00	Jiang et al.(Jiang, x. et al., 2014)
Malt bagasse	Orange solimax TGL	23.20	Fontana et al.(Fontana, K. B. et al., 2016)
Calcium alginate nanoparticles	Malachite green	277.78	Geetha et al.(Geetha, P. et al., 2016)

^a biosorption capacity presented as mmol g⁻¹

Table 2.4. Summary of algal or fungal biomass used as biosorbent on synthetic dyes

Biosorbent(s) biomass)	(Algal	Synthetic dye(s)	Biosorption capacity (mg g⁻¹/ removal %)	Source
<i>Spirogyra sp. 102</i>		Direct Brown	80% (based on 5 ppm)	Mohan et al.(Mohan, S. V. et al., 2008)
<i>Nostoc linckia</i>		Methyl Red	81.97%	El-Sheekh et al.(El-Sheekh,
<i>Lyngbya lagerlerimi</i>		Orange II	47.06%	

<i>Chlorella vulgaris</i>	G-Red (FN-3G)	59.11% (based on 20 ppm)	M. M. et al., 2009)
<i>Scenedesmus quadricauda</i>	Remazol Brilliant Blue R	48.30	Ergene et al.(Ergene, A. et al., 2009)
<i>Chlorella vulgaris</i>	Supranol Red 3BW Lanaset Red 2GA Levafix Navy Blue EBNA	35.62 44.98 43.17	Lim et al.(Lim, S. L. et al., 2010)
Biosorbent (fungal biomass)	Synthetic dye(s)	Biosorption capacity (mg g⁻¹)	Source
White rot Fungi	Acid green Basic orange Disperse red	98.00 61.00 76.00	Nasreen et al.(Nasreen, Z. et al., 2007)
<i>Phanerochaete chrysosporium</i>	Acid red 88 Reactive black 5 Reactive orange 16 Acid red 114	99% 100% 100% 90% (based on 24 ppm)	Ghasemi et al.(Ghasemi, F. et al., 2010)
<i>Aspergillus niger</i>	Congo red	99% (based on 10 ppm)	Karthikeyan et al.(Karthikeyan, K. et al., 2010)
<i>Aspergillus flavus</i> <i>Alternaria sp. / Penicillium sp.</i>	Acid red 151 Orange 2	98% 58% (based on 20 ppm)	Ali et al.(Ali, N. et al., 2010)
<i>Trametes versicolor</i>	Sirius Blue K-CFN	62.62	Erden et al.(Erden, E. et al., 2011)
<i>Phanerochaete chrysosporium</i>	Direct red 80	100% (based on 20 ppm)	Sen et al.(Sen, K. et al., 2012)
<i>Coriolus versicolor</i>	Acid orange II	85% (based on 33-100 ppm)	Hai et al.(Hai, F. I. et al., 2012)
<i>Aspergillus versicolor</i>	Reactive black 5	227.27	Huang et al.(Huang, J. et al., 2016)
<i>Penicillium ochrochloron</i>	Reactive blue 13	14.58	Aytar et al.(Aytar, P. et al., 2016)

Table 2.5. Summary of bacterial biomass used as biosorbent on synthetic dyes

Biosorbent	Synthetic dye(s)	Biosorption capacity (mg g ⁻¹ / removal %)	Source
<i>Staphylococcus arlettae</i>	Reactive Yellow 107 Reactive Black 5 Direct Blue 71	99.00% 99.00% 96.00% (based on 100 ppm)	Elisangela et al.(Elisangela, F. et al., 2009)
<i>Staphylococcus aureus</i>	Orange II Sudan III	76.00% 97.00% (based on 6 ppm)	Pan et al.(pan, H. et al., 2011)
<i>Pseudomonas sp.</i>	Reactive Red 2,	52% (based on 5000ppm)	Kalyani et al.(Kalyani, D. C. et al., 2009)
<i>Pseudomonas aeruginosa</i>	Remazol Red	97% (based on 50 ppm)	Ghodake et al.(Ghodake, G. et al., 2011a)
<i>Bacillus cereus</i>	Reactive red 195	97% (based on 200 ppm)	Modi et al.(Modi, H. A. et al., 2010)
<i>Bacillus cereus</i>	Cibacron Black PSG, Cibacron Red P4B	67.00% 81.00%	Ola et al.(Ola, I. O. et al., 2010a)
<i>Listeria sp.</i>	Black B Black HFGR Red B5	69.00% 74.00% 70.00% (based on 50 ppm)	Anburaj et al.(Anburaj, J. et al., 2011)
<i>Sphingomonas paucimobilis</i>	Methyl red	98.00% (based on 850pm)	Ayed et al.(Ayed, L. et al., 2011)
<i>Micrococcus sp.</i>	Orange MR	93.18% (based on 100pm)	Rajee et al.(Rajee, O. & Patterson, J., 2011)
<i>Shewanella oneidensis</i>	Reactive black 5 Congo red	100.00% 100.00% (based on 50 µM)	Wu et al.(Wu, J. et al., 2009)
<i>Shewanella sp.</i>	Acid orange 7	98.00%	Wang et al.(Wang, J. et

			al., 2012)
<i>Acinetobacter calcoaceticus</i>	Amaranth	92.00% (based on 50 ppm)	Ghodake et al.(Ghodake, G. et al., 2011a)
<i>Rhodopseudomonas palustris</i>	Reactive Red 195	100.00% (based on 0.1% dye)	Celik et al.(Celik, L. et al., 2012)
<i>Lentinus edodes</i>	Congo red	143.67	Gimenez et al.(Gimenez, G. G. et al., 2014)
	Bordeaux red	500.00	
	Methyl violet	381.68	

Table 2.6. Summary of yeast biomass used as biosorbent on synthetic dyes

Biosorbent	Synthetic dye(s)	Biosorption capacity (mg g ⁻¹ / removal %)	Source
<i>Candida tropicalis</i>	Basic Violet 3	85.30% (based on 50 ppm)	Das et al.(Das, D. et al., 2011)
<i>Candida tropicalis</i>	Violet 90	56.28	Okur et al.(Okur, M. et al., 2014)
<i>Candida rugopelliculosa</i>	Reactive blue 13	90% (based on 2000 ppm)	Liu et al.(Liu, X. et al., 2011)
<i>Trichosporon akiyoshidainum</i>	Reactive Blue 221 Reactive Red 141 Reactive black 5	65.00% 100.00% 100.00% (based on 200 ppm)	Pajot et al.(Pajot, H. F. et al., 2011)
<i>Galactomyces geotrichum</i>	Mixture of 7 dyes	88.00% (based on 10 ppm in each dye)	Waghmode et al.(Waghmode, T.R. et al., 2011)
<i>Paraconiothyrium variabile</i>	Sudan Black Remazol Brilliant Blue R	84.00% 93.00% (based on 200 ppm)	Aghaie-Khouzani et al.(Aghaie-Khouzani, M. et al., 2012)
<i>Saccharomyces Cerevisiae</i>	Basic green 4 Basic yellow 2	96.0% 93.00% (based on 100 ppm)	Kelewou et al.(Kelewou, H. et al., 2014)
<i>Issatchenkia orientalis</i>	Reactive black 5	90.00% (based on 200 ppm)	Jafari et al.(Jafari, N. et al., 2014)
<i>Yarrowia lipolytica isf7</i>	Methyl orange	99.00% (based on 35 ppm)	Asfaram et al.(Asfaram, A. et al., 2016)

Table 2.7 Summary of non-living biomass used as biosorbent on heavy metals

Biosorbent(s)	Heavy metal species	Biosorption capacity (mg g ⁻¹)	Source
Lemon residue	Arsenic (V)	0.47	Marin-Rangel et al.(Marin-Rangel, V. M. et al., 2012)
Pine leaves		3.27	Shafique et al.(Shafique, U. et al., 2012)
Parsley		18.17	Jimenez-Cedillo et al.(Jimenez-Cedillo, M. J. et al., 2013)
<i>Vallisneria gigantea</i>	Arsenic (III)	0.05	Iriel et al.(Iriel, A. et al., 2015)
Coffee grounds	Cadmium (II)	15.65	Azouaou et al.(Azouaou, N. et al., 2010)
Castor seed hull		6.98	Sen et al.(Sen, T. K. et al., 2010)
Cashew nut shell		22.11	Kumar et al.(Kumar, P. S. et al., 2012)
Cortex banana waste		67.20	Kelly-Vargas et al.(Kelly-Vargas, K. et al., 2012)
Duckweed (<i>Lemna aequinoctialis</i>)		33.00	Chen et al.(Chen, L. et al., 2015)
Chitosan-based nanoparticles	63.50	Shaker(Shaker, M. A., 2015)	
Pine cone powder	Copper (II)	26.32	Ofomaja et al.(Ofomaja, A. E. et al., 2010)
Pineapple peel fibre		27.68	Hu et al.(Hu, X. et al., 2011)
Watermelon rind		111.10	Banerjee et al.(Banerjee, K. et al., 2013)
Bifunctionalised chitosan		0.698 ^a	de Almeida et al.(de Almeida, F. T. R. et al., 2016)
Cotton fibre	Chromium (VI)	69.15	Muxel et al.(Muxel, A. A. et al., 2011)
Bark (<i>Cupressus lusitanica</i>)		87.50	Netzahuatl-Muñoz et

			al.(Netzahuatl-Muñoz, A. R. et al., 2012)
Acid treated date palm fibre		34.12	Hossini et al.(Hossini, H. et al., 2015)
Bifunctionalised chitosan		1.91 ^a	de Almeida et al.(de Almeida, F. T. R. et al., 2016)
Pineapple peel fibre	Lead (II)	27.68	Hu et al.(Hu, X. et al., 2011)
Portulaca plant		17.24	Dubey and Shiwani(Dubey, A. & Shiwani, S., 2012)
Cortex orange waste		76.80	Kelly-Vargas et al.(Kelly-Vargas, K. et al., 2012)
Pretreated oil palm fronds		129.87	Khosravifahkhan et al.(Khosravifahkhan, S. et al., 2015)
Cassava peel		57.00	Kurniawan et al.(Kurniawan, A. et al., 2011)
Bark (<i>Moringa oleifera</i>)	Nickel (II)	30.38	Reddy et al.(Reddy, D. H. K. et al., 2011)
Orange peel		62.30	Gönen and Serin(Gönen, F. & Serin, D. S., 2012)
Seeds (<i>Litchi chinensis</i>)		66.62	Flores-Garnica et al.(Flores-Garnica, J. G. et al., 2013)
Carissa Carandas		3.76	Sharma et al.(Sharma, S. K. et al., 2015)
Syzygium aromaticum		2.96	
Bifunctionalised chitosan		0.725 ^a	de Almeida et al.(de Almeida, F. T. R. et al., 2016)

^a adsorption amount denoted as mmol g⁻¹

Table 2.8 Summary of algal biomass used as biosorbent on heavy metals

Biosorbent(s)	Heavy metal species	Biosorption capacity (mg g ⁻¹)	Source
<i>Osmundea pinnatifida</i>	Cadmium (II)	10.02	El Hassouni et al.(El Hassouni, E. et al., 2014)
<i>Hizikia fusiformis</i>		14.42	Shin and Kim(Shin, W. S. & Kim, Y. K., 2014)
<i>Chlamydomonas reinhardtii</i>	Copper (II)	0.12	Flouty and Estephane(Flouty, R. & Estephane, G., 2012)
<i>Spirulina platensis</i>		16.20	Hadiyanto et al.(Hadiyanto et al., 2014)
<i>Bifurcaria</i>	Chromium (VI)	23.40	Ainane et al.(Ainane, T. et al., 2014)
<i>Chlorella vulgaris</i>		43.30	Xie et al.(Xie, Y. et al., 2014)
<i>Arthrospira platensis</i>		40.65	Markou et al.(Markou, G. et al., 2015)
<i>Scenedesmus quadricauda</i>		46.51	Shokri Khoubestani et al.(Shokri Khoubestani, R. et al., 2015)
<i>Chlamydomonas reinhardtii</i>	Lead (II)	0.41	Flouty and Estephane(Flouty, R. & Estephane, G., 2012)
<i>Hizikia fusiformis</i>		26.75	Shin and Kim(Shin, W. S. & Kim, Y. K., 2014)
<i>Oscillatoria princeps</i> (88%), <i>Spirogyra aequinoctialis</i> (9%) and <i>Oscillatoria subbrevis</i> (3%) (mixed algae)		89.19	Brouers and Al-Musawi(Brouers, F. & Al-Musawi, T. J., 2015)
<i>Hizikia fusiformis</i>	Nickel (II)	13.90	Shin and Kim(Shin, W. S. & Kim, Y. K., 2014)
<i>Arthrospira platensis</i>		90.91	Markou et al.(Markou, G. et al., 2015)

Table 2.9 Summary of fungal biomass used as biosorbent on heavy metals

Biosorbent	Heavy metal species	Biosorption capacity (mg g ⁻¹)	Source
<i>Paecilomyces lilacinus</i>	Cadmium (II)	24.23	Zeng et al.(Zeng, X. et al., 2010)
<i>Microsphaeropsis</i> sp.		247.5	Xiao et al.(Xiao, X. et al., 2010)
<i>Trichoderma</i> sp.		133.33	Bazrafshan et al.(Bazrafshan, E. et al., 2015)
<i>Agaricus bisporus</i>	Copper (II)	73.30	Ertugay and Bayhan(Ertugay, N. & Bayhan, Y. K., 2010)
<i>Trichoderma</i> sp.		15.08	Mohsenzadeh and Shahrokhi(Mohsenzadeh, F. & Shahrokhi, F., 2013)
<i>Phanerochaete chrysosporium</i>	Chromium (VI)	93.23% (based on 100 ppm)	Marandi(Marandi, R., 2011Marandi)
<i>Phanerochaete chrysosporium</i>		98.92% (based on 10 ppm)	Murugavelh and Mohanty(Murugavelh, S. & Mohanty, K., 2012)
<i>Aspergillus niger</i>		138.26	Ghosh et al.(Ghosh, S. et al., 2015a)
<i>Aspergillus niger</i>	Lead (II)	54.05	Iskandar et al.(Iskandar, N. L. et al., 2011)
<i>Penicillium</i> sp.		76% (based on 123 ppm)	Aytar et al.(Aytar, P. et al., 2014)
<i>Lactarius salmonicolor</i>	Nickel (II)	1.16 ^a	Akar et al.(Akar, T. et al., 2013)
<i>Trametes versicolor</i>		212.50	Subbaiah and Yun(Subbaiah, M. V. & Yun, Y. S., 2013)
<i>Aspergillus awamori</i>		9.52	Shahverdi et al.(Shahverdi, F. et al., 2015)

Table 2.10 Summary of bacterial biomass used as biosorbent on heavy metals

Biosorbent(s)	Heavy metal species	Biosorption capacity (mg g ⁻¹)	Source
<i>Bacillus cereus</i>	Cadmium (II)	82.00% (based on 200 ppm)	Arivalagan et al.(Arivalagan, P. et al., 2014)
<i>Pseudomonas aeruginosa</i>		113.00	König-Péter et al.(König-Péter, A. et al., 2014)
<i>Halomonas sp.</i>		12.02	Manasi et al.(Manasi et al., 2014)
Thermophilic haloalkalitolerant strain		22.70 ^b	Alkan et al.(Alkan, H. et al., 2015)
<i>Enterobacter ludwigii</i> , <i>Zoogloea ramigerans</i> and <i>Comamonas testosteroni</i>	Copper (II)	6.52	Black et al.(Black, R. et al., 2014)
Thermophilic haloalkalitolerant strain		61.10 ^b	Alkan et al.(Alkan, H. et al., 2015)
<i>Bacillus cereus</i>		36.27% (based on 5 ppm)	Maddela et al.(Maddela, N. R. et al., 2015)
<i>Pseudomonas sp.</i>	Chromium (VI)	64.4% (reduction) (based on 160 ppm)	Farag and Zaki(Farag, S. & Zaki, S., 2010)
<i>Bacillus subtilis</i>		93% (reduction) (based on 500 ppm)	Tharannum et al.(Tharannum, S. et al., 2012)
<i>Lysinibacillus sp.</i>		98.20% (based on 30 ppm)	San et al.(San Keskin, N. O. et al., 2015a)
<i>Bacillus cereus</i> <i>Bacillus pumilus</i>	Lead (II)	22.10 28.06	Çolak et al.(Çolak, F. et al., 2011)
<i>Enterococcus faecium</i>		0.0460 ^c	Bhakta et al.(Bhakta, J. N. et al., 2012)
<i>Bacillus gibsonii</i>		333.30	Zhang et al.(Zhang, B. et al., 2013)

<i>Pseudomonas aeruginosa</i>		164.00	König-Péter et al.(König-Péter, A. et al., 2014)
<i>Lysinibacillus sp.</i>		180.5 (dead) 129.7 (live)	Prithviraj et al.(Prithviraj, D. et al., 2014)
Thermophilic haloalkalitolerant strain	Nickel (II)	33.40 ^b	Alkan et al.(Alkan, H. et al., 2015)
<i>Pseudomonas aeruginosa</i>		37.44	Sarkar and Paul(Sarkar, D. & Paul, G., 2015)
^b adsorption amount denoted as $\mu\text{mol g}^{-1}$			
^c adsorption amount denoted as $\text{mg h}^{-1} \text{g}^{-1}$			

Table 2.11 Summary of yeast biomass used as biosorbent on heavy metals

Adsorbent(s)	Heavy metal specie	Adsorption capacity (mg g ⁻¹)	Source
<i>Saccharomyces Cerevisiae</i>	Cadmium (II)	10.17	Cui et al.(Cui, L. et al., 2010)
<i>Candida tropicalis</i>		80% (based on 100 ppm)	Rehman and Anjum(Rehman, A. & Anjum, M. S., 2010)
<i>Saccharomyces Cerevisiae</i>		110.00	Tálos et al.(Tálos, K. et al., 2012)
<i>Saccharomyces Cerevisiae</i>		16.18	Nagy et al.(Nagy, B. et al., 2013)
<i>Saccharomyces cerevisiae</i>	Copper (II)	2.59	Cojocar et al.(Cojocar, C. et al., 2009)
<i>Rhodotorula mucilaginosa</i>		26.20	Salvadori et al.(Salvadori, M. R. et al., 2014)
<i>Cyberlindnera fabianii</i> <i>Wickerhamomyces anomalus</i> <i>Candida tropicalis</i>	Chromium (VI)	18.90	Bahafid et al.(Bahafid, W. et al., 2013a)
		28.14	
		29.10	
<i>Aureobasidium pullulans</i>	Lead (II)	25.00	Ghaedi et al.(Ghaedi, M. et al., 2014)
<i>Saccharomyces cerevisiae</i>		8.90	Infante et al.(Infante, J. et al., 2014)
<i>Yarrowia lipolytica</i>	Nickel (II)	95.33	Shinde et al.(Shinde, N. R. et al., 2012)
<i>Saccharomyces cerevisiae</i>		1.20	Galedar and Younesi(Galedar, M. & Younesi, H., 2013)
<i>Aureobasidium pullulans</i>		45.00	Ghaedi et al.(Ghaedi, M. et

			al., 2014)
<i>Saccharomyces cerevisiae</i>		2.80	Infante et al.(Infante, J. et al., 2014)

In the biosorption of synthetic dyes, it has been observed that there are significant differences in the adsorption capacity of the various adsorbents. For example, Han et al.(Han, R. et al., 2008) reported the removal of 14.00 mg g⁻¹ of congo red dye by using rice husk while Kadirvelu et al. (Kadirvelu, K. et al., 2003) found that banana pith could remove up to 191.4 mg g⁻¹ of the congo red dye. The significant difference is due to the particle size of the adsorbent and whether the carbonaceous materials in the adsorbent undergo activation (activation of carbon). Gong et al.(Gong, R. et al., 2008a) reported the use of acid-esterified wheat straw and Royer et al. (Royer, B et al., 2009) used citric acid to activate the carbon from pine fruit shell and both were able to remove methylene blue dye with satisfactory adsorption results. This means that non-living biomasses of plant origins usually require the activation of carbonaceous materials or further treatment in order to enhance their capacity to remove synthetic dyes. On the other hand, chitosan, which is the deacetylated form of chitin (*N*-acetylglucosamine), shows excellent adsorption of various synthetic dyes even in its original form without further chemical modifications. Dotto et al.(Dotto, G. L. et al., 2012) studied and reported the difference in the amount of tartrazine removed by using chitin versus chitosan. The ability of chitosan to remove synthetic dyes is excellent owing to its amino group at carbon-2. Compared to other cellulosic biosorbents, chitosan has a much more positive surface charge when subjected to a suitable pH environment which

greatly enhances its interactions with synthetic dyes. Moreover, the C-2 amino group means that chitosan has versatile chemical reactions which allow different types of crosslinking and grafting reactions. For example, Jiang et al. (Jiang, x. et al., 2014) reported that chitosan that is graft-copolymerised with PMMA has an adsorption capacity of reactive blue 19 dye as high as 1498.0 mg g^{-1} . Although chitosan itself demonstrates good removal of synthetic dyes, its poor chemical tolerance at low pH environments limits its applications. Therefore, in research work that followed, chemical modifications and grafting with chitosan have been extensively studied. In short, with a proper design and appropriate modifiers, non-living biomasses are good adsorbents for the removal of synthetic dyes.

The application of algal biomasses in the removal of synthetic dye is significantly different when compared with other types of biomasses. Some azo dyes are highly toxic which therefore have toxic effects on living biomasses and aquatic life, but do not affect algae very much (Solís, M. et al., 2012). Moreover, algae do not require a carbon source which is important in microbial applications. Algae derives energy through photosynthesis and hence the overall application cost of bioremediation and biosorption when algae is used is lower than that when non-living and microbial biomasses are used (Solís, M. et al., 2012). The algal removal of synthetic dyes involves bioremediation and biosorption, which comprise the aerobic and anaerobic reductions of azo dyes.

Although algae have its own advantages in treating synthetic dyes, the removal efficiency is relatively low when compared to non-living and microbial biomasses. However, a balance between the removal capacity and ease of application is also important. Microbial decolourisation is even more extensively

studied and explored in comparison to algal decolourisation. White rot fungi, *Asperigillus sp.*, *Phanerochaete sp.*, and *Penicillium sp.* are well known types of fungi that are used in decolourisation processes. Fungi have excellent adsorption ability and fast adaptation to environmental changes; however, some species require a long cultivation time thus limiting their applications. Bacteria are easy to cultivate in short periods of time and can be facultative. In terms of cultivation time, bacteria are a better option than fungi in the removal of synthetic dyes because they require a shorter time. Nevertheless, fungi species can enzymatically oxidise other possible amino products after the biodegradation of synthetic dyes (Husain, Q. & Ulber, R., 2011; Majeau, J. A. et al., 2010) while there are fewer types of bacteria that could mineralise amino products. Other than these, oxidative biodegradation by using bacteria via bacterial laccase is a better option than using fungal laccase since the former is less sensitive to pH, high temperatures and salt concentrations (Solís, M. et al., 2012). *Pseudomonas aeruginosa*, *Brevibacillus laterosporus*, *Sphingobacterium sp.*, *Acinetobacter calcoaceticus*, *Sphingomonas paucimobilis*, *Bacillus cereus* and *Micrococcus glutamicus* are examples of bacterial strains associated with oxidative decolourisation (Ayed, L. et al., 2010; Ghodake, G. et al., 2011b; Jadhav, S. B. et al., 2011; Kurade, M. B. et al., 2011; Tamboli, D. P. et al., 2010). The yeast strains in decolourisation processes are even more optimal than bacteria and fungi since yeast allows faster decolourisation, grow faster than fungi, have the same advantages of using bacteria, as well as high adsorption capacity. Among the different decolourisation processes conducted and studied, the removal of synthetic dyes is usually optimised with low pH values that range from 2-6 with the application of living and sterilised biomasses. This is due to the structure of synthetic dyes which have a salt form when dissolved in water. In low pH

environments, the adsorbent (biomass) surface accumulates a high positive charge while synthetic dyes are in their ionic form with sulfonic groups ($-\text{SO}_3^-$) which are negatively charged. Therefore, the surface adsorption is enhanced with electrostatic attraction. On the other hand, bioremediation with enzymatic reactions is also facilitated more greatly in low pH since the enzymes are more active in low pH but sensitive to high pH.

The removal of heavy metals by using biosorption is relatively more simple than that of synthetic dyes. Compared to the more complex structure of synthetic dyes, heavy metal ions are found in a free cationic form at low pHs, charged oxoanionic form in weak acidic environments, or charged hydroxo form in an aqueous medium, for example, Cr is found in the form of HCrO_4^- and CrO_4^{2-} from low to high pHs. The biosorption and redox reduction of particular heavy metal ions mainly result from biomass-metal ion interactions. However, biosorption is the main focus in the present study.

In the removal of cationic metal ions, such as As (III), As (V), Cu (II), Ni (II), Pb (II), and Cd (II), weak acidic to near neutral pH environments facilitate the capacity for their removal. On the other hand, Cr, which has an opposite charge from the cationic metal species, is found in an oxoanionic form and hence low to extremely low pH environments are reported as optimal for its removal. It is therefore vital to control the pH in removing heavy metals since metal species will precipitate in high pH environments which differs from biosorption. A pH that is carefully controlled provides optimal removal of cationic metal species. Moreover, compared to the conventional processes of precipitation, flocculation and chelation, biosorption addresses low initial concentrations of metal species

which is the primary rationale for using biosorption. Similar to synthetic dyes, most non-living biomasses, which originate from plants and agricultural wastes, are cellulosic and reported to have a lower adsorption capacity when compared to chitosan-based adsorbents. Shaker reported that chitosan-based nanoparticles have a removal capacity of 63.50 mg g^{-1} for Cd (II) which is several folds that of nut shells, seed hulls and coffee grounds.(Azouaou, N. et al., 2010; Kumar, P. S. et al., 2012; Sen, T. K. et al., 2010; Shaker, M. A., 2015). Banerjee et al.(Banerjee, K. et al., 2013) prepared watermelon rind powder at a micro-scale and subsequently subjected this adsorbent to the removal of Cu (II). The resultant capacity to remove Cu (II) is 111.10 mg g^{-1} and the biosorption was determined by following the Langmuir isotherm which showed monolayer adsorption. In the removal of heavy metal by using algal- and microbial-biomasses, surface adsorption takes place through metal chelation with numerous functional groups on the cell wall. The microorganisms are advantageous in the removal of synthetic dyes when the metal ions are removed. Nevertheless, the time to reach equilibrium with biosorption varies with the different species applied. Mishra and Malik reported the removal of Pb (II), Cr (III), Cu (II) and Ni (II) by using *Aspergillus lentulus* in which adsorption equilibrium was reached after five days of incubation(Mishra, A. & Malik, A., 2012). Shin and Kim reported the biosorption of Pb (II), Cd (II), Ni (II) and zinc (II) with a brown algae species (*Hizikia fusiformis*) and kinetics studies showed that adsorption equilibrium was reached after 180 minutes of incubation and the maximum removal capacity ranged from 3.94 to 4.52 mg g^{-1} for these four types of metal ions(Shin, W. S. & Kim, Y. K., 2014).

In short, non-living, algal and microbial biomasses can adsorb synthetic dyes and heavy metal ions with a low initial concentration yet have a high removal capacity. Different chemistries and modifications further enhance their capacity to remove dyes and heavy metals as well as tolerate greater changes in the environment. The optimal pairing of adsorbents and adsorbates optimises the time required for removal and induces a high removal capacity. Further mechanistic reviews, including the means of biosorption, bioremediation, and kinetics and isotherm modelling will be discussed in Section 2.5.

2.3.2.3 Factors that affect adsorption and biosorption efficiency

Both adsorption and biosorption are facilitated via physisorption, chemisorption or electrostatic interaction between the adsorbents and adsorbates. Therefore, physical and chemical parameters, such as the pH, temperature, presence of different ions in the solution, physical characteristics of the adsorbents, and agitation of the solution all affect the removal efficiency (Park, D. et al., 2010).

The physical characteristics of adsorbents have an important role in the adsorption process. The total surface area, porosity, rigidity, chemical and physical stability, and binding site availability determine the removal performance of particular biosorbents. Wu et al. reported that bead type of chitosan has a 2-3.8 fold greater adsorption capacity compared to flake type of chitosan for removing Cu (II) and reactive dye RR222 (Wu, F. C. et al., 2000). The bead type of chitosan has a much higher total surface area compared to the flake type and the chitosan beads are porous, thus allowing diffusion of the adsorbates into the pores. Graft-copolymerisation of chemically cross-linked chitosan not only demonstrates good adsorption capacity of Cr (VI), Ni (II) and

Cu (II), but also strengthens the chemical stability of chitosan in an acidic medium, which originally dissolves in low pH(Shankar, P. et al., 2014).

The pH of the bulk adsorbate solution very much influences the removal efficiency as the surface charge of the adsorbents greatly affects the interactions with the adsorbates(Park, D. et al., 2010). Besides the overall surface charge, the pH also affects the functional groups present on the adsorbents, such as the amino-, hydroxo-, and sulfonyl-groups, and amides. Under different pH environments, the functional groups are positively or negatively charged due to changes in the chemistry. Hence, interactions with adsorbates would be either enhanced or limited, depending on the nature of the adsorbate. The impact of ionic strength is similar to that of the pH environment. The presence of different anions and cations in waste water is inevitable. Since adsorbates and ions both have a charge, competition among all of them and between the adsorbents exists. For example, cations like Cu (II), calcium (II), and sodium (I) compete with each other toward the anionic adsorbents, which eventually affects the adsorption efficiency of Cu (II), the primary target of the removal process.

The temperature of the adsorbent solution usually gives rise to higher removal efficiency as the adsorbent molecules have higher kinetic energy to collide toward the adsorbents to form bonds(Fomina, M. & Gadd, G. M., 2014). Nevertheless, increases in the removal of the heavy metal ions is not always the result as the adsorbents might be unstable under high temperatures so that the major functional groups might be damaged or denatured in such an environment. The thermodynamics of the adsorption process also affect the results. There will be less removal of the heavy metal ions if the process is exothermic and vice versa, which is then endothermic. The agitation of the adsorbent-adsorbate

mixture also physically stimulates the adsorption process. Although a higher agitation speed allows for a more vigorous mass transfer of the mixture, some adsorbents are relatively fragile which will be damaged under vigorous agitation, thus giving rise to lower efficiency in the removal of the heavy metal ions.

2.4 Encapsulation technique for removal of dyestuffs and heavy metals from water

Biosorption is advantageous in a number of aspects which makes this process an attractive option for pollution control. Nevertheless, the application of microorganisms as part of the biosorption process imposes practical problems in terms of the separation of heavy metals and dyes. Since the microbes are micrometre in size, they clog the separation pipes and filter bed after a while. To avoid this, these biosorbents would not be recycled and are discarded after a single use, which generate large amounts of sludge so that the intentions of biosorption are contradicted (Haydar, S. et al., 2015). Therefore, encapsulation is a solution to address the problems of biosorption, in which the biosorbents (microorganisms) are encapsulated into a polymeric matrix and the moiety is subjected to further processing. Since this encapsulated form is relatively large in size, the problem of clogging during separation can be solved. Moreover, the adsorbents can be collected and adsorbed pollutants can be desorbed and collected for reuse. As a result, the selection of a suitable polymer for encapsulation and the microorganism used are highly beneficial to remediating pollutants.

2.4.1 Encapsulation materials

Among the numerous types of encapsulation materials that have been reported,

the most popular include agar, cellulose, pectin, chitosan, alginate, gelatin, polysulfone, polyurethane, polyacrylamide and polyvinyl alcohol (Vemmer, M. & Patel, A. V., 2013). Besides providing the same advantages as non-conventional biosorbents, these polymers are attractive owing to their (1) good biocompatibility with the encapsulated microbes; (2) wide range of possible physical and chemical modifications; and (3) ease and versatility of use in experimental protocols of encapsulation. Chitosan (Hsieh, F. M. et al., 2008; Huq, T. et al., 2013; Lang, W. et al., 2013; Liu, Y. G. et al., 2013; Naydenova, V. et al., 2014), alginate (Abdel Hameed, M. S., 2006; Brachkova, M. I., Duarte, M. A., & Pinto, J. F. (2010)., 2010; Cruz, I., Bashan, Y. et al., 2013; Samuel, J. et al., 2013; Tan, W. S. & Ting, A. S. Y., 2012; Tham, C. S. C. et al., 2015; Ting, A. S. Y. et al., 2013; Vijayaraghavan, K. et al., 2007) and gelatin (Mahmoud, M. E., 2015a; Samuel, J. et al., 2013; Xu, J. et al., 2011) are well known hydrogels that are explored and reported as encapsulation materials to protect microorganisms, drugs, and enzymes. Some studies have reported the use of two or more kinds of polymers to synthesise the polymeric matrix for better encapsulation efficiency or high physical and chemical stability (Cook, M. T. et al., 2013; Kumar, S. S. et al., 2012; Li, X. Y. et al., 2011; Mogharabi, M. et al., 2012; Pang, Y. et al., 2011). In terms of the remediation efficiency of the encapsulated moiety, the removal of pollutants is enhanced (Gomes, L. H. et al., 2011; Saeed, A. et al., 2009; Tan, W. S. & Ting, A. S. Y., 2012), depressed (Abdel Hameed, M. S., 2006) or similar (Batool, R. et al., 2014; Ting, A. S. Y. et al., 2013). Even though the problems of the application of single microorganisms are solved by encapsulation with a polymeric matrix, limitations of removal efficiency or similar results compared to conventional biosorption are reported. The interpretation of the removal performance by using removal efficiency

(expressed as %) or maximum capacity (expressed as q_m) gives different insights to the remediation outcome. After encapsulation of the microorganisms into a polymeric matrix, the mass of the whole moiety is greater compared to the original free polymers. From the viewpoint of removal efficiency, enhancement might be observed with significantly higher removal %. However, in calculating the maximum adsorption capacity, the adsorbed amount per unit mass is usually similar or lower compared to that of a blank polymeric matrix. Mahmoud demonstrated an inverse proportional relationship between biosorbent dosage and adsorption capacity when studying the removal of Cr (VI) by using gelatin-impregnated yeast as the biosorbent (Mahmoud, M. E., 2015a). Nevertheless, enhancements in adsorption capacity have also been reported with *Trichoderma viride* immobilised on a loofa sponge for the removal of methylene blue dye (Saeed, A. et al., 2009) and immobilised *Aspergillus niger* for the removal of Cu (II) (Tsekova, K. et al., 2010).

2.4.2 Encapsulation methods

The encapsulation of microorganisms is carried out through dripping or emulsification (Vemmer, M. & Patel, A. V., 2013). The mixing of the microbes with the polymer in a solution form followed by dripping into a hardening bath is one general approach, which does little harm to the microorganisms during the encapsulation process, unless the hardening bath is toxic to the material that is being encapsulated or there are unfavourable physical parameters in the hardening process. Another general method of encapsulation is emulsification, which comprise the water-in-oil (W/O) and oil-in-water (O/W) methods. The encapsulation target is mixed with an immiscible solution and subsequently mixed well to form an emulsion.

Coacervation/ extrusion involves the dripping of the microorganism-polymer mixture into a hardening bath through a nozzle or needle and the droplets are allowed to harden(Dong, Q. Y. et al., 2013). This method usually results in large sized hydrogel beads with a diameter that ranges from 1–4 mm. Further modifications to the basic dripping setup, for example, the application of pressure, increased number of needles or droplet breaking systems (coaxial air flow, electrostatic droplet generator, and nozzle resonance and jet-cutting methods) are used to obtain smaller droplets at larger flow rates(Vemmer, M. & Patel, A. V., 2013). The hardening of alginate beads by using divalent cations is one of the very commonly adopted methods for the encapsulation of microorganisms(Huq, T. et al., 2013). After dripping the alginate mixture into a hardening bath, the divalent calcium ions would crosslink with the alginate at the surface within milliseconds, thus forming hydrogel beads that contain water inside(Vemmer, M. & Patel, A. V., 2013). With this hydrogel, the calcium ions will diffuse into the core material and calcium ions from the bulk solution diffuse to the surface through a concentration gradient, subsequently hardening the whole hydrogel. On the other hand, by changing the order of the solution, hollow beads can be formed with the core material mixed with the hardening solution and dripping into a polymer solution. Compared to hardening from the outside to the inside, hollow beads are finished by hardening from the inside to the outside (Vemmer, M. & Patel, A. V., 2013).

Polymers such as carrageenan, gellan gum, gelatin, and agar/ agarose can be gelled by using a thermal gelation method. This approach is effective with polymers that require dynamic hardening so that gels may soften or disintegrate at higher temperatures and harden when cooled down (Vemmer, M. & Patel, A. V., 2013). A polymer-microbe mixture is dripped into cooler solution at warm temperatures. The cooling solution can be an ionic bath or immiscible phase. For polymers that are thermally irreversible and harden after cooling, no stabilising agent is required in addition to the cooling bath. Further covalent cross-linking on the gelled beads is selective based on the purpose that follows.

In terms of emulsification, the general method is to add Phase A into Phase B (in which the two phases are immiscible) to form an emulsion (Vemmer, M. & Patel, A. V., 2013). Subsequent gelation follows a similar principle to that for dripping. Thermal gelation starts with the warm organic phase that contains the polymer-core material and subsequent cooling of the organic phase gives rise to the gelling of the polymeric matrix. Ionic gelation is carried out by adding a hardening solution to the organic phase that contains the polymer-core material emulsion.

2.5 Removal of synthetic dyes and heavy metals

As mentioned in Section 2.3.2, the basic principles behind the removal of synthetic dyes and heavy metals through adsorption and biosorption involve physisorption, chemisorption and electrostatic interaction, with the possible addition of a biodegradation process if metabolic-dependent reactions are involved. After the study of the impacts imposed by physical and chemical parameters such as the pH, temperature, adsorbate-adsorbent concentration ratio

and agitation, further mechanistic study is critical in fully understanding the removal process.

2.5.1 Adsorption kinetics

Kinetics models are important and useful tools to determine the rate of adsorption and the rate-determining-step of the sorption process. The response of the sorption toward variations in conditions can also be reflected and evaluated by fitting kinetic models with experimental data. For example, the impacts on removal by the size of the sorbents, modifications of sorbents, pH and temperature selected, the sorbate diffusivity and mass transfer coefficient can be evaluated by fitting with different kinetics models(Park, D. et al., 2010).

Commonly adopted kinetics models in biosorption include pseudo first and second order kinetics, Elovich equation and an intraparticle diffusion model (Webber-Morris equation). Table 2.12 shows the mathematical expressions of the models.

Table 2.12 Kinetics models adopted in biosorption evaluation.

Kinetics model	Mathematical expression
Pseudo first order kinetics(Largergren, S., 1898)	$\log(q_e - q_t) = \log q_e - \frac{k_1}{2.303} t$
Pseudo second order kinetics(Ho, Y. S., 2006)	$\frac{t}{q_t} = \frac{1}{k_2 q_e^2} + \frac{1}{q_e} t$
Elovich equation(Zeldowitsch, J., 1934)	$q_t = \frac{1}{\beta} \ln(\alpha\beta) - \frac{1}{\beta} \ln t$
Intraparticle diffusion model(Weber, W. J. & Morris, J. C., 1963)	$q_t = k_i \cdot t^{0.5}$

k_1, k_2, α, k_i : rate constants of corresponding kinetics equations;

q_e, q_t : amount of adsorbed adsorbates at equilibrium and time t .

In most biosorption studies, both pseudo first and second order equations are applied to provide insight into the removal process, in which one of the models show a higher degree of correlation. Further kinetics modelling gives more insight to the removal mechanism. When fitting the experimental results with an intraparticle diffusion model, the point that passes through the origin indicates that intraparticle diffusion is the rate-determining-step of a particular biosorption. The diffusion model usually shows multi-linearity which implies different stages of diffusion in the whole sorption system: (1) diffusion of adsorbate from the bulk toward the surface of the adsorbent; (2) gradual adsorption step where intraparticle diffusion is controlled; and (3) equilibrium step where adsorbates diffuse slowly from the surface into the core parts(Dotto, G. L. & Pinto, L. A. A., 2012). If a biosorption system fits well with the Elovich equation, the result indicates chemisorption-based-biosorption. The Elovich equation generally applies to chemisorption kinetics, which shows satisfactory fitting to various chemisorption processes and covers a wide range of slow adsorption rates. It is often used for systems in which the adsorbing surface is

heterogeneous(Pérez-Marín, A. B. et al., 2007).

2.5.2 Adsorption isotherm modelling

Besides kinetics modelling, isotherm modelling is another important tool for evaluating adsorption. Different isotherm models have different assumptions to help understand the sorption system after mathematical correlation. Table 2.13 shows the mathematical expression of isotherm models commonly used in evaluating biosorption.

Table 2.13 Isotherm models adopted in biosorption evaluation.

Isotherm model	Mathematical expression	Isotherm abbreviations
Langmuir (I., Langmuir, 1918)	$q_e = \frac{q_m K_L C_e}{1 + K_L C_e}$	q_e : adsorbed amount at equilibrium q_m : maximum adsorption capacity C_e : concentration of adsorbate at equilibrium K_L : Langmuir isotherm constant
Freundlich (Freundlich, H., 1907)	$q_e = K_F C_e^{1/n}$	q_e : adsorbed amount at equilibrium C_e : concentration of adsorbate at equilibrium n, K_F : Freundlich isotherm constant
Temkin (Temkin, D., 1934)	$q_e = \frac{RT}{b_T} \ln(K_T C_e)$	q_e : adsorbed amount at equilibrium C_e : concentration of adsorbate at equilibrium K_T : Temkin isotherm constant b_T : constant related to heat of adsorption R : universal gas constant T : temperature
Langmuir-Freundlich (Sips, R., 1948)	$q_e = \frac{q_m K_{LF} C_e^{1/n}}{1 + K_{LF} C_e^{1/n}}$	q_e : adsorbed amount at equilibrium q_m : maximum adsorption capacity C_e : concentration of adsorbate at equilibrium n, K_{LF} : Langmuir-Freundlich isotherm constant
Redlich-Peterson (Redlich, O. & Peterson, D. L., 1959)	$q_e = \frac{q_m K_{RP} C_e}{1 + K_{RP} C_e^n}$	q_e : adsorbed amount at equilibrium C_e : concentration of adsorbate at equilibrium n, K_{RP} : Redlich-Peterson isotherm constant q_m : maximum adsorption capacity
Dubinin-Radushkevich (Dubinin, M. M. & Radushkevich, L. V., 1947)	$q_e = q_m \exp \left\{ -B_D \left[RT \ln \left(1 + \frac{1}{C_e} \right) \right]^2 \right\}$	q_e : adsorbed amount at equilibrium C_e : concentration of adsorbate at equilibrium B_D : Dubinin-Radushkevich isotherm constant q_m : maximum adsorption capacity R : universal gas constant T : temperature

The Langmuir isotherm basically assumes that (1) the adsorbent surface is homogeneous; (2) all adsorption sites are equivalent; (3) the sorption system is based on monolayer adsorption; and (4) no interactions occur between the adsorbed molecules on the adsorbent surface (Haydar, S. et al., 2015). Although a number of adsorption studies have reported results that agree with the Langmuir isotherm assumption, the model has some limitations. In reality, most adsorbents have a heterogeneous surface and also rough structure with a great number of variations. The model also deviates if the adsorption system has a high concentration of adsorbates (or high adsorbate-to-adsorbent ratio). Liu and Liu also indicated that the Langmuir isotherm offers no insights into the mechanism aspects of biosorption (Liu, Y. & Liu, Y. J., 2008). Nevertheless, when a sorption experiment fits well with an isotherm model, at least useful information can be obtained based on the isotherm model assumptions.

The Freundlich isotherm is another widely applied model in biosorption studies. Compared to the Langmuir isotherm, the Freundlich isotherm applies to adsorption on a heterogeneous surface and also addresses the limitation of the adsorbate concentration, which is not as low as that with the Langmuir isotherm (Haydar, S. et al., 2015). The Freundlich isotherm also applies to multilayer adsorption in that the adsorption is reversible and non-ideal (Haydar, S. et al., 2015).

Other isotherm models can be fitted with different biosorption systems which offer other insights into the adsorption mechanism. For instance, the Dubinin-Radushkevich isotherm describes monolayer adsorption and effect of the porous structure of a biosorbent with heterogeneous sorption behaviour,

which is more general than the Langmuir isotherm. The Temkin isotherm assumes that the heat of adsorption would decrease linearly with increases in the coverage of the adsorbent. The Redlich-Peterson isotherm has features of both the Langmuir and Freundlich isotherms for describing biosorption systems (Haydar, S. et al., 2015).

2.5.3 Metabolic-dependent removal of synthetic dyes and heavy metals

Kinetics and isotherm models are useful tools for describing adsorption and biosorption systems. Aside from the biosorption of heavy metal ions and dye on the surface of biosorbents, bioremediation by using live microorganisms is another possible means of removing synthetic dyes, and biological redox reaction for removing heavy metals. These are metabolic-dependent processes which might require the supplementation of nutrients into the bioremediation system.

2.5.3.1 Bioremediation of synthetic dyes

In reality, the toxicity of waste water usually does not favour the growth and sustenance of microorganisms, since a variety of organic and inorganic pollutants are found in the water. Hence, surface biosorption is a primary removal mechanism in this circumstance. However, if the aquatic environment allows for microorganism metabolism, or encapsulation of the microorganisms is carried out, metabolic-dependent bioremediation could take place through different mechanisms.

Fungi and yeast have been studied as the means to degrade synthetic dyes due to their extracellular, nonspecific and non-stereoselective enzymes which include lignin peroxidase (LiP), laccase and manganese peroxidase (MnP)(Hofrichter, M., 2002). Among the numerous species, white-rot fungi have been extensively studied for their efficient enzymatic degradation of synthetic dyes. Under aerobic conditions, they excrete oxidoreductase which degrades lignin and other related aromatic compounds(Ali, H., 2010). *Aspergillus* sp.(Ali, H. et al., 2009; Almeida, E. J. R. & Corso, C. R., 2014; Alvarenga, N. et al., 2014; Andleeb, S. et al., 2012; Kumar, C. G. et al., 2012; Telke, A. A. et al., 2010), *Phanerochaete* sp.(Enayatizamir, N. et al., 2011; Kiran, S., Ali, S. et al., 2012; Noreen, R. et al., 2011; Senthilkumar, S. et al., 2014), *Trametes* sp.(Adnan, L. A. et al., 2014), and *Pleurotus* sp.(Kiran, S., Ali, S. et al., 2012; Yang, X. Q. et al., 2009) are reported to successfully biodegrade synthetic dyes. However, a long growth cycle, nutrition requirements, and long hydraulic retention time are required for white-rot-fungi to carry out the biodegradation of synthetic dyes thus limiting their application. Compared to filamentous fungi, yeast strains are relatively more popular owing to their combined advantages of using fungi and bacteria: they have a fast growth rate and good resistance to harsh and changing environments(Yu, Z. & Wen, X., 2005a). With the supplementation of sucrose as the carbon source, Deivasigamani and Das reported the successful biodegradation of Basic violet 3 dye by using *Candida krusei*(Deivasigamani, C. & Das, N., 2011). Yeast strains such as *Debaryomyces* sp., *Saccharomyces* sp., *Galactomyces* sp. and *Trichosporon* sp. have also been reported to biodegrade azo dyes(Jadhav, S.U. et al., 2008; Lucas, M.S. et al., 2006; Martorell, M.M. et al., 2012; Pajot, H. F. et al., 2008; Tan, L. et al., 2013; Vitor, V. & Corso, C.R., 2008; Waghmode, T.R. et al., 2011; Yang, Q. et al., 2003; Yu, Z. & Wen, X.,

2005b).

Algae and bacterial strains are reported to biodegrade synthetic dyes with the aid of azoreductase, which enzymatically cleaves azo dyes at the $-N=N-$ diazo bond to produce aromatic amine fragments as the end products. Algae species such as *Chlorella* sp.(Omar, H. H., 2008), *Cladophora* sp.(Khataee, A. R. & Dehghan, G., 2011) and *Oscillatoria* sp.(Priya, B. et al., 2011; Shankar, A. M. et al., 2013) show successful degradation of synthetic dyes while *Bacillus* sp.(Khelifi, E. et al., 2012; Shah, M. P. et al., 2013a; Shah, M. P. et al., 2014), *Pseudomonas* sp.(Du, L. N. et al., 2011; Jadhav, J. P. et al., 2010; Kalme, S. D. et al., 2007; Khan, S. S. et al., 2015; Saranraj, P. et al., 2010; Shah, M. P. et al., 2013b; Tuttolomondo, M. V. et al., 2014), and *Enterobacter* sp.(H., Wang et al., 2009; Wang, H. et al., 2009) are bacteria species that have been reported to biodegrade synthetic dyes. The enzymatic reaction by azoreductase is anaerobic(Khan, R. et al., 2013). With suitable carbon and nitrogen sources as the nutrient supply, the anaerobic enzymatic cleavage of azo dyes could be achieved, in which the rate of the bioremediation is dependent on the nutrient source and the structure of the dye molecules(Stolz, A., 2001). If encapsulation of microorganisms is accompanied with bioremediation, the limitations of the gaseous exchange through the polymeric matrix to the microorganisms further enhance favourable conditions for anaerobic bioremediation. However, the carbon and nitrogen sources might also be rejected from the bulk solution into the polymeric matrix. On the other hand, some bacteria strains undergo aerobic bioremediation which is specific to the substrate, compared to non-specific anaerobic degradation as mentioned earlier(Khan, R. et al., 2013). In general, it is more difficult for analogous sulfonated azo dyes, with the sulfonyl group in the *para* position to the azo bond,

to be biodegraded compared to the original chromophores without the sulfonyl group(Khan, R. et al., 2013).

2.5.3.2 Biotransformation of heavy metal

Unlike synthetic dyes with a complex chemical structure, heavy metal ions in water are ionic species or simple complexes chelated with water molecules or counter ions. Therefore, instead of metabolic bioremediation which is complicated, the metabolic-dependent processes of bioaccumulation and biotransformation are used to remove heavy metals by using microorganisms. Bioaccumulation is the process after the biosorption of particular adsorbates onto the surface of the biosorbents. The adsorbed molecules are transported into the inner part of the cells through the membrane layer to achieve bioaccumulation(Ahemad, M. & Kibret, M., 2013; Soares, E. V. & Soares, H. M., 2012). The process of bioaccumulation can be analysed with transmission electron microscopy (TEM). Anand et al. reported work on bioaccumulation found in *Trichoderma viride*(Anand, P. et al., 2006); bacterial strains such as *Citrobacter sp.*, *Thiobacillus ferrooxidans*, *Bacillus sp.*, *Pseudomonas sp.*, *Micrococcus sp.*, *Rhizopus sp.*, *Aspergillus sp.* and *Saccharomyces sp.* have also been reported to exhibit the bioaccumulation of different heavy metals(Ahemad, M., 2012). On the other hand, biotransformation is the change in the oxidation state of various heavy metal species from the metabolism of the microorganisms that are being applied. Although fewer studies are reported compared to the biosorption of heavy metals, the reduction of Cr (VI) to Cr (III) was reported in Somasundaram et al.(Somasundaram, V. et al., 2009), Sharma and Adholeya(Sharma, S. & Adholeya, A., 2012), Bahafid et al.(Bahafid, W. et al., 2011) and Zahoor and Rehman(Zahoor, A., & Rehman, A. (2009). , 2009).

Immobilised forms of Cr-reducing bacteria (*Pseudomonas* sp.) as well as the cell-free extract from *Arthrobacter* are also published (Elangovan, R. et al., 2010; Pang, Y. et al., 2011). Fungi and yeast are also capable in reducing Cr (VI) to (III) under aerobic conditions.

2.6 Chapter Summary

Water pollution problems have been negatively affecting aquatic life and the health of human beings for a long period of time. Conventional methods are no longer adequate for dealing with pollution. Therefore, biosorption is now a non-conventional means that is very effective for treating water pollution by removing synthetic dyes and heavy metal ions. Although there are numerous types of biomasses, non-living biomasses with plant origins and from agricultural wastes, as well as algal and microbial biomasses, work well to remove pollutants. Nevertheless, there is still room to optimise biosorbents such as by improving their sorption capacity at low concentrations of synthetic dyes and heavy metals instead of focusing on the maximum adsorption capacity (q_m).

Encapsulation techniques have been introduced into biosorption processes to optimise the use of microorganisms when removing water pollutants. They are a promising means of solving separation problems associated with the use of microbial biomasses and also allow for the protection of the encapsulated microorganisms when subjected to undesirable bulk environments. Although the separation problems can be minimised, the advantages of using naked microorganisms in biosorption are usually lost after encapsulation. Many researchers have therefore reported the encapsulation of dead microorganisms and subsequently evaluated the removal performance. The rationale for using

dead microorganisms is that there is a higher removal capacity accompanied with the use of heat-treated dead microorganisms compared to live microbes. The limitations of using live microorganisms, such as their nutrient supply which is costly, and toxic effects of the substrate, are also eliminated. Therefore, the encapsulation of dead microbes has become very popular in the biosorption field. On the other hand, live microorganisms can biodegrade other types of organic and inorganic compounds, and not just synthetic dyes and heavy metal ions. Therefore, if an appropriate encapsulation design can be found for live microorganisms, multi-functional adsorbents will be the result which could be used in the biosorption mechanism and result in different types of biodegradation. Some research work have reported the use of encapsulated live microorganisms with a bulk nutrient supply which is one of the ways to increase the functions of adsorbents. However, the design in these research studies is similar to the application of naked microbes. There are few studies that evaluate the encapsulation of both nutrients and microorganisms inside a polymeric matrix. With the inclusion of nutrients inside the matrix, the encapsulated microorganisms are able to undergo biological processes and at the same time, no extra bulk nutrients are required. Protection against the toxicity of substrates is also an advantage with this method. In short, the methods of encapsulating live microorganisms to remove synthetic dyes and heavy metal ions can be further advanced and are worth exploring.

Mechanistic studies are crucial in the evaluation of biosorption to understand how substrates are adsorbed onto adsorbents as well as the rate-determining steps. Many isotherm and kinetics models have been fitted well and used to explain the adsorption nature of particular adsorbents with different adsorbates. Among the

studies on biosorption, q_m is a very important factor used to evaluate the removal performance of an adsorbent. In this study, the q_{ms} of hundreds to thousands of milligrams per gram for synthetic dyes and heavy metals are reported. Encapsulated live microorganisms, however, demonstrate insignificant increments in adsorption capacity or even decreased adsorption when compared to sole polymers. . As a result, the encapsulation of live microorganisms in biosorption is limited in terms of the q_m . Nevertheless, the original rationale of using biomasses for biosorption is to address very low concentrations of synthetic dyes and heavy metals, and thus the q_m may not be the decisive factor of the overall biosorbent process. Even if particular biomasses demonstrate a very large q_m , they should be able to maintain a high level of efficiency when working with diluted substrates. From the literature review, it is found that researchers usually conclude their work by using the q_m and removal mechanisms, but the adsorption characteristics with regard to substrate concentration have not been their focus. While q_m is informative at equilibrium, the adsorption characteristics of different biosorbents are more important in real applications.

Above all, as shown in the literature review, biosorption with the use of different types of biomasses to address the removal of synthetic dyes and heavy metal ions has been extensively studied and explored. It has been reported that encapsulated microorganisms used as biosorbents provide a good performance in removing synthetic dyes and heavy metals. Although a similar or even reduced q_m is primarily the outcome of the various studies, alternative methods as well as studies on the characteristics of encapsulated microorganisms are still lacking. With such research gaps, there is room to design an experiment that can evaluate the characteristics of encapsulated microorganisms for removing synthetic dyes and heavy metal ions.

CHAPTER 3 RESEARCH METHODOLOGY

3.1 Introduction

In this chapter, the research methods of this study will be discussed. The methods that are used for the (1) removal of synthetic dyes and heavy metal ions, (2) characterisation through various instrumentations, (3) synthesis of biosorbents and preparation of microorganisms, as well as (4) fitting of the data in kinetics and isotherm models, will be described.

3.2 Experimental design

The removal of synthetic dyes and heavy metal ions was carried out through several steps. The first step was the selection of the encapsulation materials, microorganisms and target adsorbates. After carrying out a literature review, suitable encapsulation materials (chitosan and alginate) and microorganisms (*L. casei* and *C. krusei*) were chosen in consideration of their biocompatibility with each other and their capability of removing synthetic dyes and heavy metal ions. The selection of the synthetic dyes (Direct Red 80 (DR80), Reactive Yellow 25 (RY25), Acid Blue 25 (AB25), and Reactive Blue (RB19) was based on their common use in the dyeing industry. The type of heavy metal ions (copper(II)) was chosen based on the volume found in industrial discharge and their biohazard significance. The second step was the synthesis of the hydrogel beads with the encapsulated microorganisms. The third step was the characterisation of the synthesised biosorbents. The last step was the evaluation of the removal performance with optimisation experiments and mechanistic studies. Figure 3.1 shows the flow of the experimental design of the research work.

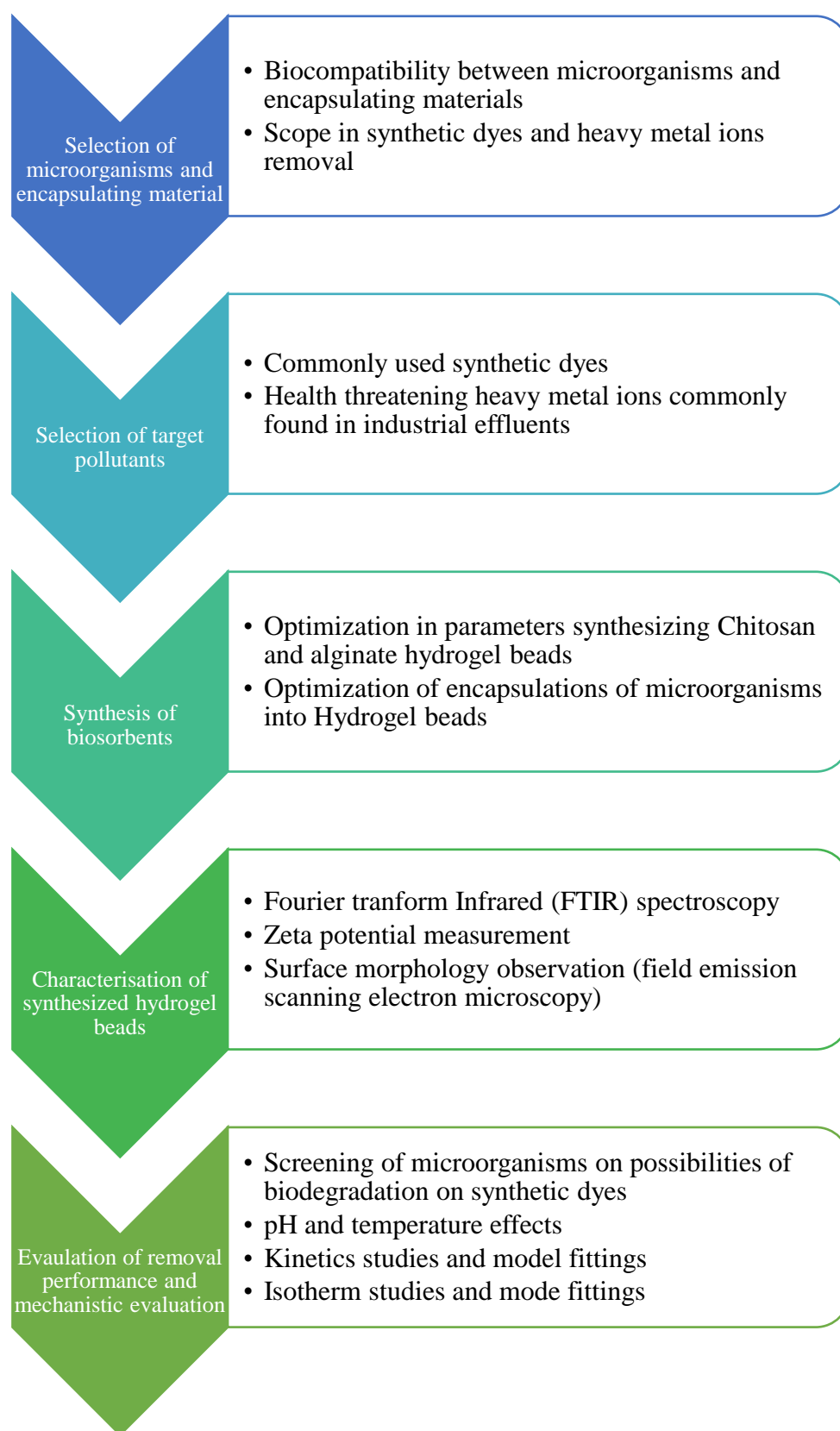
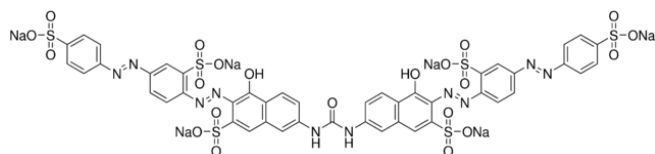


Figure 3.1 Experimental design for the study removal of synthetic dyes and heavy metal ions.

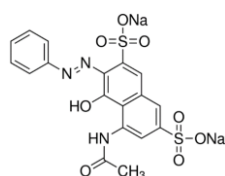
3.3 Materials and reagents

All of the chemical reagents and solvents were analytical grade (unless otherwise specified). Sodium hydroxide (NaOH) in pellet form was supplied from VWR International LLC, nitric acid 65% v/v (HNO₃) and hydrochloric acid (37% v/v) were obtained from Sigma Aldrich LLC. Synthetic dyes studied were Direct Red80 (DR80, dye content 25%), Acid Red 1 (AR1, dye content 60%), Acid Orange 8 (AO8, dye content 65%), Acid Yellow 17 (AY17, dye content 60%), Acid Blue25 (AB25, dye content 45%), Acid Red 37 Diammonium Salt form (AR37, dye content 70%), Reactive Blue 4 (RB4, dye content 35%), Reactive Blue 19 (RB19, dye content 50%), Reactive Yellow 25 and Palatine Chrome Black 6BN (PCB 6BN) were supplied from Sigma Aldrich LLC. The heavy metal salts including potassium dichromate (99.5%), copper (II) nitrate trihydrate (99%), nickel (II) nitrate hexahydrate, (99%), lead (II) nitrate (99%+), and the metal ion standards all of 1000±4 ppm for chromium, copper, lead and nickel in nitric acid were supplied from Fisher Scientific and Acros Organics. Chitosan (practical grade from shrimp shells, ≥75% deacetylation degree) was supplied from Sigma Aldrich LLC. Sodium alginate (derived from *Laminaria hyperborean*, maximum impurity 15%) was supplied from UniChem Co. Glutaraldehyde (50% w/v), sodium triphosphate pentabasic (≥98%) were supplied from Sigma Aldrich LLC. and calcium chloride (≥96%) were obtained from UniChem Co. The solvents used throughout the study included acetone, ethanol, methanol and deionised (DI) water were obtained from VWR International LLC. The culture media, including de Man, Rogosa and Sharpe (MRS) broth and agar, yeast mold (YM) broth and agar and nutrient broth and agar, were supplied by BD Co.; and D(+) glucose, sucrose, and D(-) fructose were supplied by Sigma-Aldrich LLC. The microorganism cultures (ATCC 393 *Lactobacillus casei* (*L. casei*), ATCC

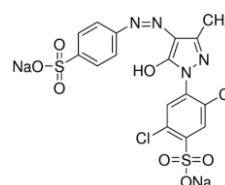
11778 *Bacillus cereus* (*B. cereus*), ATCC 49128 *Pseudomonas putida* (*P. putida*), ATCC 13048 *Enterobacter aerogenes* (*E. aerogenes*) and ATCC 14243 *Candida krusei* (*C. krusei*) were obtained from ATCC Co. All of the stock solutions and dilutions were prepared with DI water. Figure 3.2 shows the chemical structure of the synthetic dyes used in this study.



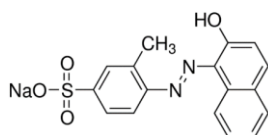
Direct Red 80



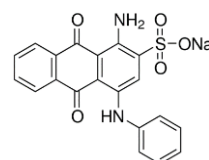
Acid Red 1



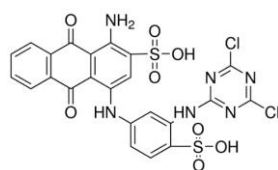
Acid Yellow 17



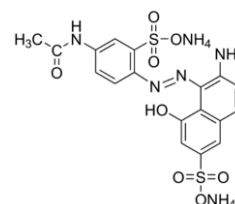
Acid Orange 8



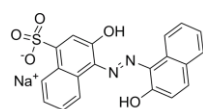
Acid Blue 25



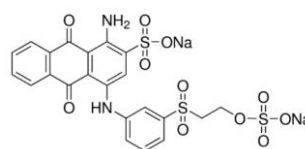
Reactive Blue 4



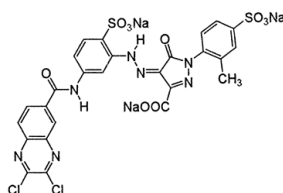
Acid Red 37 Diammonium Salt form



Palatine Chrome Black 6BN



Reactive Blue 19



Reactive Yellow 25

Figure 3.2 Chemical structures of synthetic dyes used in this study.

3.4 Instrumentation and characterisation

3.4.1 Biosorption experiment

All of the biosorption experiments and inoculations of the microorganism cultures were conducted in an OLS 200 orbital shaking water bath (Grant Instruments, shown in Figure 3.3) at 150 rpm and different temperatures. The pH values of the solutions were measured by using a Mettler Toledo MP220 pH meter.



Figure 3.3 Biosorption experiments conducted in OLS 200 orbital shaking water bath (Grant Instruments).

Purifications of the solutions were carried out through centrifugation on a Centurion Scientific K3 series centrifuge. The surface morphology of the biosorbents was observed by using a JEOL-6335F field emission scanning electron microscope (SEM). All of the samples were coated with a Pd/Au alloy for 3 minutes prior to examination by using the SEM. Zeta potential measurements were carried out by using a ZetaPlus zeta potential analyser (BrookHaven Instrument Co.) and Fourier transform infrared (FTIR) analyses of the biosorbents were obtained with a Perkin Elmer Spectrum 100 FTIR spectrometer. The metal ion concentrations were measured with a Perkin Elmer (AAAnalyst 800) atomic absorption spectrometer at particular wavelengths in accordance with the metal species. The dye concentrations were measured with a Perkin Elmer Lambda 18 UV-VIS spectrophotometer. The freeze dry process was conducted by using a FreeZone 2.5 L freeze dry system (Labconco) at 0.120 mbar and -51°C.

3.5 Culturing and inoculation of microorganisms

L. casei was cultured with MRS broth and agar, and *C. krusei* with YM broth and agar. *B. cereus*, *E. aerogenes* and *P. putida* were cultured with nutrient broth and agar. In general, after sterilisation at 121°C and 15 psi for 15-20 minutes, agar was poured into the petri dishes and allowed to cool for solidification. Streaking was done by using sterilised disposable inoculation loops of 10 µl in volume. Broth culturing was conducted by transferring a loopful culture from a prepared culture dish to a sterilised broth in a baffled-bottom flask that was 250 ml in volume. *L. casei* was cultured at 37°C for 5 days, *C. krusei* at 30°C for 24 hours and the other microorganisms at 37°C for 24 hours in accordance with standard procedures of ATCC Co.

3.6 Screening of non-encapsulated microorganisms on biodegradation of synthetic dyes

The biodegradation of synthetic dyes is one of the applications associated with microorganisms in biosorption as mentioned in Chapter 2. Therefore, prior to encapsulation, the biodegradation ability of the microorganisms in this study were tested with the use of aerobic and anaerobic biodegradation. Each type of the biodegradation screening was respectively conducted on agar and mixed with dye solutions.

3.6.1 Trials of aerobic and anaerobic biodegradation with agar

Agar was first sterilised per the procedure outlined in Section 3.5. Before the agar cooled and solidified, each dye solution was mixed with the agar in which the final concentration of each mixture was equivalent to 0.03 mM of the synthetic dyes. The mixtures were then poured into petri dishes respectively and allowed to cool and solidify. Three spots of microorganism strains with approximately 10^9 colony forming unit (CFU) ml^{-1} were streaked on the agar and inoculated at appropriate temperatures for 24 to 48 hours. In terms of the anaerobic biodegradation, the streaked agar plates were sealed tightly with parafilm to limit the amount of gaseous diffusion from outside.

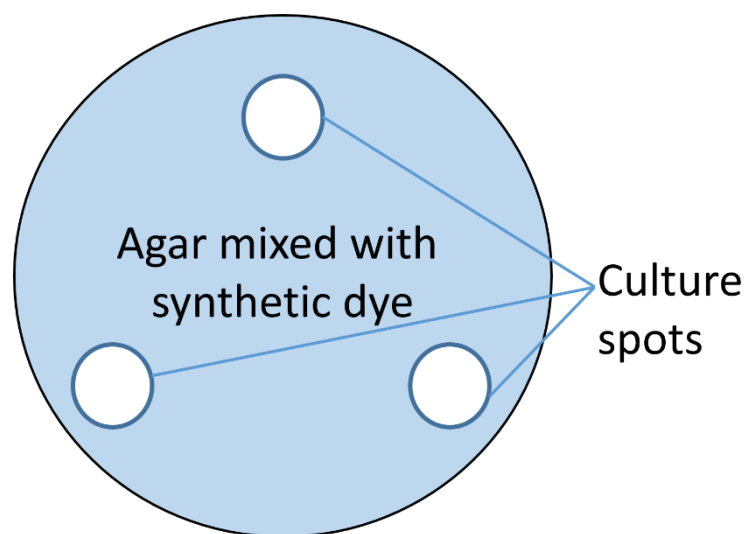


Figure 3.5 Schematic diagram of streaking of culture material onto agar plates for aerobic/ anaerobic biodegradations of synthetic dyes.

3.7 Synthesis of biosorbents

3.7.1 Chitosan hydrogel beads

Three chitosan hydrogel beads were synthesised; by coacervation (chitosan hydrogel beads: CB), chemical crosslinking (crosslinked chitosan hydrogel beads: GCB) and ionotropic crosslinking (chitosan hydrogel beads crosslinked with NaTPP: TPPCB). The chitosan used in the experiments was practical grade with a deacetylation degree of $\geq 75\%$.

3.7.1.1 Chitosan beads synthesised by coacervation

Chitosan (1.4% w/v) was prepared with 1.4% (v/v) glacial acetic acid in DI water until complete dissolution. The chitosan solution was then centrifuged at 6000 rpm for 10 min and the supernatant was gathered for use. Methanolic sodium hydroxide (NaOH; 0.5 M) was prepared by dissolving NaOH pellets in DI water and mixed with methanol at a volume ratio of 8:2. A syringe with a 25 G needle

tip was used for the coacervation process. Chitosan solution (10 mL) was injected into 50 mL of methanolic NaOH with a syringe pump that was operated at 2 ml min⁻¹. Chitosan beads immediately formed in the constantly agitated hardening alkaline medium. After stirring for 60 minutes, the chitosan beads were filtered and thoroughly washed with distilled water.

3.7.1.2 Chemically crosslinked chitosan beads

Crosslinked chitosan hydrogel beads were synthesised by mixing CB with a glutaraldehyde solution (0.5% w/v) at room temperature for 15 minutes. The crosslinked chitosan beads were filtered and thoroughly washed with distilled water.

3.7.1.3 Ionotropically crosslinked chitosan beads

Chitosan (1.5% w/v) was prepared with 1.5% (v/v) glacial acetic acid in DI water until complete dissolution. The solution was then centrifuged at 6000 rpm for 10 minutes and the supernatant was gathered for use. A sodium tripolyphosphate (NaTPP; 2% (w/v)) solution was prepared with DI water followed by pH adjustment with nitric acid (HNO₃) to a pH of 6-7. The chitosan solution was transferred into a syringe equipped with a 25 G needle tip, and subsequently added drop wise at 10 ml each time into 50 ml of the NaTPP solution with a tip-solution surface distance of approximately 4 cm. TPPCB immediately formed after contact with the NaTPP bath. The beads were post-hardened for 60 minutes and then filtered and rinsed thoroughly with DI water.

3.7.2 Alginate hydrogel beads

Sodium alginate derived from *Laminaria hyperborean* was used for the synthesis of the alginate hydrogel beads. The sodium alginate solution (3.6% (w/v)) was prepared by dissolving sodium alginate in DI water overnight. After complete dissolution, the solution was centrifuged at 6000 rpm for 10 minutes and the supernatant was gathered for bead generation. The alginate solution was diluted to 1.8% w/v and then transferred into a syringe equipped with a 25 G needle tip, and subsequently added drop wise into a 50 mM calcium chloride (CaCl₂) solution. The ratio of alginate solution to CaCl₂ solution was 1:20 ml. Alginate beads (CaAlg) immediately formed after contact with the CaCl₂ in a hardening bath. The beads were post-hardened for 60 minutes and then filtered and rinsed thoroughly with DI water.

3.7.3 Encapsulation of microorganisms

To encapsulate the *L. casei*, the harvested culture was first freeze dried for 24 hours at 0.120 mbar and -51°C and stored at 4°C until encapsulation. The freeze-dried *L. casei* was first rehydrated in the MRS broth and then mixed with the chitosan solution at a volume ratio of 1:9. The final concentration was maintained as 1.5% (w/v) chitosan in 1.5% (v/v) glacial acetic acid with 0.2% (w/v) *L. casei*. The mixture was then dripped into the methanolic NaOH (MCB) and NaTPP solution as discussed in Sections 3.7.1.1 and 3.7.1.3 respectively. The TPPCB with the encapsulated *L. casei* was subsequently freeze dried in the same conditions mentioned above for biosorption use (MTPPCB).

C. krusei was cultured in YM broth for 24 hours. The harvested culture was then directly mixed with the sodium alginate solution as outlined in Section 3.7.2 at a

volume ratio of 1:1. The final alginate concentration was maintained at 1.8% w/v. The mixture was then dripped into the CaCl₂ solution and subsequently hardened for 60 minutes (MCAAlg).

3.8 Characterisation of biosorbents

3.8.1 Fourier Transform Infrared Spectroscopy

All of the samples were dried overnight in a desiccator prior to FTIR analyses, which were carried out by using a Perkin-Elmer Spectrum 100 FTIR spectrometer. The dried and pressed pellets were fabricated by grinding different samples with FTIR grade KBr by using an agate mortar.

3.8.2 Zeta Potential Measurement

All of the samples were dried (equivalent to 100 mg of dried mass), grounded and mixed with 100 mL of DI water. The mixtures were then stirred at 1000 rpm with a magnetic stirrer for 24 hours. The suspensions were subjected to Zeta potential measurements with a ZetaPlus Zeta potential analyser (BrookHarven Instrument Co.). Before the measurement, the suspensions were withdrawn into different vials and the pre-assigned pH values were adjusted by using various concentrations of HNO₃ and NaOH solutions respectively without the addition of background electrolytes.

3.8.3 Viability of microorganisms

After the preparation of the biosorbents, 20 mg of each sample was weighed, grinded and rehydrated in the MRS broth solution. A series of dilution of each mixture was conducted and then transferred onto an MRS agar plate for 5 days of inoculation at a temperature of 37°C. The viability of the encapsulated *L. casei* is expressed as the CFU/g of the MTB and the encapsulated amount is expressed as the mg *L. casei*/g MTB which is measured by mass balance.

3.8.4 Surface morphology

The biosorbents were air dried overnight before the surface morphology analysis. Cross sections of the samples were cut with a surgery cutter to observe the internal morphologies. The samples were fixed onto an aluminium stub and then coated with a thin layer of Pd/Au alloy for 3 minutes by using a sputter coater. Afterward, the samples were analysed with a JOEL-6335F SEM and an acceleration voltage of 5.0 kV and current of 12.0 μ A.

3.9 Batch Biosorption Experiments

Batch biosorption experiments were conducted to study the effects of different parameters, such as the temperature and pH, and also used to evaluate the removal performance of the synthesised biosorbents and microorganisms adopted. Kinetics and isotherm experiments were carried out and the experimental data were fitted into related models.

3.9.1 Removal of synthetic dyes/ heavy metal ions

Pre-assigned amounts of biosorbents (CB, GCB, MCB, TPPCB, MTPPCB, CaAlg, MCaAlg, *L. casei*, *C. krusei*) were mixed with adsorbates (synthetic

dyes/ heavy metal ions) of pre-determined concentrations in 100 ml borosilicate glass bottles equipped with a blue screw cap. The bottles with the mixtures were transferred to the OLS 200 orbital shaking water bath and then shook at 150 rpm and various temperatures. At predetermined time intervals, the aliquots were withdrawn and purified by centrifugation at 14,000 rpm for 2 minutes. The supernatants were further diluted to appropriate concentrations for spectroscopic analyses. The synthetic dyes concentrations were analysed by using a Perkin-Elmer Lambda 18 UV-VIS spectrometer and heavy metal ions by using a Perkin-Elmer AAnalyst 800 atomic absorption spectrometer. All of the dilutions were conducted with DI water. For heavy metal measurements, standard metal ion solutions were diluted accordingly for calibration and all of the measurements were conducted in triplicate. For the dye measurements, calibration of the dye solutions was carried out by dissolving analytical grade dye powders followed by subsequent dilutions. All of the measurements were carried in triplicate.

3.9.2 pH effects

The experiments on the effects of pH on dye removal were carried out at 37°C and that of heavy metal ion removal at 30°C. All of the pH values were adjusted and maintained with various concentrations of HNO₃ and NaOH throughout the biosorption process.

pH values of 2, 3.4, 4.6 and 5.5 were used to evaluate the biosorption that used CB, GCB and MCB. Three grams of biosorbents were weighed and mixed with 50 ml of 100 mg L⁻¹ (ppm) of DR80, RY25 and AB25 and the dye concentrations were recorded at the equilibrium stage. With TPPCB and MTPPCB, 0.1 g of

biosorbents were weighed and mixed with 50 ml of 0.15 mM Reactive blue 19. In the heavy metal ion removal experiments, CaAlg and MCaAlg were used as the biosorbents. Then, 20 ml of a 1.5 mM copper (II) solution was mixed with 2 ml of biosorbents at pH values of 1.2, 2.0, 3.1, 4.1, and 5.2. At the equilibrium stage of the biosorptions, aliquots were withdrawn followed by suitable dilutions and spectroscopic analysis as outlined in Section 3.8.1. For biosorptions with non-encapsulated microorganisms (0.1g L^{-1}), centrifugal purifications were carried out prior to the dilutions and spectroscopic analyses.

3.9.3 Temperature effects

The experiments on the effects of temperature were carried out at pre-determined temperatures in the orbital shaking water bath in which the temperatures were kept constant throughout the biosorption equilibrium. For biosorption with CB, GCB, and MCB, temperatures of 25°C , 37°C and 50°C were used with 50 ml of 100 mg L^{-1} DR80, RY25 and AB25 at pH 3.4. Biosorption with CaAlg, MCaAlg and *C. krusei* were studied at 30°C , 40°C and 50°C with 20 ml of 1.5 mM copper (II) at pH 5.2. The experimental process and spectroscopic measurements were carried out as outlined in Section 3.8.1.

3.9.4 Biosorption kinetics

Kinetics experiments on synthetic dye removal were performed by (1) transferring 3 g of CB to 50 ml of 100 mg L^{-1} DR80, RY25 and AB25. The mixture was shaken for 5 hours at pHs of 3.4, 4.6 and 5.5 in the orbital shaking water bath at 37°C ; (2) 0.1 g of TPPCB and MTPPCB were transferred to 50 ml of 1.5 mM RB19 at 37°C at pH 3 for 24 hours; (3) 2 ml CaAlg, 2 ml MCaAlg and 0.1g L^{-1} cultured *C. krusei* were transferred to 20 ml of a 0.05 mM copper (II)

solution at a temperature of 30°C and pH of 5.2 for 24 hours. At regular time intervals, the concentrations of the dye and heavy metal ions were measured and the adsorbed amount of dyes, q_t (mg g⁻¹ or mmol g⁻¹) at time t (min) were calculated as follows:

$$q_t = \frac{C_0 - C_t}{M} \times V \quad (1)$$

where C_0 is the initial concentration of the dye and heavy metal solutions in mg g⁻¹ or mmol g⁻¹ and C_t is the concentration of the dye and heavy metal solutions at a pre-determined time interval, M is the mass of the adsorbent and V is the volume of the dye and heavy metal solutions. The experimental data were fitted into pseudo first order kinetics, pseudo second order kinetics and intraparticle diffusion models. GraphPad Prism 6.0 was used to simulate the experimental data with linear regression analysis.

3.9.5 Biosorption isotherms

Isotherm studies on the removal of DR80, RY25 and AB25 with CB was determined by mixing 3 grams of CB with 50 mL of the dye solution at different initial concentrations (0-200 mg L⁻¹). The mixture was shaken for 24 hours at pH 5.5 for all three dyes in the orbital shaking water bath at 37°C. A copper (II) solution of 20 ml in the range of 0.05 mM to 1.5 mM at 30°C and pH of 5.2 as mixed with 2 ml CaAlg, 2 ml MCAAlg and 1 ml cultured *C. krusei* respectively for the isotherm experiments. C_e (mg g⁻¹ or mmol g⁻¹) of the dye and the metal ion solutions were measured after 24 hours of biosorption. Langmuir and Freundlich isotherms were used for the modelling of the experimental data with

linear regression analysis (GraphPad Prism 6.0).

3.10 Chapter Summary

The research methods for the removal of synthetic dyes and heavy metal ions with encapsulated microorganisms have been outlined and discussed in this chapter. After carrying out a literature review, suitable microorganisms, encapsulation materials, target synthetic dyes and metal ions are selected for study and evaluation. The screening of the microorganisms on their possibility of biodegrading synthetic dyes is carried out with aerobic and anaerobic biodegradation processes by using agar and a solution. The synthesis of hydrogel beads to encapsulate the microorganisms in this study has been reviewed and optimised. Systematic characterisation of the biosorbents, including the use of FTIR analysis, zeta potential measurement, and estimation of microorganism viability after encapsulation and surface morphology have been conducted to evaluate the biosorbents. Batch biosorption experiments on the removal of different synthetic dyes and heavy metal ions are conducted. The effects of the pH and temperature are examined. Kinetics studies and isotherm modelling are also carried out to understand the removal mechanisms of the dyes and heavy metal ions by the biosorbents.

CHAPTER 4 SYNTHESIS OF BIOSORBENTS

4.1 Introduction

In this chapter, the synthesis of biosorbents will be outlined and discussed. The synthesis of the biosorbents is done via a coacervation technique based on the encapsulation of microorganisms. The synthesis parameters and characterisation of chitosan hydrogel beads (CB), crosslinked chitosan beads (glutaraldehyde crosslinked chitosan beads (GCB)), ionotropic crosslinked chitosan hydrogel beads (tripolyphosphate-crosslinked chitosan hydrogel beads (TPPCB)), calcium alginate hydrogel beads (CaAlg), *L. casei*-encapsulated hydrogel beads (MCB, MTPPCB) and *C. casei*-encapsulated beads (MCAAlg) will be included in the discussion.

4.2 Synthesis of chitosan-based hydrogel beads

Chitosan is one of the most common biosorbents examined in previous studies on the removal of synthetic dyes and heavy metal ions because chitosan has reactive amino groups at the carbon-2 position. Chitosan is a polymer composed of *N*-glucosamine and *N*-acetylglucosamine consecutive units. The amount of *N*-glucosamine varies because it depends on the degree of deacetylation (DD%).

Figure 4.1 shows the chemical structure of chitosan.

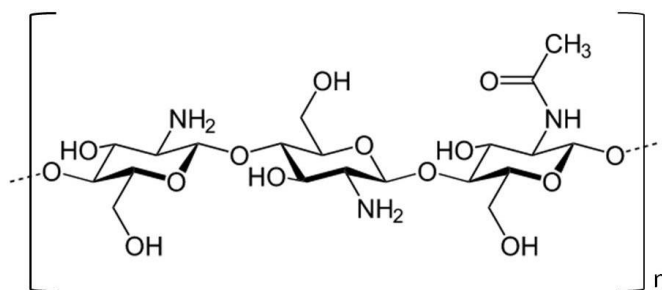


Figure 4.1 Chemical structure of chitosan.

Chitosan forms a gel when subjected to an acidic medium at $\text{pH} < 4-4.5$. This can be either a pro or con in biosorption processes. If the biosorption conditions are acidic, chitosan in the gel form cannot properly remove the target pollutants, but would work well in alkaline conditions. Therefore, the crosslinking reaction of chitosan has been studied by number of researchers in order to enhance the physical and chemical stability of chitosan. On the other hand, besides chemical crosslinking, chitosan can also be transformed into different physical states, for example, flakes, hydrogel beads, micro-particles, nano-particles, electrospun fibers, etc., which are usually further crosslinked after the transformation. In this study, two types of chitosan hydrogel beads are synthesized and evaluated: CB formed by coacervation through neutralization and coacervation through ionotropic crosslinking (thus TPPCB). CB is further crosslinked with glutaraldehyde while TPPCB is subsequently freeze-dried for the removal of synthetic dyes.

4.2.1 Chitosan hydrogel beads – coacervation through neutralization

The synthesis of CB by coacervation was successfully performed by using a methanolic sodium hydroxide solution for the hardening medium. The chitosan was first dissolved in acetic acid to form a gel, followed by dipping into a sodium hydroxide solution. The chitosan neutralized and formed into hydrogel beads after solidification as a gel in the sodium hydroxide solution. A number of factors influence the resultant bead morphology: (1) the volume ratio of methanol to sodium hydroxide; (2) concentration of chitosan solution; (3) total concentration of sodium hydroxide in the methanol alkaline bath; and (4) agitation speed of the alkaline bath. The ease of the bead formation, size, shape, etc., are all attributed to these factors. The methanol in the alkaline bath is important as methanol competes as a hydrophilic solvent to precipitate out the chitosan hence giving beads (Peniche, C. et al., 2003). The use of only a sodium hydroxide solution would provide irregular shaped and soft hydrogels. The methanol therefore controls the chitosan solution-drip to sink into the alkaline bath and thus harden the beads in all directions. A methanol-sodium hydroxide ratio of 2:8 is optimal for controlled sinking of the chitosan beads into the alkaline bath. The alkalinity of the bath is crucial since the formation of the beads is also dependent on the neutralization of acid-dissolved chitosan (Zhao, F. et al., 2007). A certain amount of alkalinity is required to successfully harden the beads but too much alkalinity will require a much longer time for rinsing after the reaction. It was found that 0.5 M of the total OH⁻ is adequate enough to synthesize the chitosan beads. Besides these two factors, the agitation speed also contributed to the shaping of the beads in the alkaline bath. A slow agitation speed provides enough time for the formation of spherical beads while a high agitation speed results in

elongation of the beads due to the hydraulic force. After the drop of chitosan solution sank into the alkaline bath, the hardening usually required 15-30 minutes until completion. Hence the agitation speed cannot be too fast so as to avoid changing the shape and size distribution of the beads. It was found that a speed of 200-400 rpm provides a good spherical shape. The chitosan concentration was also found to affect the synthesis of the beads in practice. A higher chitosan concentration provides high molarity and viscosity. The molarity affects the chitosan content of each bead granule while the viscosity affects the solution ejection speed and ease of incorporating microorganisms in later modifications. An overly low concentration of chitosan solution means that chitosan beads will not form, or hydrogels will be formed that are too physically soft to use in further experiments. A suitable concentration for the synthesis of beads is 1.5% (w/v) of chitosan solution dissolved in 1.5% (w/v) acetic acid. Figure 4.2 shows the flow diagram of the synthesis of CB.

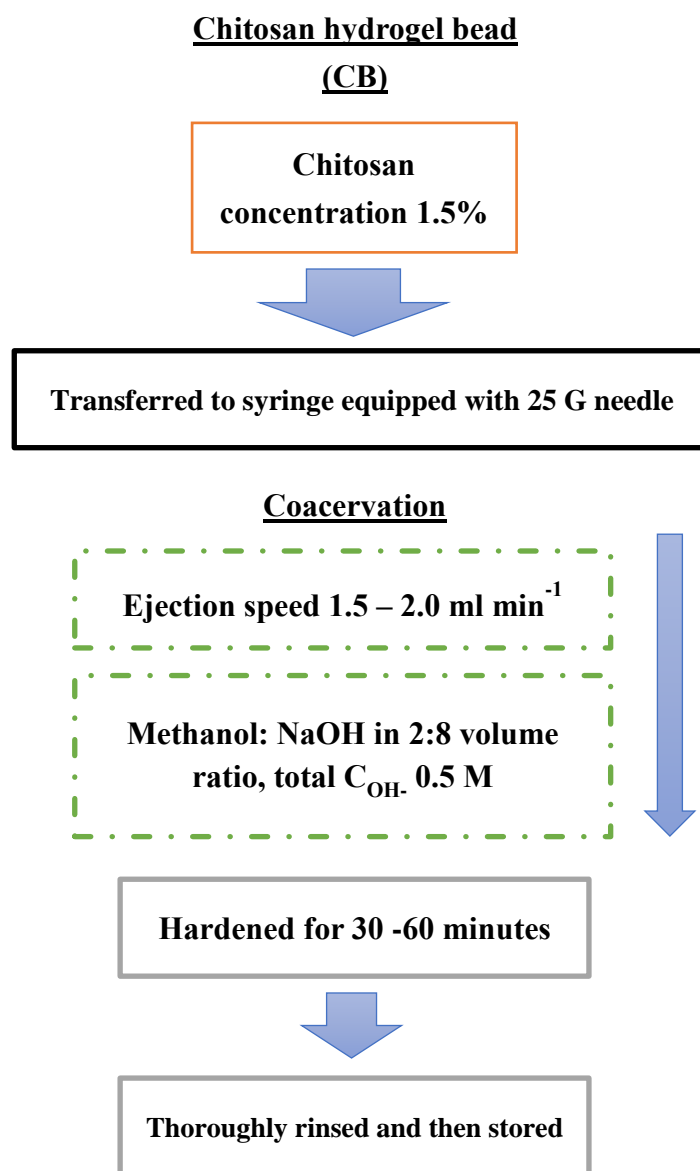


Figure 4.2 Flow diagram of synthesis of chitosan hydrogel beads (CB).

4.2.2 Crosslinked chitosan hydrogel beads

Chemical crosslinking will increase the chemical stability of chitosan beads and enhance their chemical functionality. In this study, glutaraldehyde is used as the crosslinking agent on CB.

The synthesis was simple and fast. The crosslinking reaction comprised the formation of imide bonds between the amino groups in the chitosan and the aldehyde groups in the glutaraldehyde. The reaction occurred at room temperature and 0.5% (w/v) glutaraldehyde in deionized water was mixed with the prepared CB and allowed to crosslink. In order to catalyze the reaction, the CB-glutaraldehyde mixture was first allowed to partially crosslink at 30°C for 30 minutes. Then, 100 μ l of 10 M nitric acid (HNO_3) was added to facilitate the formation of imide bonding between the amino and aldehyde groups. If acid is added at the beginning, dissolution of CB would be observed and weak hydrogels obtained. That is, the early addition of acid dissolves the CB prior to the catalytic reaction. The protonation of the carbonyl groups in the glutaraldehyde promoted nucleophilic attacks from the amino groups in the chitosan, hence speeding up the reaction. A simplified reaction scheme is shown in Figure 4.3. Thorough rinsing was required to ensure that no residue was left inside the beads.

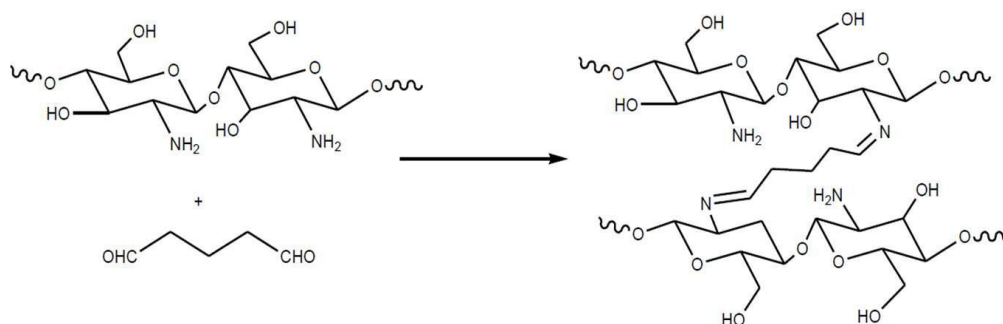


Figure 4.3 Reaction scheme of formation of imide bond - crosslinking between chitosan and glutaraldehyde.

4.2.3 Ionotropic crosslinked chitosan hydrogel beads

Although CB and GCB can be used to encapsulate microorganisms, the synthesis involves reagents which reduce the viability of the encapsulated cultures. In order to maintain the viability of the encapsulated cultures, tripolyphosphate-crosslinked chitosan hydrogel beads (TPPCB) were synthesized as an alternative to the synthesis of microorganism-embedded beads (will be discussed in Section 4.4). The formation was achieved by ionic interaction between the chitosan gel solution and polyanion sodium tripolyphosphate (NaTPP). The synthesis procedure was simpler and faster than coacervation through neutralization. Only 0.5% (w/ v) of the NaTPP solution, without the addition of alcohol, was adequate enough to form chitosan beads. The only consideration was the distance between the syringe outlet and bath surface which should have a distance of approximately 4 cm apart in order to obtain a good spherical shape for the hydrogel beads. There is another advantage to NaTPP-crosslinking, which is the flexibility of the pH conditions. pH is one of the most important factors that affect the viability of microorganisms. It was found that the NaTPP solution could harden the chitosan beads in a pH range of 6-9. This is a crucial step to increase the encapsulation efficiency if live

microorganisms are to be encapsulated, as numerous bacteria strains grow at pH 6.0-7.5. Figure 4.4 is a flow diagram of the synthesis of TPPCB and Table 4.1 summarizes the synthesis conditions of different kinds of the chitosan beads adopted in this study.

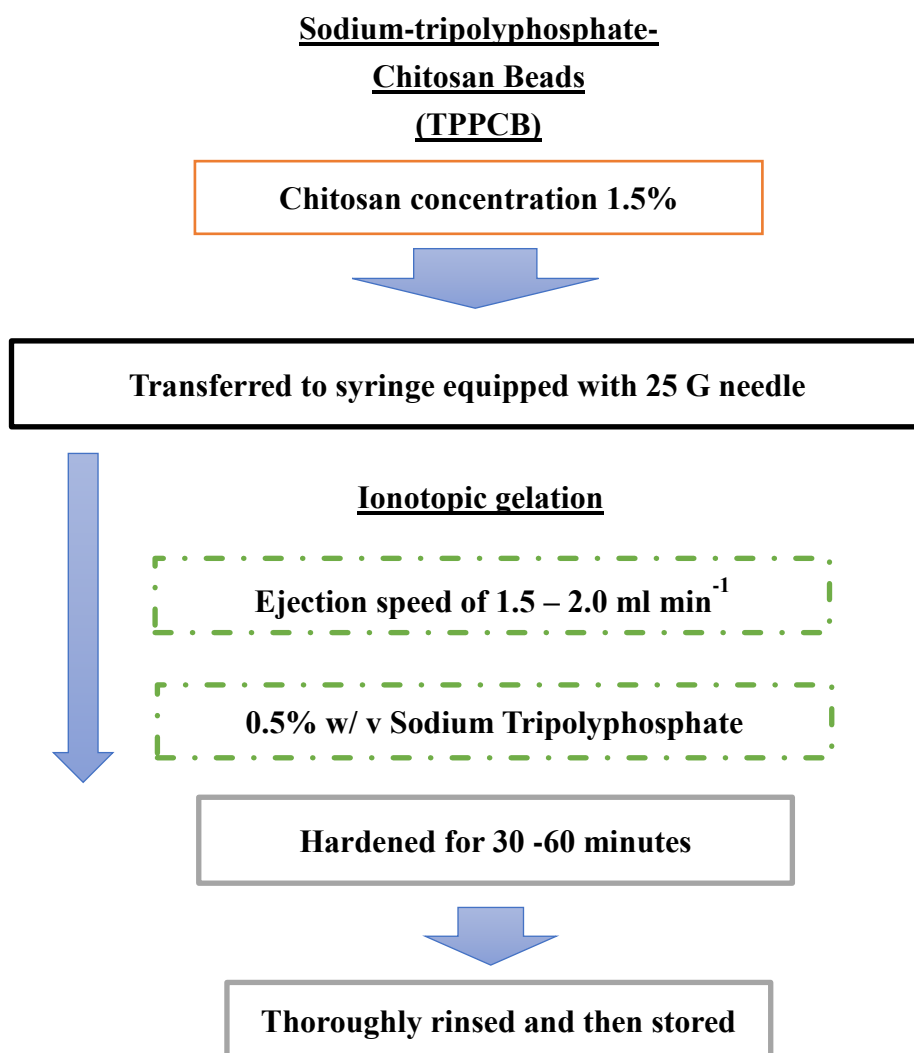


Figure 4.4 Flow diagram of synthesis of ionotopic crosslinked chitosan hydrogel beads (TPPCB).

Table 4.1 Summary of optimized synthesis conditions for different kinds of chitosan beads in this study.

	CB	GCB	TPPCB
Chitosan solution concentration	1.5%	-	1.5%
Hardening bath	0.5M – 1M NaOH	0.5% (w/v) GLA	0.5% (w/v) NaTPP
Hardening bath composition	MeT: NaOH – 2:8	-	-
Agitation speed	200 rpm (stirring)	120 rpm (shaking)	400 rpm (stirring)
Syringe outlet – bath distance	0.5 – 1.0 cm	-	3.0 – 4.0 cm

NaOH = sodium hydroxide; MeT = methanol; NaTPP = sodium tripolyphosphate; GLA = glutaraldehyde.

4.3 Synthesis of alginate-based hydrogel beads

Alginate is a polysaccharide composed of (1-4)-linked β -D-mannuronate and its C-5 epimer α -L-guluronate residues. Sodium alginate is extracted from seaweed, in which first, acid is extracted which is converted into sodium salt. Sodium salt is then extracted and diluted, thus resulting in sodium alginate, which can be applied or used in reactions to produce other types of salts. Sodium alginate can be dissolved in water without heating or pH tuning. It is well used in research work, the food industry and the pharmaceutical field. In the pharmaceutical and medicine manufacturing industry, alginate is popularly used to encapsulate microorganisms due to its high compatibility with the encapsulated cultures and good biocompatibility with various materials. In this study, sodium alginate is used as a component of the polymeric wall material for the encapsulation of

microorganisms to remove heavy metal ions. Figure 4.5 shows the structure of alginate.

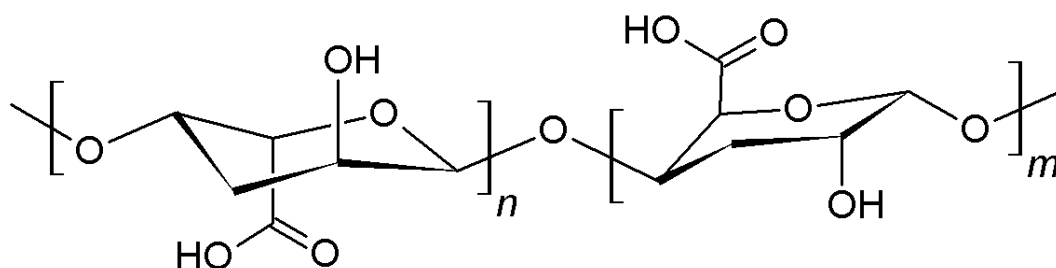


Figure 4.5 Chemical structure of alginate.

For the synthesis of the calcium alginate hydrogel beads (CaAlg), sodium alginate was first dissolved in deionized water overnight to allow for complete dissolution. After centrifugation, the supernatant was ready to use for the synthesis of the hydrogel beads. Calcium chloride (50 mM) was used as the hardening reagent. Since the sodium salt of alginate has ionic carboxylate groups, ionotropic bridging can be achieved by using divalent cations as the counter ions. The concentration of sodium alginate affects the morphology of the hydrogel beads, and therefore several concentrations were chosen and the optimized concentration was found to be 1.8% w/v. This optimal value allows the successful formation of spherical shaped CaAlg as well as good mixing of microorganisms. Moreover, like the synthesis of CB, when the sodium alginate solution was dripped into the calcium chloride bath, the distance between the solution surface and needle tip had to be around 4 cm. Less space between the two would mean failure of bead formation in which the drop of sodium alginate would remain on the solution surface but not sink and form beads. The agitation speed of the bath was optimized to 600 – 700 rpm. Figure 4.6 shows the flow

diagram of the synthesis of CaAlg.

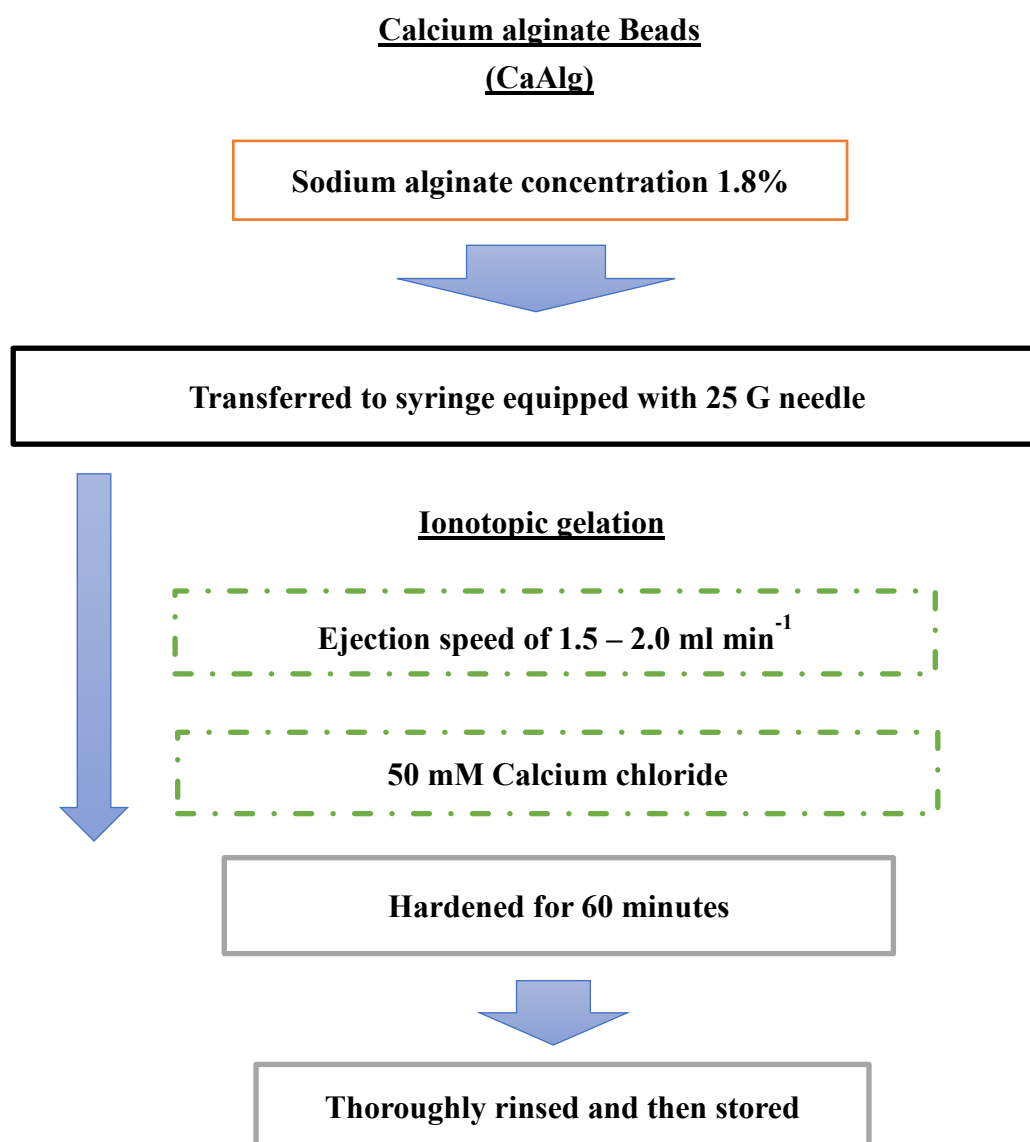


Figure 4.6 Flow diagram of the synthesis of calcium alginate hydrogel beads.

4.4 Selection and encapsulation of microorganisms

In this study, the encapsulation of microorganisms is a major modification of biosorbents to remove synthetic dyes and heavy metal ions. Several microbe cultures were selected for use after carrying out a literature review. Several criteria were adopted to determine whether the cultures are suitable for encapsulation and also the removal experiments, including whether:

- (1) the microbes are biologically non-hazardous. This allows a more reliable application of the biosorbents in water pollution control processes,
- (2) the microbes are biocompatible with the encapsulation material, and
- (3) the microbes have potential to biodegrade synthetic dyes.

4.4.1 Screening of microorganisms for removal of synthetic dyes and heavy metal ions

As mentioned in Chapter 3, the microbes were subjected to screening processes to see whether they could biodegrade synthetic dyes. *B. cereus*, *E. aerogenes*, *L. casei* and *P. putida* were subjected to aerobic and anaerobic degradation in the screening tests. After successful plate streaking, two observations were made: there was growth of the cultures and presence of clear zones around the spot of culture. The growth of the cultures indicate whether the synthetic dyes are toxic to the microorganisms at particular concentrations and the clear zones indicate biodegradation of the synthetic dyes into colorless organic compounds. If the approach was mixing cultures with dye solutions, observation of the color changes would indicate if there was biodegradation. Tables 4.2 and 4.3 summarize the results of the aerobic and anaerobic degradation in the screening

tests respectively.

Table 4.2 Summary of aerobic degradation results with agar streaking and dye solutions on *B. cereus*, *E. aerogenes*, *L. casei* and *P. putida*

	Agar streaking		Use of dye solution
	Clear zone	Culture growth	Decolorization
Synthetic dye	Clear zone	Culture growth	Decolorization
AB25	Negative	Positive	Negative
AR1	Negative	Positive	Negative
AR37	Negative	Positive	Negative
AO8	Negative	Positive	Negative
AY17	Negative	Positive	Negative
DR80	Negative	Positive	Negative
RB4	Negative	Positive	Negative
RB19	Negative	Positive	Negative
RY25	Negative	Positive	Negative
PCB 6BN	Negative	Positive	Negative

Table 4.3 Summary of anaerobic degradation results with agar streaking and dye solutions on *B. cereus*, *E. aerogenes*, *L. casei* and *P. putida*

	Agar streaking		Use of dye solution
	Clear zone	Culture growth	Decolorization
Synthetic dye			
AB25	Negative	Positive	Negative
AR1	Negative	Positive	Negative
AR37	Negative	Positive	Negative
AO8	Negative	Positive	Negative
AY17	Negative	Positive	Negative
DR80	Negative	Positive	Negative
RB4	Negative	Positive	Negative
RB19	Negative	Positive	Negative
RY25	Negative	Positive	Negative
PCB 6BN	Negative	Positive	Negative

Tables 4.2 and 4.3 show that there are no clear zones on the streaked agar plate nor decolourization in both the aerobic and anaerobic screening tests, but the cultures grew normally on the agar. This shows that the cultures have normal metabolism; however, they do not metabolize the synthetic dyes. The culture mediums used were obtained from a standard procedure. The MRS broth contained proteose peptone No.3 (carbon source), beef extract (carbon source), yeast extract (carbon source), dextrose, polysorbate 80, ammonium citrate (nitrogen source), sodium acetate, magnesium sulfate, manganese sulfate and

dipotassium phosphate while the nutrient broth contained beef extract (carbon source) and peptone (carbon source). In terms of the compositions in the broth and agar, it can be concluded that the carbon and nitrogen sources cannot facilitate the biodegradation of the synthetic dyes. On the other hand, the synthetic dyes cannot be utilized as the carbon source for metabolism to occur. Also, from the view point of the nutrient sources, the enzymatic reactions are a concern. Since the growth of the cultures was not affected by the incorporated synthetic dyes, the enzymes were supposed to be secreted by normal metabolism. Azoreductase, which can degrade azo dyes by attacking the azo bonds, is the anaerobic enzyme. In the anaerobic screening tests, an anaerobic environment was created by sealing the petri dishes for agar streaking and pumping nitrogen for the dye solutions. One of the possible reasons for negative decolourization could be attributed to the chemical structure of the synthetic dyes. The literature has suggested that the *para*-position of the sulphonyl groups to the azo bonds on the synthetic dyes are inhibitors to enzymatic reaction from azoreductase. This matches the dye substrates chosen in this study as well as the outcome. Although inhibition could be the reason, it is still worthwhile to carry out the biodegradation experiments with the use of other methods. As a result, from the screening of the biodegradation, no microorganism was found to be dominant for encapsulation. An encapsulation trial was then implemented as the next step to confirm which microorganism would work best.

In terms of selecting the microorganism for the removal of heavy metal ions, the focus was simply on the biocompatibility of the microorganism with the encapsulation material and the ability of the species to cope with the metal ion substrates since ionic metal species are not biodegradable. *Candida* sp. has been one of the species explored and shows a good removal performance of heavy metal ions. Among *Candida* sp., *C. krusei* is one of the species that has not been unexplored in the removal of heavy metal ions. Hence, it is chosen to evaluate its potential in the removal of heavy metal ions in this study.

4.4.2 Encapsulation of microorganisms

As mentioned in the previous subsections, encapsulating live culture in a polymeric matrix is the goal in this study. Although the chosen cultures showed negative biodegradation on synthetic dyes, it is still worthwhile to encapsulate live culture. If the cultures are live, other biological means can also be used aside from the suggested reactions in this study, which makes the encapsulation of live cultures more functional in practical applications.

B. cereus, *E. aerogenes*, *L. casei* and *P. putida* were encapsulated with CB for the primary trial. It was found that none of the cultures can maintain their viability after encapsulation with CB. Chitosan is well known for its antibacterial property. Therefore, it is already challenging to encapsulate bacterial strains with chitosan. Moreover, in the synthesis of CB, methanol and sodium hydroxide were used in the hardening bath. These two reagents have a negative influence on the viability of the cultures. Among the four cultures, *L. casei* has been explored in depth for applications in the food industry and pharmaceuticals, but not in

research on the environment. Since *L. casei* has yet to be explored for the removal of synthetic dyes and heavy metal ions, it is chosen as the encapsulated species in the present study. Since CB reduces the viability of *L. casei* after encapsulation, encapsulation with TPPCB was conducted instead and a positive result was obtained. Figure 4.7 shows the inoculation loop of *L. casei* on MRS agar plates at different stages.

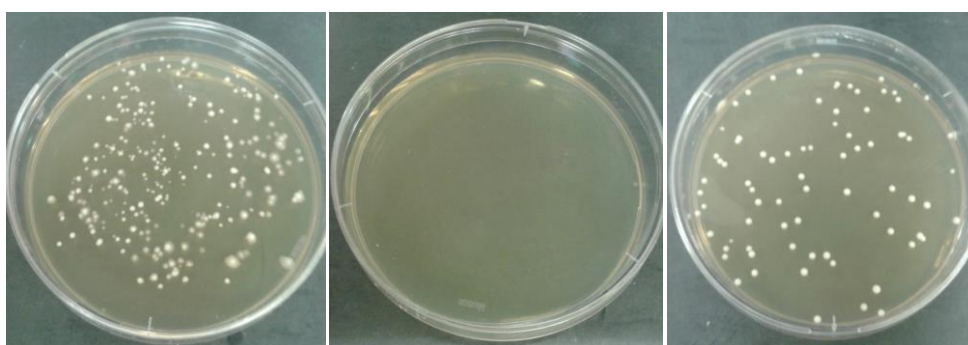


Figure 4.7 10^6 CFU ml⁻¹ inoculation loop of *L. casei* on MRS agar plates. Left: *L. casei*-chitosan solution mixture; middle: *L. casei*-encapsulated CB (MCB); right: *L. casei*-encapsulated TPPCB (MTPPCB).

It was observed from the inoculation results that *L. casei* survives when mixed with the chitosan solution but loses viability after the coacervation process. On the other hand, the less harmful ionotropic crosslinking with TPPCB showed satisfactory viability. Although *L. casei*-encapsulated CB (MCB) could not encapsulate live *L. casei*, it was subsequently evaluated for synthetic dye removal as well as in GCB. TPPCB and MTPPCB were also used to evaluate the removal of RB19. On the other hand, the encapsulation of live *C. krusei* has also been achieved with calcium alginate which was used for heavy metal removal. The removal performance will be discussed in the next chapter.

4.5 Characterisation of biosorbents

The characterisation of biosorbents is important for understanding the nature of the biosorbents and hence evaluating the removal performance. The characterisation processes of FTIR analysis, zeta potential measurement and SEM analysis will be discussed in the following sections.

4.5.1 FTIR analysis

FTIR is mainly used to analyse functional groups on substrates, which can provide information on possible changes before and after reactions and processes. Figure 4.8 shows the FTIR spectra of CB and GCB; Figure 4.9, MTPPCB and TPPCB and *L. casei*; and Figure 4.10, CaAlg, MCaAlg and *C. krusei*.

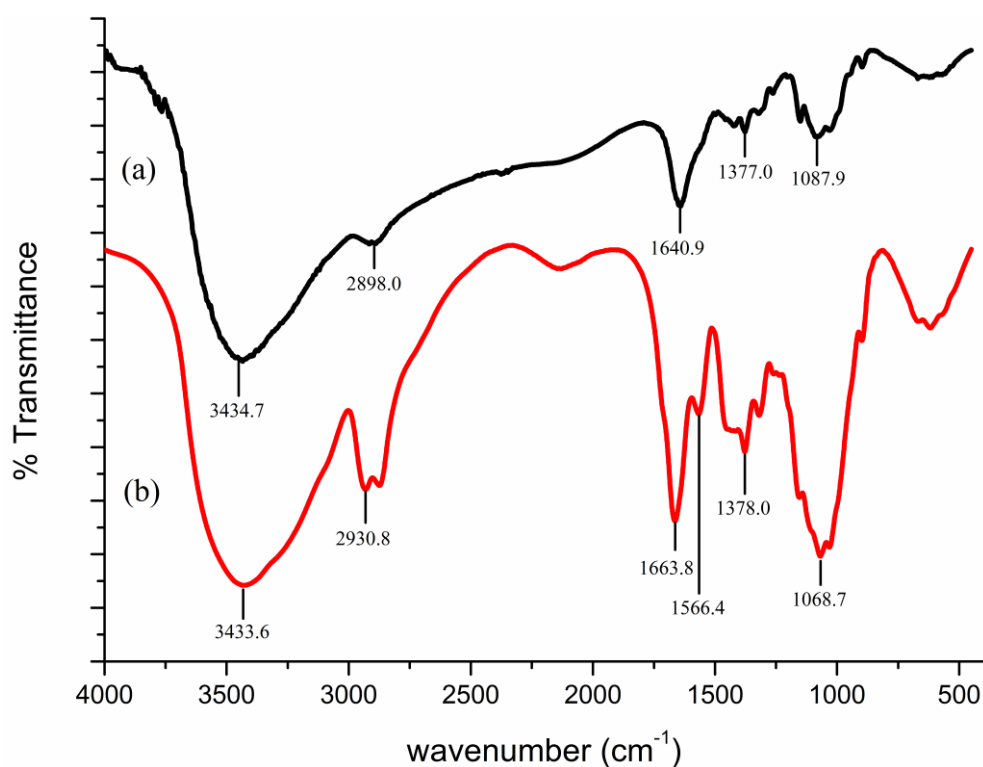


Figure 4.8 FTIR spectra of (a) CB and (b) GCB.

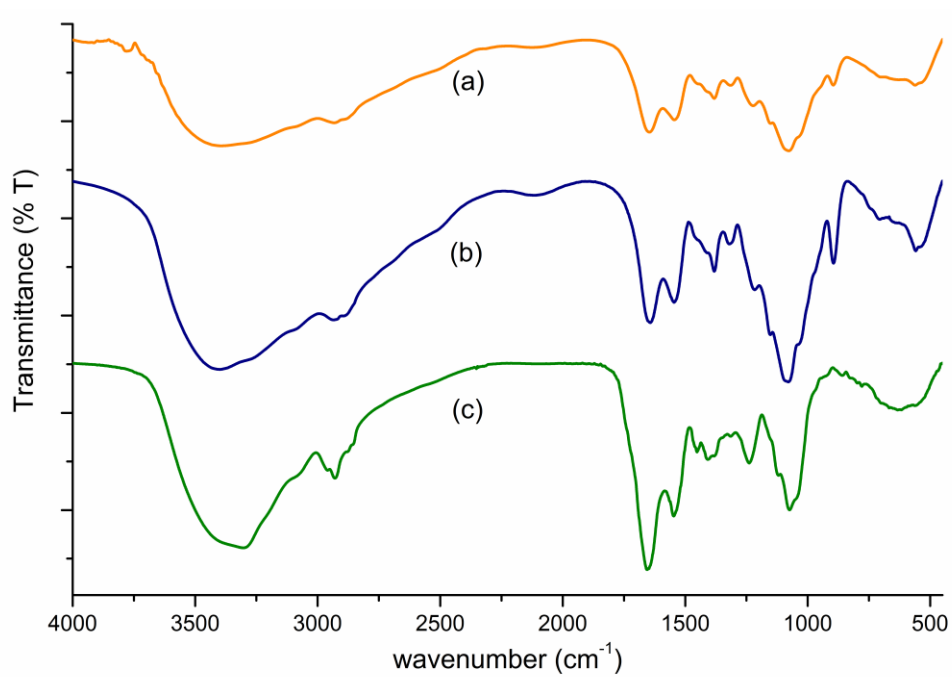


Figure 4.9 FTIR spectra of (a) MTPPCB and (b) TPPCB and (c) *L. casei*.

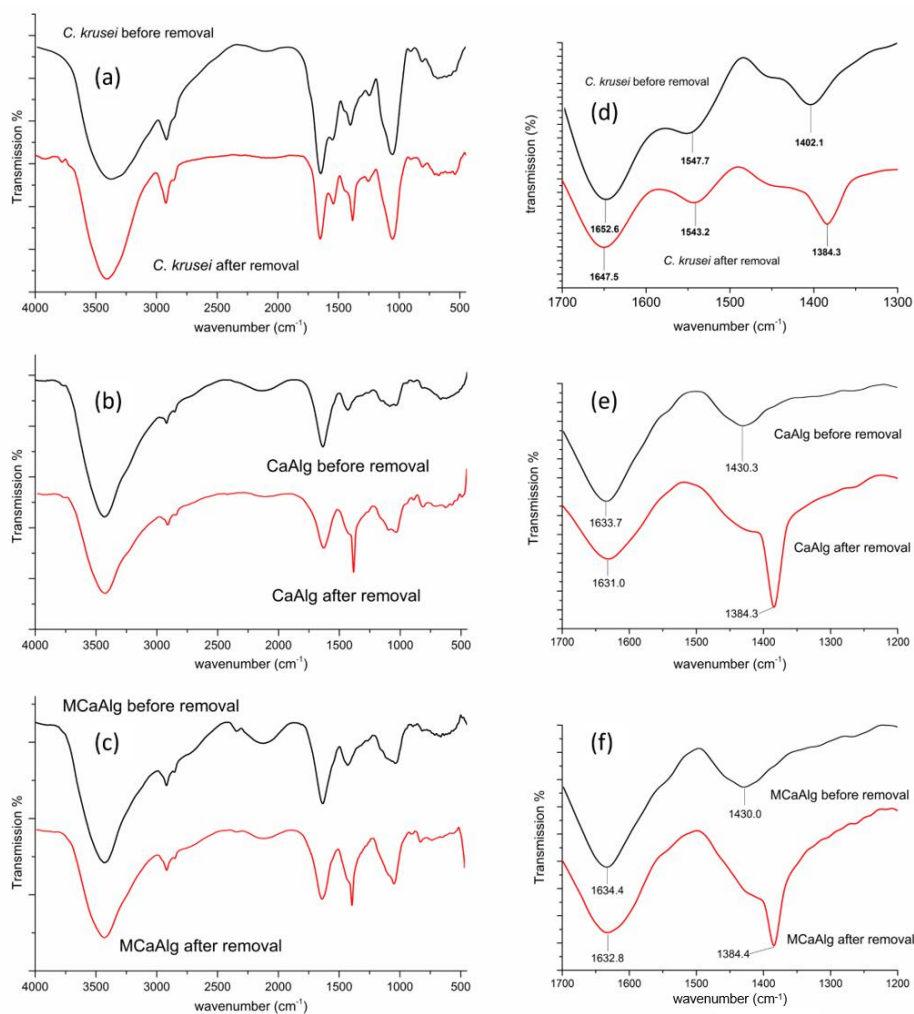


Figure 4.10 FTIR spectra of (a) *C. krusei*, (b) CaAlg and (c) MCAAlg. (d-f): spectra of the region of 1200-1700 cm^{-1} for *C. krusei*, CaAlg and MCAAlg respectively.

Figures 4.8(a) and 4.8(b) show the FTIR spectra of CB and GCB respectively. In analysing the CB, the absorption band at 1640.9 cm^{-1} is attributed to the N-H bending of the primary amine and 1087.9 cm^{-1} to C-N stretching. As for the GCB, the absorption band at 1663.8 cm^{-1} is the C=N bond stretching vibration which was formed via crosslinking with glutaraldehyde and the absorption band at 1566.4 cm^{-1} is the N-H bending of the amide which is present as a result of the incomplete deacetylation of the chitosan. Besides the corresponding

characteristic absorption peaks, other common peaks can be observed from the two spectra, including O-H stretching near 3433 cm^{-1} , C-H stretching of the sp^3 carbon near 2900 cm^{-1} , and C-O-C stretching of ether around 1377 cm^{-1} (El-Reash, Y. A. et al., 2011; Zhou, L. et al., 2010).

Figures 4.9(a), 4.9(b), and 4.9(c) show the FTIR spectra of MTPPCB, TPPCB and *L. casei* respectively. *L. casei* is a gram-positive bacterium. The cell wall has a large amount of peptidoglycan in the outer layer(Schär-Zammaretti, P. & Ubbink, J., 2003). The peptidoglycan layer contains a polymeric network of *N*-acetylglucosamine and *N*-acetylmuramic acids. On the other hand, chitosan is composed of glucosamine and *N*-acetylglucosamine. Therefore, the three spectra share common absorption bands in the presence of glucosamine and *N*-acetylglucosamine units (amido, amino, ether and alcoholic absorption bands). Both the TPPCB and MTPPCB showed the presence of N-H bending at 895 cm^{-1} while *L. casei* did not. This is due to the presence of the primary amino groups on chitosan. Another common absorption band is related to the presence of P=O, which is responsible for the phosphodiester bonds on *L. casei*(Schär-Zammaretti, P. & Ubbink, J., 2003) and NaTPP in TPPCB and MTPPCB after ionotropic crosslinking. However, it can be observed that there are two P=O absorption bands in the FTIR spectra of TPPCB and MTPPCB (overlapping with the C-O-C absorption band), and just one in that of *L. casei*. A possible reason could be the presence of different P=O planes on the NaTPP ions after the crosslinking reaction (different planes of P=O) while the phosphodiester bond only has one plane of the P=O bond(Luk, C. H. J. et al., 2015). Due to the presence of *N*-acetylmuramic acid, the spectrum of *L. casei* shows the presence

of carboxylic O-H bending while this is not found in the spectrum of TBBCB and MTPPCB.

Figures 4.10(a), 4.10(b), and 4.10(c) show the FTIR spectra of CaAlg, MCaAlg and *C. krusei* before and after metal biosorption (copper(II) removal, which will be discussed in a later chapter) respectively. The major functional groups found in the three kinds of biosorbents before copper(II) biosorption are similar, mainly alcoholic -OH (3390-3436 cm^{-1}), alkane C-H (~ 2920 cm^{-1}), salt form of carboxylate COO^- (1384 -1652 cm^{-1})(Daemi, H. & Barikani, M. , 2012) and ether C-O-C (~ 1040 cm^{-1}). The polymeric network of CaAlg is composed of covalently linked consecutive pairs of salts of alginic acid(Bahafid, W. et al., 2013c), with calcium ions as the divalent cross-linking cation. Since both CaAlg and MCaAlg are mainly composed of calcium alginate polymeric networks, they share a similar IR spectrum. On the other hand, *C. krusei* is a yeast species with a cell wall that is mainly composed of chitin (poly-*N*-acetylglucosamine) and glucan (poly-*D*-glucose)(Feldmann, H., 2012). Hence, the IR spectrum of *C. krusei* shows the presence of amino N-H (1543-1647 cm^{-1}) and carboxylate COO^- (1384-1402 cm^{-1}) absorption peaks.

Figures 4.10(d), 4.10(e) and 4.10(f) also show the FTIR spectra of the three biosorbents after copper(II) biosorption. Since significant changes occurred in the absorption of the biosorbents, it is also discussed in this section. After the biosorption of copper(II), shift of absorption band occurred in *C. krusei* and new absorption band were observed with CaAlg and MCaAlg. The carboxylate COO^- of *C. krusei* shifted from 1402.1 cm^{-1} to 1384.3 cm^{-1} ; new asymmetric and

symmetric COO^- absorption band of CaAlg and MAcAlg appeared around 1384.3 cm^{-1} respectively. Before the biosorption of copper(II), the alginate polymeric network was bridged in the presence of the calcium divalent cations and the asymmetric and symmetric COO^- absorbed the IR at around 1430 cm^{-1} . After the biosorption of copper(II), the absorption peak at 1384 cm^{-1} showed up. This means the counter ions among the polymeric matrix had changed, and it was most likely attributed to the participation of copper(II) ions. On the other hand, the asymmetric and symmetric COO^- absorption of *C. krusei* shifted from 1402.1 cm^{-1} to 1384.3 cm^{-1} , which means the major biosorption sites for copper(II) removal is the carboxylate COO^- group on the cell wall.

4.5.2 Zeta Potential Measurement

Zeta potential measurement is another important means of characterizing biosorbents in terms of the surface charge. Hence, further evaluation of the biosorption performance is warranted. In this section, the zeta potential of CB, GCB, TPPCB, MTTPCB and *L. casei* will be outlined and discussed. Figure 4.11 shows the zeta potential plot of CB and GCB and Figure 4.12 shows the zeta potential plot of TPPCB, MTTPCB and *L. casei*.

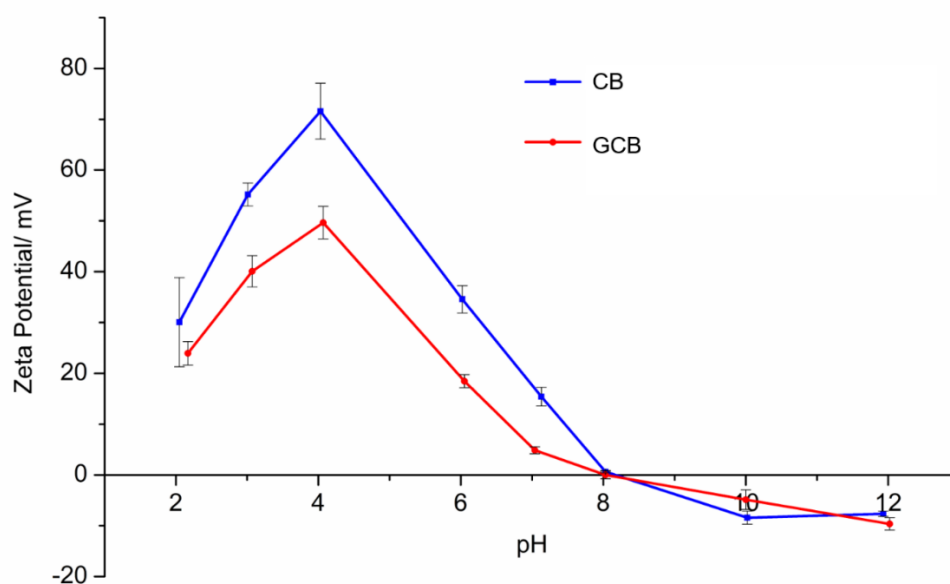


Figure 4.11 Zeta potential plot of CB and GCB as a function of pH.

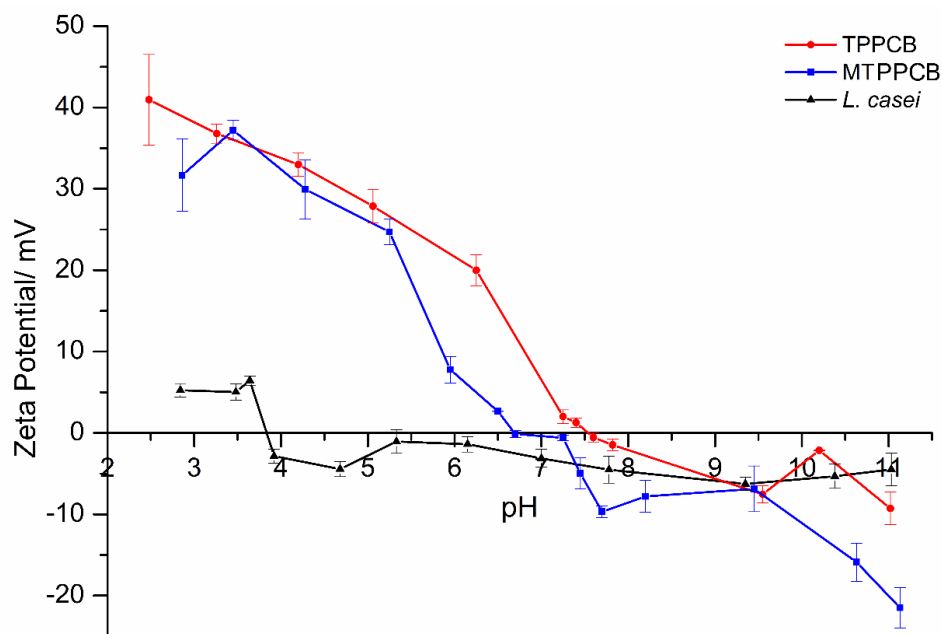


Figure 4.12 Zeta potential plot of TPPCB, MTPPCB and *L. casei* as a function of pH.

Chitosan has numerous -NH_2 and -OH groups which contribute to different surface charges upon interaction with protons and hydroxides in acidic and alkaline mediums. Figure 4.10 shows the zeta potential of CB and GCB with a pH 2-12. The overall zeta potential of both biosorbents is positive in an acidic medium and negative in an alkaline medium or a pH of 8 and more. The isoelectric point was reached at around pH 8 for both beads, where the surface charge of the beads was neutral. The zeta potential of CB before the isoelectric point is more positive than that of GCB. This could be attributed to the protonation of the amino group (R-NH_2) on chitosan into the corresponding protonated form (R-NH_3^+). The availability of the primary amino groups on chitosan is reduced after crosslinking with glutaraldehyde which were converted to imide (R-C=N). Therefore, the zeta potential of CB is relatively more positive due to increased protonation of CB. This is also true vice versa; the negative zeta

potential of CB and GCB obtained beyond the isoelectric points is possibly due to the surface interaction with OH⁻ ions.

Figure 4.12 shows the zeta potential of TPPCB, MTPPCB and *L. casei* respectively. The three demonstrate a similar trend with more positive zeta potential at low pH and less positive or negative value at high pH, similar to the results of CB and GCB. The isoelectric point of TPPCB is around 7.5 while MTPPCB has an isoelectric point of 6.8, and *L. casei* has an isoelectric point near pH 3.8. The low isoelectric point and negative zeta potential of *L. casei* imply that the microbial cells have numerous negatively-charged functional groups on the cell wall, hence the net surface charge is neutral around pH 3.8 and becomes net negative when the pH is increased. Moreover, the zeta potential of MTPPCB is overall less positive than that of TPPCB. Since MTPPCB is a combination of *L. casei* and TPPCB, the overall zeta potential is therefore less positive.

4.5.3 Scanning Electron Microscopy Analysis

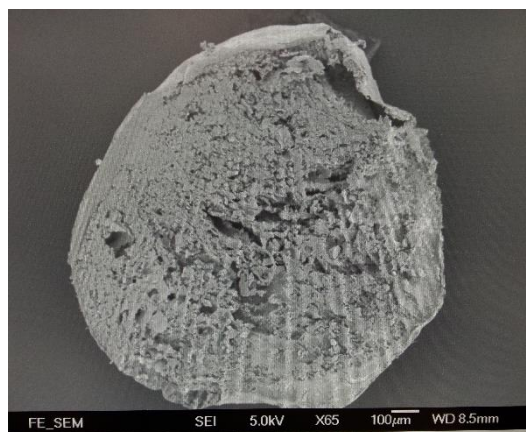
Since live *L. casei* was successfully encapsulated in MTPPCB, SEM images of TPPCB and MTPPCB were taken to observe the internal structure of the hydrogel beads.

Figure 4.12 shows the different SEM images of TPPCB and MTPPCB. Since the hydrogel was freeze-dried for proper analysis, the hydrogel beads have shrunk. Figures 4.13(a) and 4.13(b) shows smooth surface of TPPCB and the inner structure of TPPCB was constructed with layers of chitosan with relatively lower

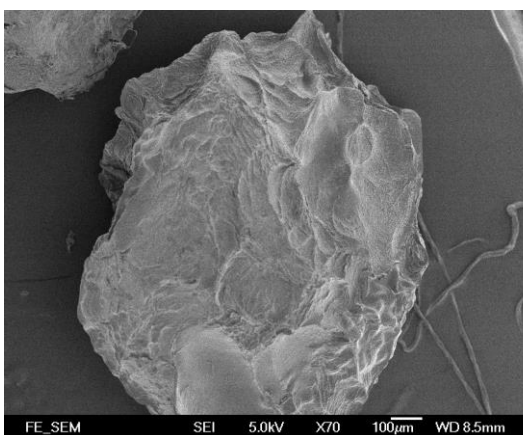
porosity compared to MTPPCB. On the other hand, it was observed from Figures 4.13(c) and 4.13(d) that the surface of the MTPPCB is smooth and the inner structure is porous, with a large space found at the center which is characteristic of the coacervation technique. Figures 4.13(e), 4.13(f), 4.13(g) and 4.13(h) are the inner surfaces and space of MTPPCB. Smooth layers and aggregates of *L. casei* are found. Since the hydrogel beads were freeze-dried, the aggregation of the culture might be due to the vacuum drying process. Otherwise, the strains would be evenly distributed within the polymeric matrix when the beads are in the original swollen state.



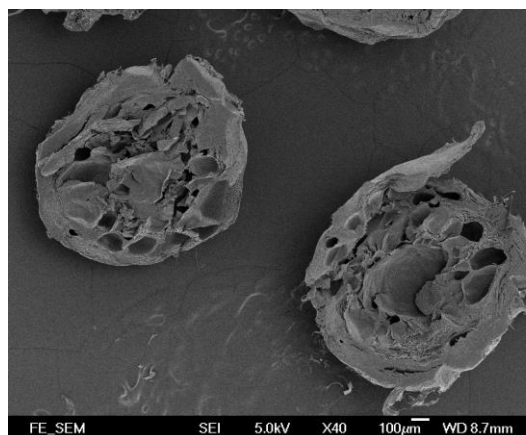
(a)



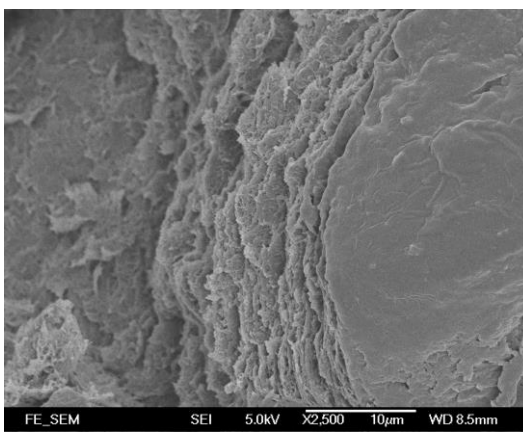
(b)



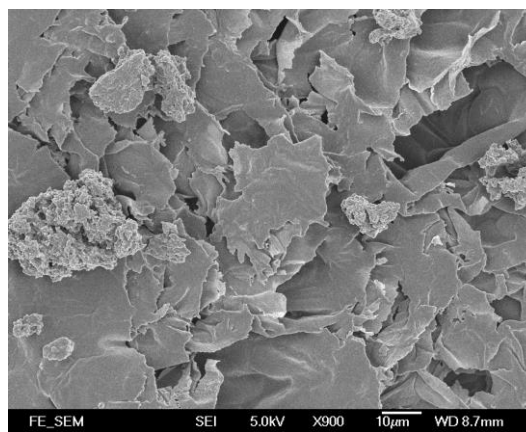
(c)



(d)



(e)



(f)

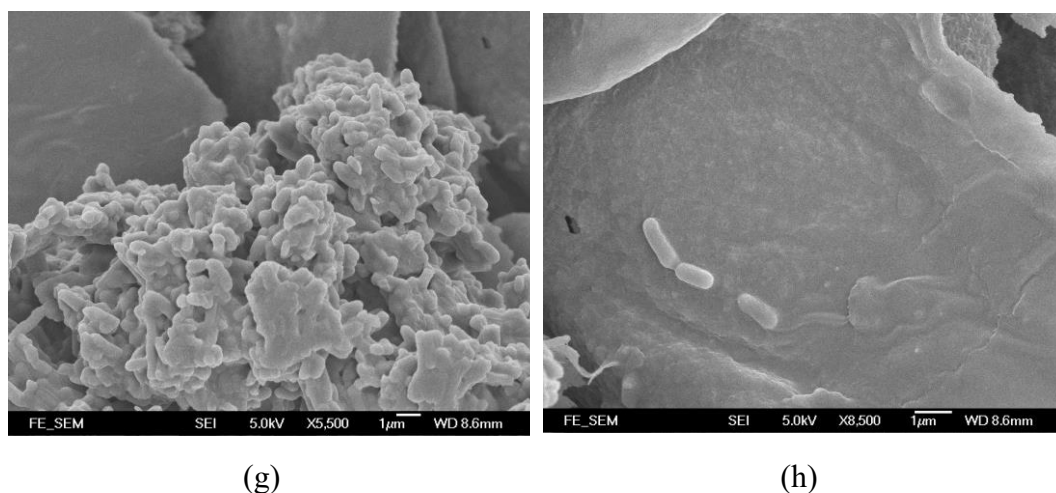


Figure 4.13 SEM images of: (a) and (b) TPPCB; (c) to (h) MTPPCB.

4.6 Chapter Summary

In this chapter, the synthesis and characterisation of the biosorbents have been outlined and discussed. Coacervation through neutralization was used to synthesize CB and GCB from methanolic sodium hydroxide. TPPCB and MTPPCB were synthesized via coacervation with ionotropic crosslinking, and CaAlg and MCaAlg were synthesized via coacervation with divalent cation crosslinking. Spherical hydrogel beads were synthesized by optimizing the concentration of the polymer concentration and hardening bath as well as the distance between the needle tip and solution surface during dripping of the polymeric process.

After optimizing the synthesis of the biosorbents, different cultures were screened by using aerobic and anaerobic approaches to determine the biodegradation performance of the synthetic dyes as well as the toxicity tolerance at particular dye concentrations. With normal metabolism and growth, none of the selected strains could biodegrade the synthetic dyes with their respective

cultured nutrient mediums. As a result, *L. casei*, which was biocompatible with chitosan, was chosen as the encapsulation strain for CB. On the other hand, *C. krusei*, which is a *Candida* sp., has not yet been extensively studied and therefore chosen for encapsulation in alginate hydrogel beads for the removal of heavy metal ions, owing to the satisfactory performance of *Candida* sp. in metal ion removal. Live strains could also be encapsulated in MTPPCB and MCaAlg in that the synthesis method did not exert negative impacts on the viability of the strains.

FTIR, zeta potential measurements and SEM analyses were conducted to characterize the biosorbents. The different characteristics of the functional groups of the biosorbents were analyzed and discussed. The zeta potential of the different biosorbents were measured in that the surface charge distribution of the biosorbent was examined. The SEM images revealed the morphology of MTPPCB and the encapsulated *L. casei* was also clearly imaged thus showing evidence of successful encapsulation.

Chapter 5 BIOSORPTION OF SYNTHETIC DYES

5.1 Introduction

In this chapter, the biosorption of synthetic dyes with the microorganisms and synthesized biosorbents of interest will be reported and discussed. The removal of synthetic dyes by using chitosan hydrogel beads will be evaluated. The effects of the pH and temperature, and mechanistic studies with kinetics and isotherm modelling are included in the discussion.

5.2 Biosorption of synthetic dyes: chitosan-based biosorbents

In this section, the biosorption of different synthetic dyes by using chitosan hydrogel beads will be outlined and discussed. The biosorption of DR80, RY25 and AB25 dyes was carried out with CB and GCB while that of the RB19 dye was conducted with TPPCB and MTPPCB.

5.2.1 Removal of DR80, RY25 and AB25 dyes: chitosan hydrogel beads

DR80, RY25 and AB25 dyes are commonly used in the dyeing industry. These three dyes are therefore applied to examine the biosorption performance of CB and GCB with the optimization of different parameters as well as for mechanistic evaluations. Moreover, *L. casei*, which is a lactic acid bacterium, is well known as a “good bacterium” for human beings (Vodnar, D. C. et al., 2010). Besides applications in the food and pharmaceutical industries, the potential of *L. casei* in removing synthetic dyes is worth exploring. Therefore, the effects of encapsulating *L. casei* for biosorption are also discussed in this section.

5.2.1.1 Effect of pH

Figure 5.1 shows the effect of the pH on the biosorption of the three types of synthetic dyes. 50 ml of 100 mg L⁻¹ dye solutions were used and the biosorptions were conducted at 37°C with 3.0 g of biosorbents. pHs of 2, 3.4, 4.6 and 5.5 are examined. The highest removal efficiency for all three dyes is observed at pH 2 which accords with the results found in Chiou et al.(Chiou, M. S. et al., 2004), who investigated the adsorption of Reactive Red 189 with crosslinked chitosan beads, and Kyzas and Lazaridis(Kyzas, G. Z. & Lazaridis, N. K., 2009) who performed removed Remazol Yellow Gelb 3RS by using chitosan derivatives. The high removal percentage of the three anionic dyes could be attributed to the electrostatic interaction between the protonated amino groups of the chitosan beads and the sulphonyl conjugate groups on the dye molecules. These interactions are consistent with the zeta potential measurements. In an acidic environment, the beads have a highly positive surface charge. This allows for strong interactions between the chitosan beads and the dye molecules. The biosorption of the DR80 dye at all pH levels resulted in a dye removal of more than 90%. This could be explained by the multiple functional groups and large molecular structure of the dye molecules which resulted in the facilitation of strong attraction with the chitosan beads even when the number of protonated amino groups available decreased with increased pH. However, there was a significant reduction in the percentage of decolourisation of the AB25 and RY25 dyes when the pH was increased from 2, which could be due to the chemical structure of the dye molecules. A relatively higher removal efficiency was demonstrated with the chitosan beads on the AB25 dye in comparison to the RY25 dye. The number of SO₃⁻ functional groups found in both dyes was the

same. The RY25 dye has a comparatively bulkier structure than the AB25 dye. Accordingly, the biosorption of RY25 molecules into the bulk solution might be prevented by the already-adsorbed-RY25 molecules on the chitosan bead surface. This resulted in a lower percentage of adsorption of the RY25 dye. Although the AB25 molecules have a ramified structure which prevents them from removal by diffusion, the less bulky structure of the dye molecules could reduce the steric hindrance of subsequent dye molecule adsorption. As a result, the AB25 dye showed a higher percentage of decolorisation than the RY25 dye at pHs higher than 2.

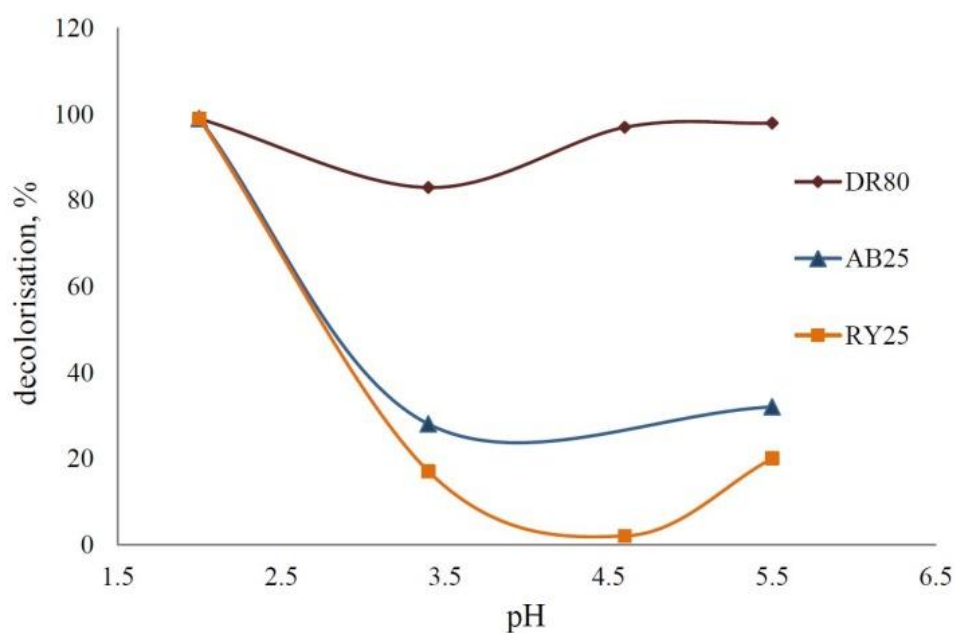


Figure 5.1 Effect of pH on removal of DR80, AB25 and RY25(Luk, C. H. J. et al., 2014).

5.2.1.2 Effect of Temperature

Figures 5.2(a), 5.2 (b) and 5.2(c) show the effect of temperature on the biosorption of the DR80, AB25 and RY25 dyes, respectively. All three biosorptions were conducted with 50ml of 100 mg L⁻¹ dye solutions and 3.0 g of biosorbents at pH 5.5. After 300 min, the highest amount of removal was realized with the DR80 dye at any temperature in comparison to the removal of the AB25 and RY25 dyes. This is consistent with the results on the effects of pH in that the DR80 dye could be basically biosorbed with high efficiency owing to its chemical structure. The initial biosorption rate of the DR80 dye at 50°C is the highest among the three different temperatures. The equilibrium adsorption amounts were about 86% for all three temperatures. A similar trend is observed in a study on DR80 dye by Saleem et al (Saleem, M. et al., 2007). The increase in the dye biosorption rate with respect to temperature indicates that the biosorption of the DR80 dye is an endothermic process. According to Mazengarb and Roberts (Mazengarb, S. & Roberts, G. A., 2009), direct dyes can diffuse into chitosan films during the adsorption process due to the amorphous nature of the chitosan films and the diffusion coefficient of the dyes which decreases with temperature. This can therefore explain for the higher removal percentage of the DR80 dye with increased diffusion rate into the enlarged chitosan pores at higher temperatures in the adsorption process and vice versa. On the other hand, the effects of temperature are comparatively insignificant for the AB25 and RY25 dyes. The adsorption kinetics of the RY25 dye at all temperatures were found to be similar to a maximum adsorption capacity of around 20% while that of AB25 was higher with a value of about 30%. The reason for the higher biosorption capacity might be due to the less bulky structure of the AB25 dye which enhances the

adsorption of the dye molecules from the bulk solution, similar to that mentioned in the previous section. Both the initial biosorption rate and equilibrium amount of removal of AB25 dye slightly decreased when the temperature was increased from 25°C to 50°C. This suggests that the adsorption of the AB25 dye is relatively exothermic and involves a physical process (Ho, Y. S. & McKay, G., 1998). Furthermore, according to Prado et al. (Prado, A. G. et al., 2004), the intramolecular interaction between the $-\text{SO}_3^-$ and the $-\text{NH}_2$ groups of the dye molecules, which are *ortho* to each other, also reduces the effectiveness of the interactions between the sulphonyl groups on the dye and protonated amino groups on the chitosan.

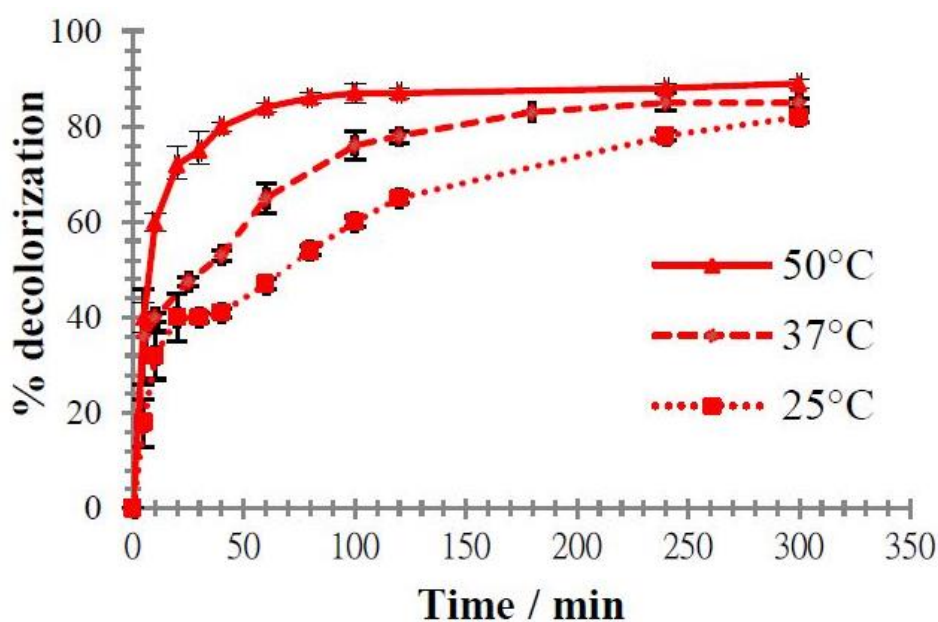


Figure 5.2(a) Effect of temperature on removal of DR80 (Luk, C. H. J. et al., 2014).

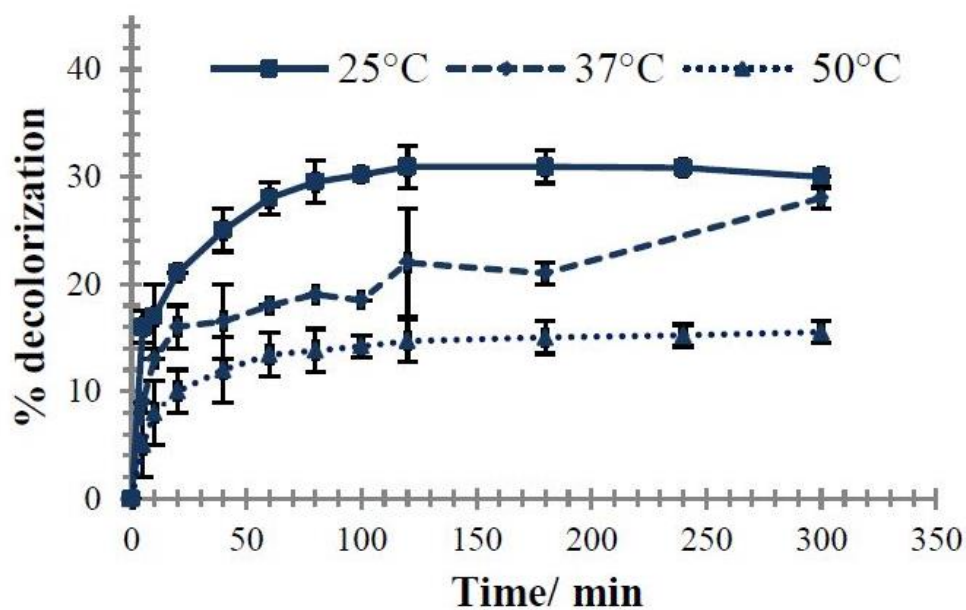


Figure 5.2(b) Effect of temperature on removal of AB25(Luk, C. H. J. et al., 2014).

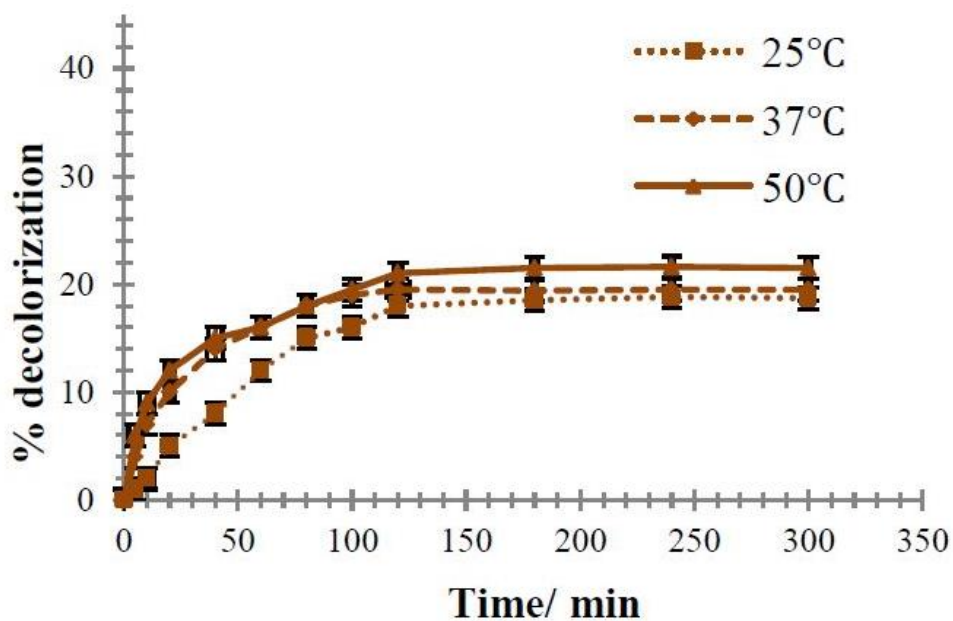


Figure 5.2(c) Effect of temperature on removal of RY25(Luk, C. H. J. et al., 2014).

5.2.1.3 Effect of crosslinking

The effects of crosslinking with glutaraldehyde on the biosorption of the DR80, AB25 and RY25 dyes are shown in Figures 5.3(a), 5.3(b) and 5.3(c), respectively. All three biosorptions were conducted with 50ml of 100 mg L⁻¹ dye solutions and 3.0 g of biosorbents at pH 5.5. The percentage of removal of the DR80 dye could be as high as 95% while that of the AB25 and RY25 dyes were only approximately 20% to 30% with the use of CB. However, with the use of GCB, the removal of the RY25 dye was increased to more than 70% while that of the DR80 dye was drastically reduced to less than 40%. As mentioned in the previous section, the removal of the DR80 dye is attributed to high degree of molecular as well as electrostatic interactions between the anionic sulphonyl and the cationic amino groups. The average pore size of the GCB was reduced by crosslinking with the amine groups of the chitosan beads. A reduction in the pore size also reduced the possibility of long, branched dye molecules so that the sulphonyl groups could bond to the inner pores of the bead, therefore greatly reducing the contact surface area for the attachment of the dye molecules. Moreover, the reduced number of protonable amino groups due to crosslinking is another factor that contributed to the significant decrease in the removal of the DR80 dye. The biosorption capacities of the RY25 and AB25 dyes were increased through the crosslinking of CB as they depend more on the molecular attractive force for dye removal. Hence, the crosslinking of the chitosan beads with a larger molecular attractive force enhanced the biosorption of the two dyes. In addition, when compared to the AB25 dye, the removal of the RY25 dye was much more prominent when using crosslinked chitosan beads. This could be attributed to the structural effects on the intramolecular interaction between the

sulphonyl and amino groups on the dye molecules.

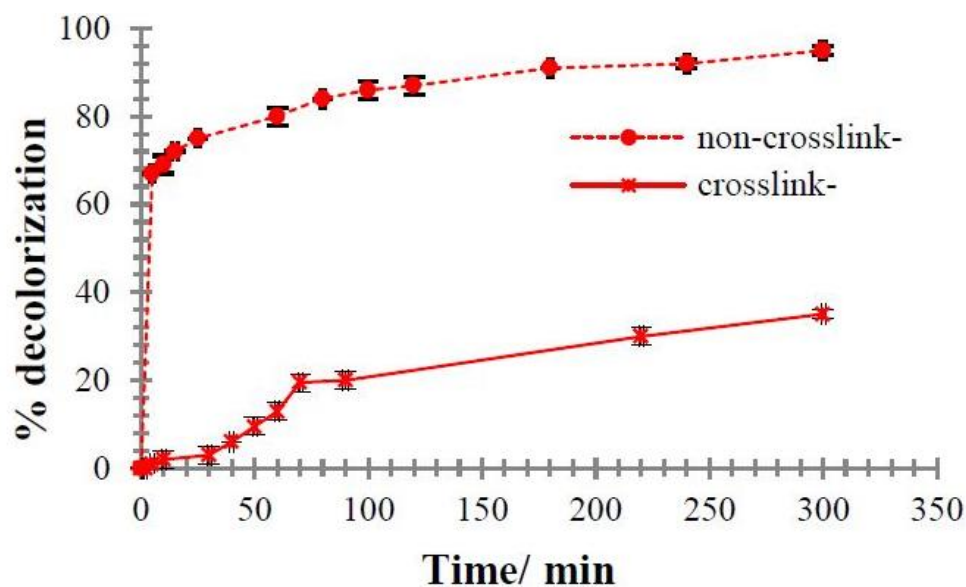


Figure 5.3 (a) Effect of crosslink on the biosorption of DR80(Luk, C. H. J. et al., 2014).

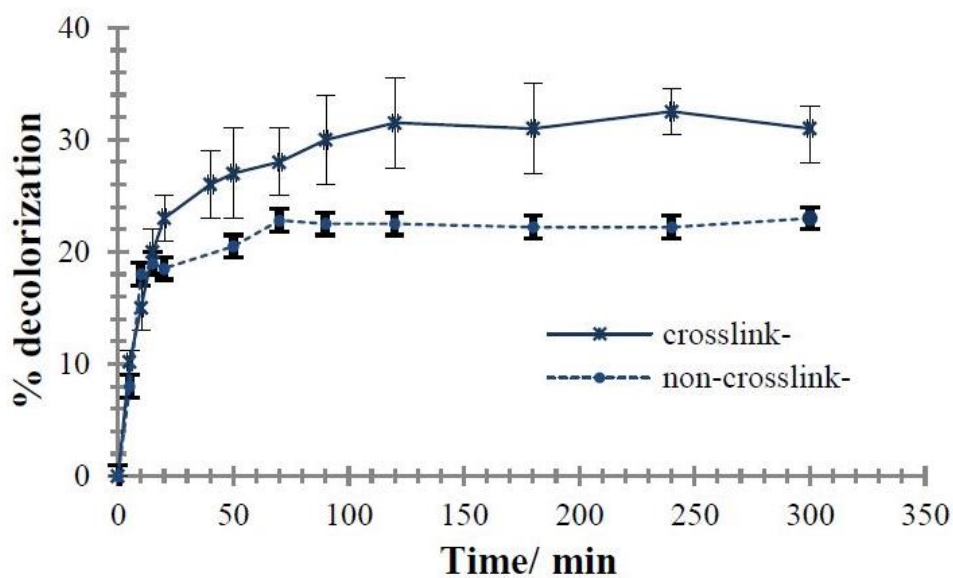


Figure 5.3 (b) Effect of crosslink on the biosorption of AB25(Luk, C. H. J. et al., 2014).

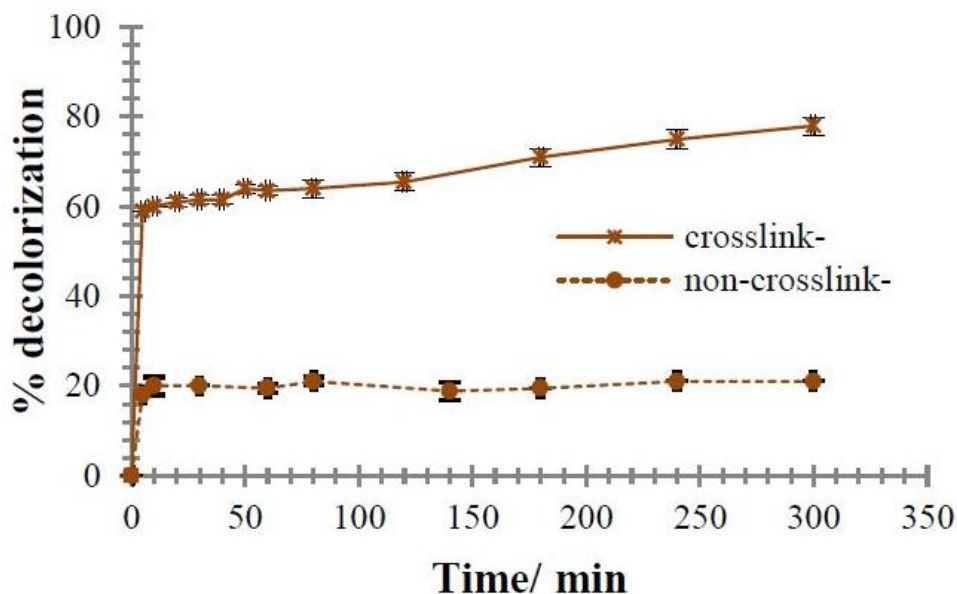


Figure 5.3 (c) Effect of crosslink on the biosorption of RY25(Luk, C. H. J. et al., 2014).

5.2.1.4 Effect from encapsulated *L. casei*

L. casei was encapsulated in GCB and the biosorption results are shown in Figures 5.4(a), 5.4(b) and 5.4(c). Figure 5.4(d) shows the biosorption of DR80 by *L. casei*-encapsulated-CB (Dyes: 50ml, 100 mg L⁻¹; pH 5.5; 37°C; Biosorbents: 3.0g; *L. casei* dosage: 11.5 mg ml⁻¹). GCB without *L. casei* only removed about 33% of the DR80 dye while the decolourisation percentage of those that contained the bacteria was 80%. The crosslinked beads had a reduced pore size which prevents the diffusion of the dye molecules into the inner pores of the beads. With the presence of the bacteria, additional biosorption sites were provided so that the binding of the dye molecules onto these various functional groups becomes possible thereby increasing the adsorption capacity. Apart from that, the removal capacity of the *L. casei*-encapsulated-CB for the DR80 dye could attain a percentage of removal that is greater than 80%. This correlated to the significant reduction in removal capacity when the pore size is reduced.

However, the maximum percentage of biosorption within the incubation time for both *L. casei*-encapsulated-CB and *L. casei*-encapsulated-GCB was still lower than that of the CB (around 93%). This once again demonstrates the adoption of the diffusion mechanism in addition to surface adsorption with the DR80 dye, which would be much more inhibited when the pore size is reduced or blocked by the encapsulated bacteria. On the other hand, the encapsulation of *L. casei* could promote the removal efficiency of AB25 by about 10%. With the incorporation of the bacteria, an increased number of interactions between the adsorption sites and dye molecules counterbalanced the negative effect brought about by fewer amino sites through crosslinking. It was also possible that the various functional groups of the bacteria could hold the dye molecules in a tighter way which strengthens the counterbalancing effect.

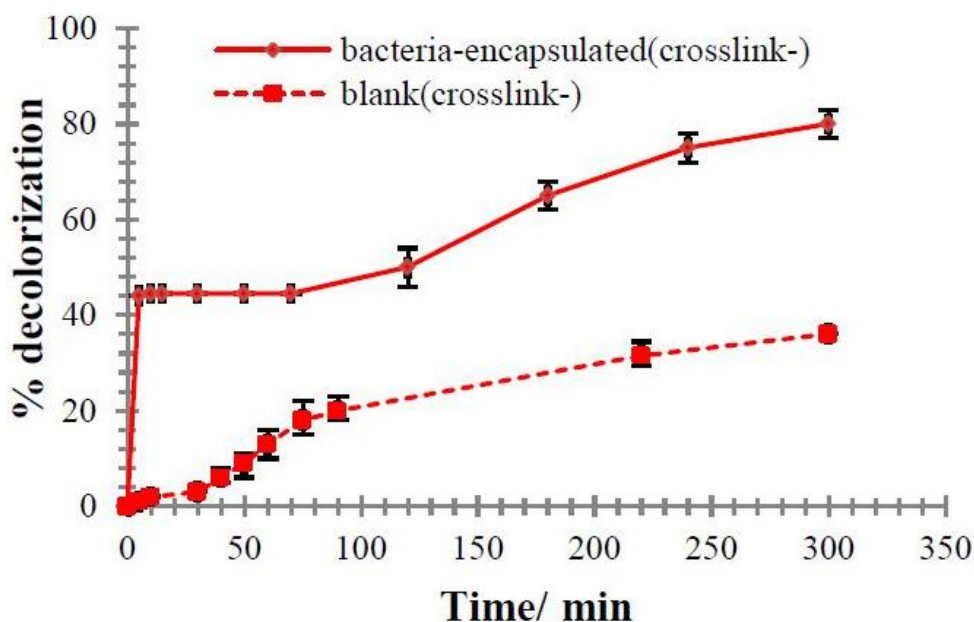


Figure 5.4(a) Effect of encapsulating *L. casei* on the biosorption of DR80 (GCB)(Luk, C. H. J. et al., 2014).

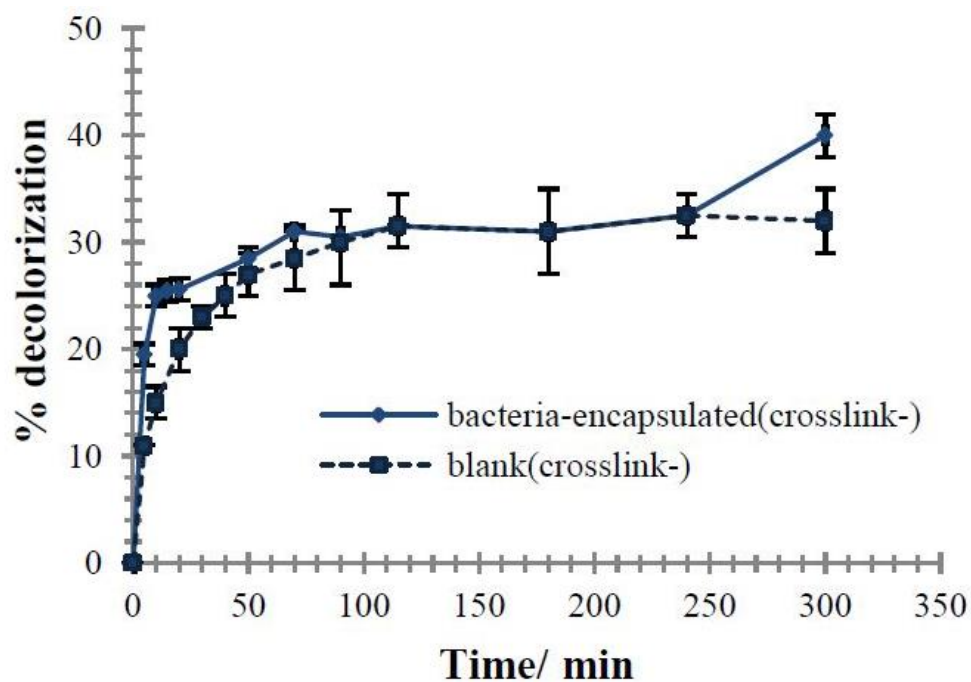


Figure 5.4 (b) Effect of encapsulating *L. casei* on the biosorption of AB25 (GCB)(Luk, C. H. J. et al., 2014).

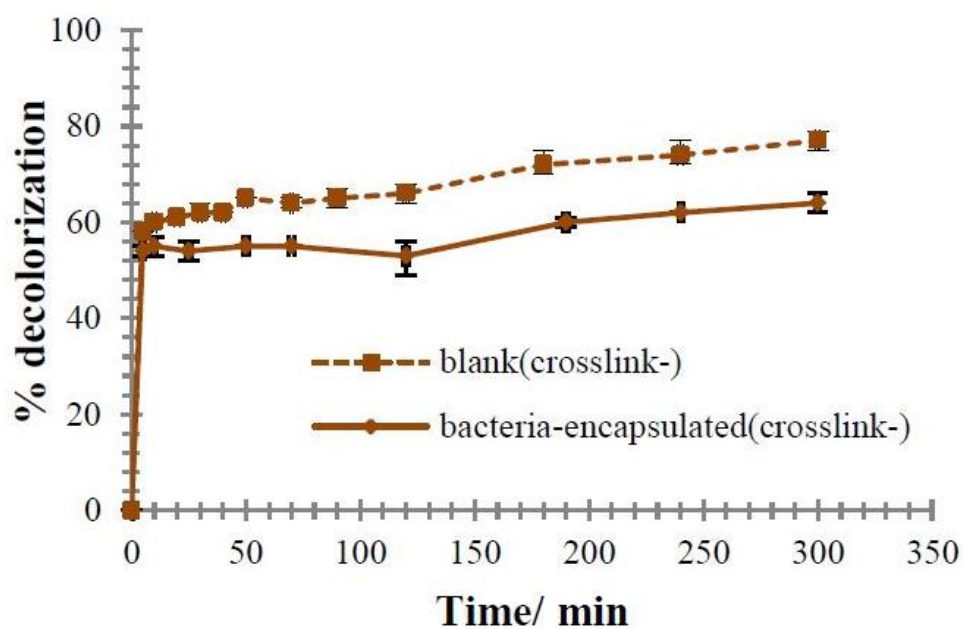


Figure 5.4 (c) Effect of encapsulating *L. casei* on the biosorption of RY25 (GCB)(Luk, C. H. J. et al., 2014).

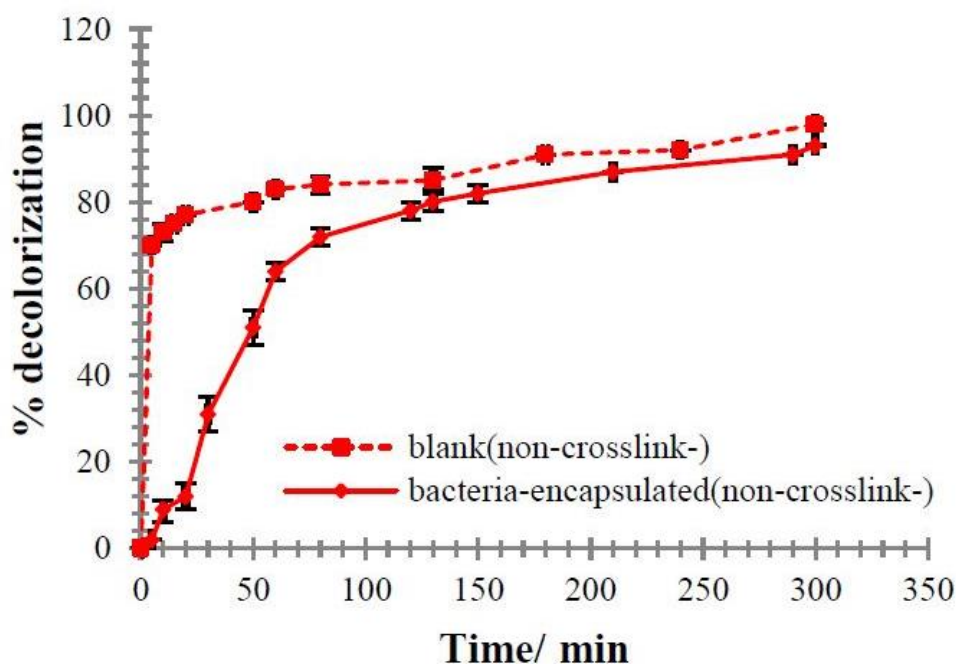


Figure 5.4 (d) Effect of encapsulating *L. casei* on the biosorption of DR80 (CB)(Luk, C. H. J. et al., 2014).

5.2.1.5 Kinetics and isotherm modelling

The application of different kinetics models provides more information on the adsorption mechanism, including the adsorption rate and the rate determining steps. Several kinetics equations are commonly adopted in the evaluation of biosorption, and the kinetics modelling of dye removal by using the chitosan beads of the three synthetic dyes were evaluated with the pseudo first order(Lagergren, S., 1898) and pseudo second order(Ho, Y. S. & McKay, G. , 1998) models. Table 5.1 shows the kinetic parameters of the model fitting.

It has been suggested that the first order model does not fit well with a wide range of contact time in the adsorption experiments(Mazengarb, S. & Roberts, G. A., 2009). The results obtained in the present study are found to follow the same trend with the kinetic parameters which showed good correlation to the

pseudo-second-order model, i.e. 0.990 for DR80 dye, 0.960 for RY25 dye, and 0.955 for AB25 dye at pH 3.4. This indicated that the biosorption system predominantly follows the pseudo-second-order model, and the rate controlling step of the overall process appeared to be chemisorption instead of a mass transport mechanism. Besides the present work, pseudo-second-order models have been successfully applied to fit the kinetic data of eosin Y by the chitosan hydrobeads(Chatterjee, S. et al., 2005), Reactive Red 189 by the crosslinked chitosan beads(Chiou, M. S. & Li, H. Y., 2003), and Remazol Yellow Gelb 3RS and Basic Yellow 37 by the chitosan derivatives(Kyzas, G. Z. & Lazaridis, N. K., 2009).

Table 5.1 Kinetics parameters for biosorption of DR80, RY25 and AB25 dyes with chitosan beads(Luk, C. H. J. et al., 2014).

Dye	DR80		RY25		AB25	
	k_2 ($\text{kg g}^{-1} \text{min}^{-1}$)	R^2	k_2 ($\text{kg g}^{-1} \text{min}^{-1}$)	R^2	k_2 ($\text{kg g}^{-1} \text{min}^{-1}$)	R^2
pH 3.4	1.74×10^{-3}	0.990	0.02	0.959	4.95×10^{-3}	0.955
pH 4.6	3.03×10^{-3}	0.998	0.01	0.964	0.388	0.998
pH 5.5	4.39×10^{-3}	0.998	0.01	0.991	0.02	0.998

The adsorption isotherms of the DR80, RY25 and AB25 dyes in pH 5.5 at 37°C by using the crosslinked beads were compared with the Freundlich and Langmuir isotherm models(Luk, C. H. J. et al., 2014). It was found that the equilibrium adsorption capacity increased with an increase in the dye concentration which ranged from 0-200 mg L⁻¹. The fitting parameters of the two models are listed in Table 5.2.

The relatively low correlation coefficients showed that the Langmuir isotherm has a poor agreement with the experimental data which suggested that the biosorption processes of this study did not occur in monolayer biosorption. On the contrary, the Freundlich isotherm fits the experimental data quite well with high correlation coefficients, thus confirming the goodness of fit, i.e. $R^2 > 0.9888$, for all three anionic dyes. The consistency of the Freundlich isotherm with the data revealed that biosorption might occur in heterogeneous adsorption sites. In addition, the interaction between the dye molecules and biosorbents could also vary in accordance with the protonation equilibrium of the different dyes(Copello, G. J. et al., 2011). Since this isotherm did not predict any saturation on the adsorbent surface, thus the existence of physisorption was found and the occurrence of infinite surface coverage(Kyzas, G. Z. & Lazaridis, N. K., 2009). Although the experimental data did not fit the Langmuir isotherm well, the q_{max} value that represents the maximum dye adsorption by the monolayer reflects the ease of the removal of the DR80 dye which was almost twofold more than that of the RY25 and AB25 dyes, and more than a hundred times the rate respectively. As a matter of fact, the protonation of the amino groups of chitosan would not be as effective as that under a pH environment of 5.5. As previously mentioned, the

crosslinking of chitosan beads reduced the number of available protonated amino groups for surface adsorption. Hence, the relatively high removal of the DR80 dye could be due to a much higher number of sulphonyl groups on each dye molecule.

The q_{max} of the Langmuir isotherm and K_F of the Freundlich model in mmol g^{-1} are also included in Table 5.2. This showed that the isotherm constants are of the reverse order when compared to the constants in mg g^{-1} , i.e. AB25 dye has the largest value while DR80 dye has the lowest. This was attributed to the different molecular masses of the three dyes. From the viewpoint of the number of moles, the actual amount of each adsorbate depends on the molecular mass when the same weight of dye is dissolved. Since the molecular masses of the three dyes are of descending order, i.e. from DR80 to RY25 and then to AB25, thus the number of moles in the solution during adsorption was in the reverse order. As a result, when the isotherm model was interpreted in mmol g^{-1} , it gave a different outcome. It is worth examining whether molar or mass quantity is more appropriate when studying a particular type of adsorption. In this study, weight quantity was chosen to obtain a better idea of practical water treatment.

Table 5.2. Biosorption isotherm parameters of DR80, RY25 and AB25 dyes by using crosslinked chitosan beads(Luk, C. H. J. et al., 2014).

		DR80	RY25	AB25
Langmuir	q_{max} (mg g ⁻¹)	610.5	368.3	443.3
	q_{max} (mmol g ⁻¹)	0.4446	0.4671	1.065
	K_L (L mg ⁻¹)	0.0049	0.0079	0.0827
	R^2	0.9105	0.8973	0.9233
Freundlich	K_F (mg g ⁻¹)	0.3856	0.5563	0.3656
	K_F (mmol g ⁻¹)	0.00028	0.00071	0.00088
	n	1.050	1.374	1.035
	R^2	0.9998	0.9987	0.9888

5.2.2 Removal of RB19: freeze-dried chitosan hydrogel beads

In this section, an evaluation on the biosorption of the RB19 dye by using freeze-dried hydrogel beads will be outlined and discussed. The freeze-drying technique is one of the most well known methods for maintaining the stability of biochemical and biological species(Anal, A. K. & Singh, H., 2007; Krasaekoopt, W. et al., 2003; Picot, A. & Lacroix, C., 2004). Nevertheless, this technique has not been explored with biosorption. In the previous section, it was found that the application of encapsulated *L. casei* on the biosorption of synthetic dyes cannot maintain the viability of the bacterium in the hydrogel beads, while the freeze-dried chitosan beads, MTPPCB, were able to maintain the viability of *L. casei*. As a result, an evaluation of TPPCB and MTPPCB on the biosorption of the RB19 dye is presented in this section. Figure 5.5 shows the TPPCB and MTPPCB after freeze-drying.

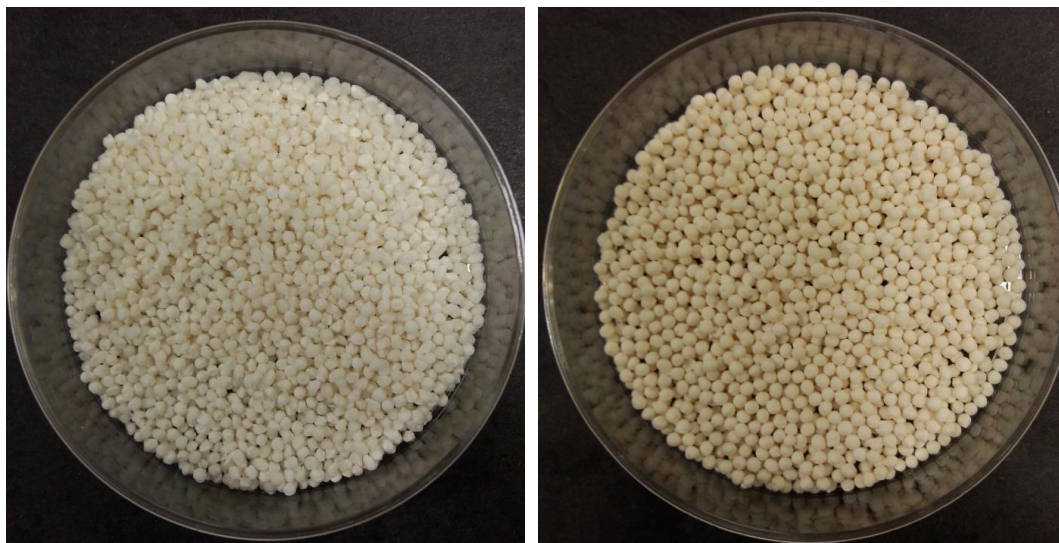


Figure 5.5 Freeze-dried TPPCB (left) and MTPPCB (right)(Luk, C. H. J. et al., 2015)

5.2.2.1 Effect of pH

Figure 5.6 shows the biosorption of the RB19 dye by using TPPCB at pHs of 3, 5.5 and 9 (dye: 50ml, 0.15 mM; 37°C; TPPCB: 2.0 g L⁻¹).(Luk, C. H. J. et al., 2015). It was found that within 24-hours of biosorption, the chitosan beads that were not freeze-dried would dissolve into gel at pH 3 while the freeze-dried chitosan beads did not do so. Although the latter became wet again with the biosorption, they were more stable chemically compared to the former. On the other hand, the freeze-dried chitosan beads were relatively more brittle than chitosan beads that were not freeze-dried which were rather elastic.

The initial rate of biosorption at pHs 3 and 5.5 was faster than that at pH 9 but overall the initial rates of biosorption at the three pHs did not demonstrate large differences. The equilibrium biosorption at pHs 3 and 9 was higher than that at pH 5, with the highest removal efficiency of $\geq 99\%$ at pH 3. The biosorption of a particular synthetic dye is closely related to the biosorbate-biosorbent

interactions at different pHs. The biosorption capacity of TPPCB followed a trend that corresponded to the zeta potential measurement (see Chapter 4) except for that at pH 9. In acidic pH environments, TPPCB interacts with the bulk protons, hence there is a highly positive surface charge. On the other hand, the RB19 dye molecules are found in their conjugate base form. As a result, positively charged TPPCB strongly attracted the anionic RB19 dye molecules. From this point of view, a higher bulk pH should give rise to less positive surface charge on TPPCB, hence less effective biosorption of the RB19 dye. Therefore, the biosorption equilibrium was reduced to around 82% at pH 5.5 compared to pH 3. However, the adsorption equilibrium at pH 9 was unexpectedly high which is comparable to that of pH 3. It was observed that there is a shoulder around 40% biosorption at a time of approximately 50 min, which follows the trend of the biosorption in terms of the effects of pH. However, increments of adsorption were later observed until the equilibrium adsorption reached approximately 95%. At a high pH, the RB19 molecules were completely ionized and found in its conjugate base form while TPPCB had a net negative surface charge surrounded by hydroxide ions. Normally, an opposite charge repulsion would mean suppressed removal. One possible reason was the presence of hydrogen bonding between TPPCB and the RB19 dye molecules which have amino and anthraquinone groups. The effect of hydrogen bonding helped to increase the removal efficiency for an even better outcome than that with pH 5.5.

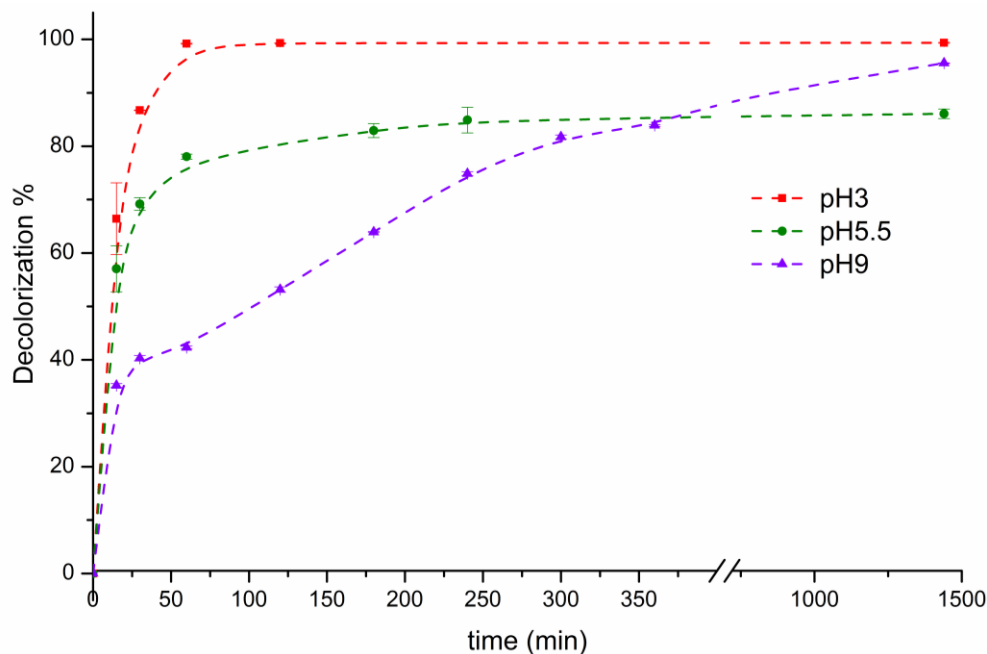


Figure 5.6 Effect of pH on removal of RB19 by TPPCB.(Luk, C. H. J. et al., 2015)

5.2.2.2 Kinetics study

After the study of the effects of pH on the removal of the RB19 dye by using TPPCB, the optimum pH was applied to both the TPPCB and MTPPCB and fitted into the pseudo first order(Lagergren, S., 1898), pseudo second order(Ho, Y. S. & McKay, G. , 1998) and intraparticle diffusion models(Weber, W. J. & Morris, J. C., 1963) to observe the kinetics of the biosorption. Figure 5.7(a) shows the plots of the removal of the RB19 dye by using MTB and TPPCB; Figures 5.7(b), 5.7(c) and 5.7(d) show the fitting of the kinetic model to the pseudo first order, pseudo second order, and intraparticle diffusion models respectively. The kinetic experiments were conducted with 50 ml of 1.5 mM RB19 at 37°C and pH 3 with 0.1 g of biosorbents. Table 5.3 summarizes the kinetics parameters of the modelling.

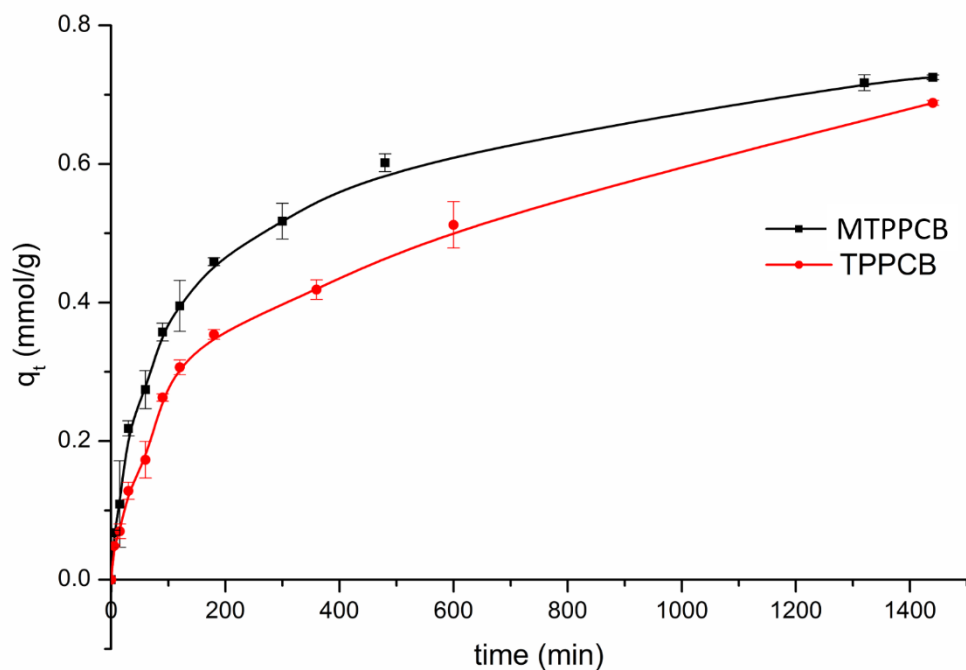


Figure 5.7(a) Removal of RB19 by MTB and TPPCB(Luk, C. H. J. et al., 2015).

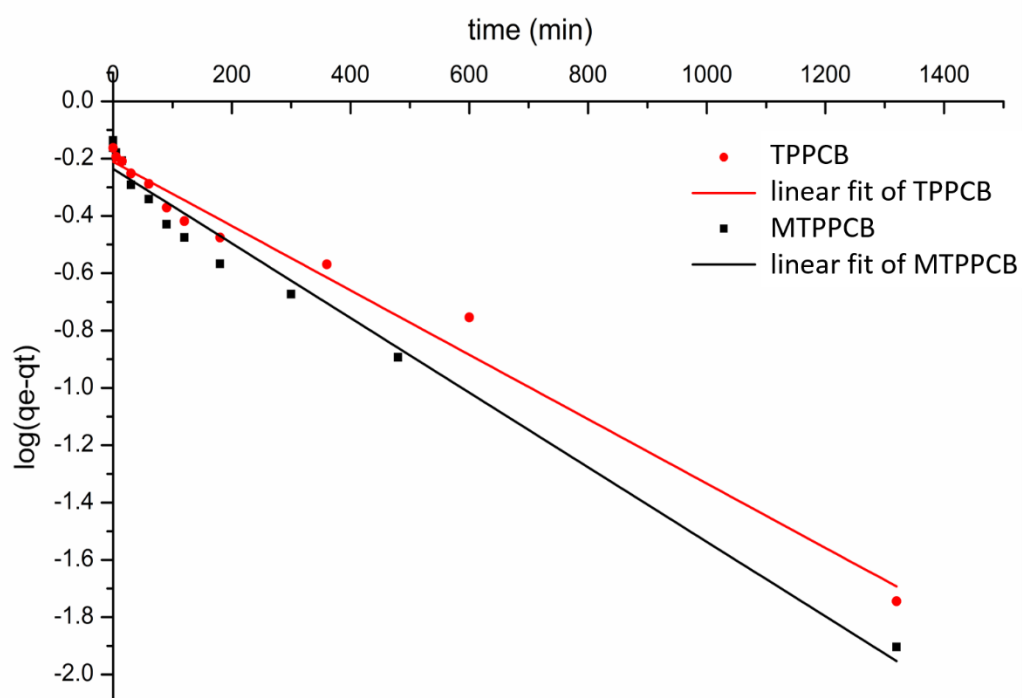


Figure 5.7(b) Pseudo-first order modelling of the removal of RB19(Luk, C. H. J. et al., 2015).

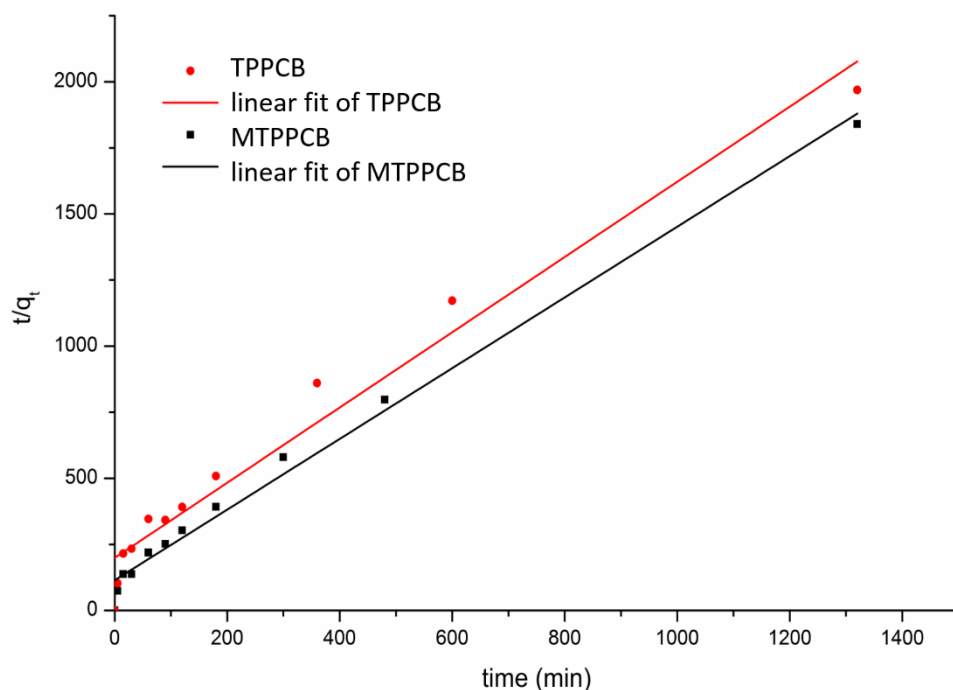


Figure 5.7(c) Pseudo-second order modelling of the removal of RB19(Luk, C. H. J. et al., 2015).

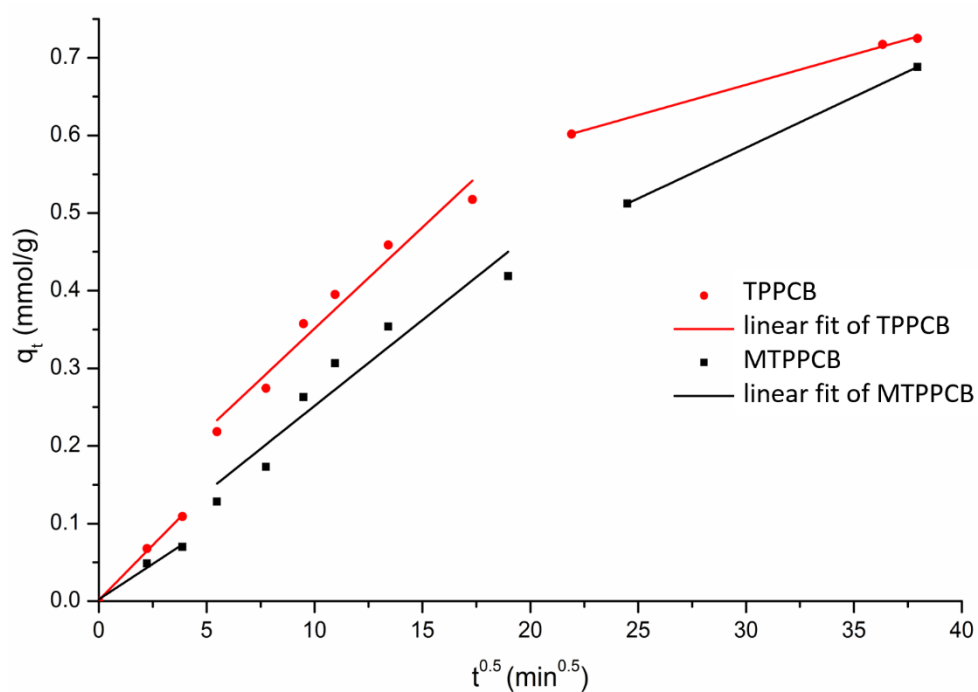


Figure 5.7(d) Intraparticle diffusion modelling of the removal of RB19(Luk, C. H. J. et al., 2015).

Table 5.3 Kinetics parameters of biosorption of RB19 by MTPPCB and TPPCB.

	Pseudo first order			Pseudo second order		
	k_1	q_e	R^2	k_2	q_e	R^2
	(min^{-1})	(mmol g^{-1})		($\text{g}^{-1} \text{mmol}^{-1} \text{min}^{-1}$)	(mmol g^{-1})	
MTPPCB	0.0030	0.5811	0.9791	0.0157	0.7477	0.9894
TPPCB	0.0026	0.6157	0.9794	0.0102	0.7028	0.9647
Intraparticle diffusion						
	MTPPCB			TPPCB		
k_i						
($\text{mmol g}^{-1} \text{min}^{-0.5}$)	0.0283	0.0261	0.0078	0.0182	0.0221	0.013
R^2	0.9955	0.9549	0.9975	0.9643	0.9016	-

From the plotting of the removal of the RB19 dye as a function of time, the initial rate and overall q_t (amount of RB19 adsorbed per mass of biosorbent at time t) of the MTB were faster and higher than those of TPPCB, respectively. However, the q_e was not significantly different. When the biosorptions were fitted in the pseudo first order model, the MTB and TPPCB showed an R^2 of 0.9791 and 0.9794 respectively with similar rate constants (0.0030 min^{-1} for MTB and 0.0026 min^{-1} for TPPCB). On the other hand, when both biosorptions were fitted in the pseudo second order model, the R^2 of the MTB was 0.9894 which showed greater agreement while that of the TPPCB was not well fitted to the model when compared to the pseudo first order model ($R^2 = 0.9647$). For the intraparticle diffusion modelling, multi-linearity was observed on both biosorptions. The high values of R^2 in the initial step (> 0.99) were attributed to the surface biosorption while those in the equilibrium stage could be regarded as further diffusion inside the biosorbents. In the mid-stage, the correlation coefficients of the intraparticle

diffusion fitting of MTB was 0.9549 and that of TPPCB was 0.9016. Although the correlation coefficients were not satisfactory, the two fittings that passed through the origin indicated the possibility of intraparticle diffusion.

5.3 Chapter Summary

The biosorption synthetic dyes by chitosan-based hydrogel beads have been described and discussed in this chapter. Chitosan hydrogel beads, in the crosslinked form as well as encapsulation of *L. casei*, were adopted to evaluate the biosorption of the DR80, AB25 and RY25 dyes. The effect of the pH showed that an acidic environment facilitates the removal of the three synthetic dyes compared to higher pH conditions. DR80 and RY25 dyes were both biosorbed to a higher extent by increasing the temperature while that of AB25 was deteriorated due to the exothermic nature of the biosorption. GCB provided different impacts on the biosorption of the three synthetic dyes. By limiting the pore size after crosslinking, the DR80 dye was not well biosorbed compared to the biosorption by CB, while AB25 and RY25 were both enhanced by the crosslinking. *L. casei* was thus encapsulated into GCB and the combined biosorbent facilitate the biosorption of the DR80 dye by increasing the available functional groups to attract dye molecules. The pseudo-second-order kinetic model successfully fitted the biosorptions of the three anionic dyes at different pH values, which indicated that the overall dye removal processes were chemisorption-controlled. The Freundlich isotherm model agreed very well with the equilibrium adsorption data at different initial concentrations of the three anionic dyes. The encapsulation of *L. casei* was further subjected to the biosorption of another synthetic dye, RB19, and the chitosan hydrogel beads

were synthesized with ionotropic crosslinking which was biologically more friendly to the culture in that the viability was successfully maintained. TPPCB and MTPPCB, the biosorbents that encapsulate the cultures, were freeze-dried and it was found that the biosorbents became physically and chemically more stable than the hydrogel form. Further investigations on the effects of pH revealed that acidic and alkaline environments could facilitate the biosorption of RB19 by TPPCB. At 37°C and under a pH 5.5, a kinetic study of TPPCB and MTPPCB were conducted and it was found that MTPPCB fits better with pseudo second order kinetics while TPPCB fitted better with the pseudo-first-order. Both biosorbents show partial agreement with the intraparticle diffusion model indicating possible diffusion kinetics during the biosorption of RB19.

Chapter 6 BIOSORPTION OF HEAVY METAL IONS

6.1 Introduction

In this chapter, the biosorption of heavy metal ions with the microorganisms and synthesized biosorbents of interest will be reported and discussed. The removal of heavy metal ions by using alginate hydrogel beads and encapsulated *C. krusei* will be evaluated. The effects of the pH and temperature, and mechanistic studies with kinetics and isotherm modelling are included in the discussion.

6.2 Biosorption of heavy metal ions: alginate-based biosorbents

In this section, the removal of heavy metal ions by using alginate hydrogel beads will be discussed. Chromium (VI), nickel (II), lead (II) and copper (II) are used to evaluate the removal performance of the synthesized hydrogel beads as well as non-encapsulated and encapsulated *C. krusei*. These metal ions are commonly used species in numerous industries which are inevitably found in the residues after application. Therefore, they are chosen for this study to study the removal of heavy metal ions.

6.2.1 Preliminary studies on heavy metal ion removal

The biosorption of heavy metal species very much depends on the pH environment. Different metal species have different forms at different pH ranges. Among the more commonly studied heavy metal ions, the speciation of chromium (VI) is relatively advanced at different pH values. Equations (6.1) to (6.3) show the possible forms of chromium (VI) dissociated in a water environment (Cotton, F. A. & Wilkinson, G. , 1980; Greenwood, N. N. & Earnshaw, A., 1984).



The speciation of chromium (VI) depends on the pH and chromium concentration in the solution. At low ppm scale concentrations, CrO_4^{2-} predominantly exists. At pH <1, H_2CrO_4 is found, and with increasing pH, HCrO_4^- predominates. Beyond pH 7, fully deprotonated CrO_4^{2-} is found. On the other hand, the other three divalent metal ions, nickel (II), copper (II) and lead (II), share similar speciations in different pH ranges. In an extreme acidic medium, the divalent metal ions exist in the form of M^{n+} . Upon increasing the pH value, the concentration of hydroxo-metal species increases, until the medium becomes a weak alkaline and a strong alkaline medium, the metal hydroxides precipitate out. With such speciation characteristics, the biosorption of metal species are greatly dependent on the solution pH in which soluble metal species are the target substrate.

In the biosorption trial of chromium, 5 ml of 1.8% (w/v) calcium alginate was used as the biosorbent, with different amounts of encapsulated *C. krusei* to investigate the effect of the culture and the encapsulated amount on the removal of chromium (VI). Chromium (VI) (20 ml of 1 mM) at pH 2.5 and 30°C was mixed with the biosorbents. Table 6.1 shows the results of the biosorption.

Table 6.1 Biosorption of chromium (VI) by alginate-based hydrogel beads.

Biosorbent	Biosorbent concentration (g L ⁻¹)	Removal %	q_e (mmol g ⁻¹)
5 ml of 1.8% (w/v) CaAlg (no <i>C. krusei</i> encapsulated)	4.5	6.621	0.0147
5 ml of 1.8% (w/v) CaAlg (10 mg <i>C. krusei</i> encapsulated)	5.0	19.305	0.0386
5 ml of 1.8% (w/v) CaAlg (100 mg <i>C. krusei</i> encapsulated)	9.0	50.629	0.0563

From Table 6.1, it can be observed that a large number of biosorbents are used to evaluate the removal performance on Cr (VI) removal. It was found that the removal efficiency and q_e of the three biosorbents are not satisfactory (not >95%). When 10 mg of *C. krusei* was encapsulated, the removal efficiency increased to 19.305% in comparison to 6.621% from CaAlg. When the encapsulation amount further increased to 100 mg, the removal efficiency is further increased to 50.629%. Nevertheless, with an increment of 10 folds of the culture, the removal efficiency only improved by around 2.5 folds.

At a pH of 2.5, HCrO_4^- and CrO_4^{2-} are the two species found in the solution. With such a low pH environment, both CaAlg and MCaAlg are associated with relatively dense positive surface charges. The positive surface attracted the anionic chromium species and hence the biosorption occurred. However, the result revealed that CaAlg and MCaAlg are not suitable biosorbents for chromium (VI) since the removal efficiency and q_e from the three biosorbents adopted are not satisfactory when compared to other biosorbents being

studied (Bahafid, W. et al., 2013b; Ghosh, S. et al., 2015b; Hołda, A., 2013; Mahmoud, M. E., 2015b; San Keskin, N. O. et al., 2015b). This could be because of the insufficient electrostatic attraction between the biosorbents and the chromium species. Moreover, unlike other cationic metal species, the anionic chromium species were in their oxo-form which is relatively electronegative. This contributed to the repulsion between the adsorbed adsorbates and the bulk adsorbates. As a result, CaAlg and MCaAlg are not suitable biosorbents for chromium (VI).

On the other hand, cationic copper (II), nickel (II) and lead (II) were also biosorbed by using CaAlg and MCaAlg. All three types of metal ions are divalent, with nickel and copper in the same period of the periodic table while lead is down the group and period of the periodic table. In the biosorption experiments of the three divalent metal species, non-encapsulated *C. krusei* was also used as a biosorbent to determine whether a plain culture could biosorb the metal species. Table 6.2 shows the preliminary biosorption results of copper (II), nickel (II) and lead (II) by using *C. krusei*, CaAlg and MCaAlg. Each metal solution was made up to 1.5mM and 20ml for the experiments. The solutions were maintained at pH 5 and 30°C for 24-hour-biosorption.

Table 6.2 Biosorption of copper (II), nickel (II) and lead (II) with alginate-based hydrogel beads.

Biosorbent	Biosorbent concentration (g L ⁻¹)	Removal %	q _e (mmol g ⁻¹)
Copper (II)			
20 mg <i>C. krusei</i>	1.0	31.146	0.4240
2 ml of 1.8% (w/v) CaAlg (no <i>C. krusei</i> encapsulated)	1.8	73.116	0.6091
2 ml of 1.8% (w/v) CaAlg (20 mg <i>C. krusei</i> encapsulated)	2.8	75.540	0.4046
Nickel (II)			
20 mg <i>C. krusei</i>	1.0	3.951	0.0592
2 ml of 1.8% (w/v) CaAlg (no <i>C. krusei</i> encapsulated)	1.8	26.952	0.2246
2 ml of 1.8% (w/v) CaAlg (20 mg <i>C. krusei</i> encapsulated)	2.8	21.446	0.1149
Lead (II) (pH 3 biosorption)			
20 mg <i>C. krusei</i>	1.0	36.875	0.5353
2 ml of 1.8% (w/v) CaAlg (no <i>C. krusei</i> encapsulated)	1.8	87.913	0.7168
2 ml of 1.8% (w/v) CaAlg (20 mg <i>C. krusei</i> encapsulated)	2.8	86.570	0.4538

As shown in Table 6.2, each metal ion is biosorbed at 1.5 mM, 30°C, and pH 5 for copper (II) and nickel (II). When lead (II) was biosorbed at pH 5, the mixture became opaque if *C. krusei* and MCaAlg were used in the biosorption. This implies that the yeast cultures influence the precipitation of lead (II) which should not occur at pH 5. Since 1.5 mM of lead (II) is a relatively high concentration, 0.2 mM of lead (II) at pH 5 was also used but the mixture still became opaque in the biosorption experiments. Therefore, the biosorption of lead (II) was performed at pH 3. From both the removal efficiency and q_e , nickel (II) was found to have the lowest values compared to lead (II) and copper(II) with similar trends of removal efficiency. Since metal hydroxides will be precipitated out when the pH is further increased, a weak acidic environment was used for the biosorption. In short, CaAlg and MCaAlg are not good biosorbents for chromium (VI) and nickel (II) while copper (II) and lead (II) are removed with satisfactory results but further optimization and evaluation are required. In later sections, further studies on the removal of copper (II) by using CaAlg and MCaAlg are discussed.

6.3 Biosorption of copper (II): alginate-type hydrogel beads

In this section, the biosorption of copper (II) will be outlined and discussed. The effects of pH and temperature, as well as kinetics and isotherm modelling will be discussed. After further optimization, it was found that a lower concentration of *C. krusei* could also reach a similar equilibrium biosorption compared to the 1 g L⁻¹ adopted in the preliminary experiments as described in the previous section. Figure 6.1 shows the biosorption of copper(II) by using non-encapsulated *C. krusei* as a function of the concentration of culture (Cu (II): 20 ml, 1.5 mM, 30°C, pH 5.2). This shows that the optimum concentration is 0.2 g L⁻¹ which is similar

to that of 0.1 g L^{-1} . The result shows similar trend to that in Mahmoud(Mahmoud, M. E., 2015b) on the biosorption of chromium (VI) by using a gel-yeast biosorbent, where the q_e was inversely proportional to the biosorbent concentrations. Therefore, the encapsulation concentration as well as the plain culture dosage adopted in further biosorption studies are reduced to 0.1 g L^{-1} as the optimum concentration.

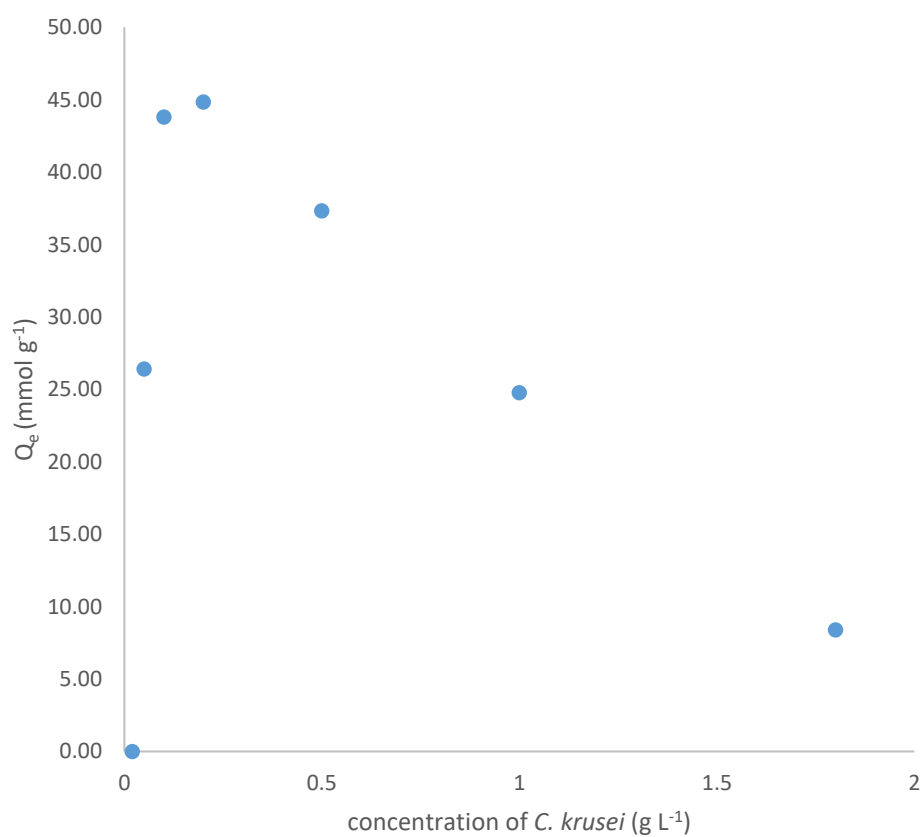


Figure 6.1 Biosorption of copper (II) by plain *C. krusei* as a function of culture concentration.

6.3.1 Effect of pH

Figure 6.2 shows the equilibrium q_e of copper (II) by using *C. krusei*, CaAlg and MCaAlg at different pHs from 1.2 to 5.2 (Cu (II): 20 ml; 1.5 mM; 30°C. 2 ml of 1.8% (w/v) of CaAlg and MCaAlg was used. Non-encapsulated and encapsulated *C. krusei*: 0.1 gL⁻¹). It can be observed that a higher pH in the bulk solution results in higher removal efficiency. The optimal pH for the removal of copper is 5.2, with 0.687 mmol g⁻¹ removed by *C. krusei*, 0.431 mmol g⁻¹ by CaAlg and 0.617 mmol g⁻¹ by MCaAlg. In examining the metal ion removal process, the speciation of the metal ions at different pHs and the interactions between the biosorbent and metal ions were taken into consideration. At acidic pH, copper(II) predominantly exists as the Cu²⁺ form. When the removal process was subjected to very low pH environments (pH 1.2 to 2), the carboxylate COO⁻ possessed on the biosorbents were protonated in majority, i.e. R-COOH. Coordination of copper(II) ions to the protonated carboxylate groups were not likely to occur hence resulted in a minimal amount of removal. When the environment was less acidic, the proportion of the conjugate form of the carboxylate COO⁻ on the biosorbents became higher. At an optimal pH of 5.2, the interaction between the biosorbents and copper(II) ions were optimized. This scenario related to the FTIR analysis in which copper(II) coordination was the primary removal mechanism between copper(II) and the biosorbents.

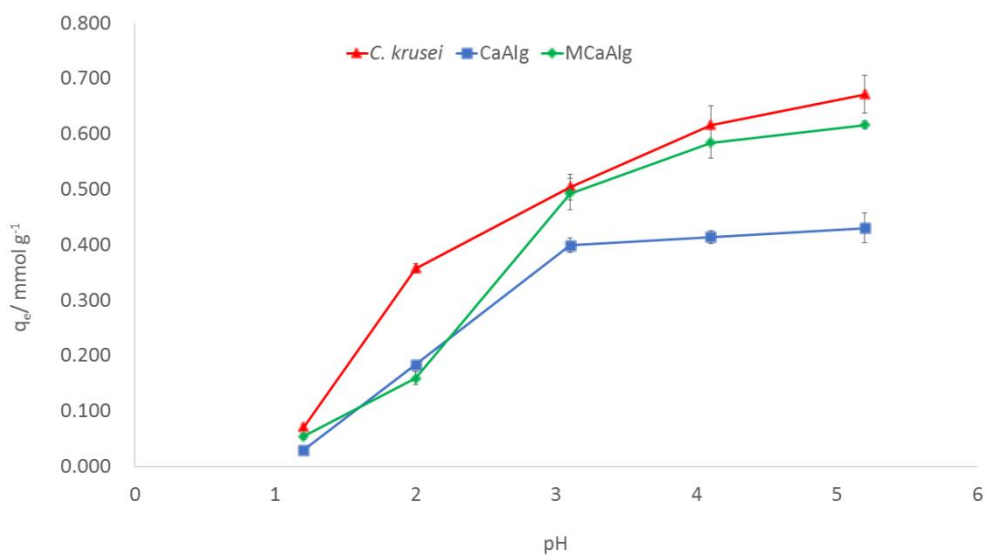


Figure 6.2 Effect of pH on *C. krusei*, CaAlg and MCAAlg in biosorption of copper (II).

6.3.2 Effect of Temperature

Figure 6.3 shows the effects of temperature on the removal of copper (II) by the three adsorbents at temperatures of 30°C, 40°C and 50°C respectively (Cu (II): 20 ml; 1.5 mM; pH 5.2. 2 ml of 1.8% (w/v) of CaAlg and MCAAlg was used. Non-encapsulated and encapsulated *C. krusei*: 0.1 gL⁻¹). An increase in the removal capacity by *C. krusei*, was observed when the temperature was increased from 30°C (0.616 mmol g⁻¹) to 40°C (0.716 mmol g⁻¹) but the removal capacity was reduced if the temperature was further increased to 50°C (0.419 mmol g⁻¹). On the other hand, a trend of increase was observed for both CaAlg and MCAAlg: CaAlg achieved 0.469 mmol g⁻¹ at 30°C, 0.517 mmol g⁻¹ at 40°C and 0.568 mmol g⁻¹ at 50°C; MCAAlg achieved 0.571 mmol g⁻¹ at 30°C, 0.637 mmol g⁻¹ at 40°C and 0.685 mmol g⁻¹ at 50°C. Besides the general trend of increase, MCAAlg also showed a higher removal capacity in all three temperatures when compared to

CaAlg. From the results of CaAlg and MCaAlg, the copper(II) removal was more favourable when increasing temperatures while that of *C. krusei* alone was not. In the case of CaAlg and MCaAlg, the coordination of copper(II) to the carboxylate groups was facilitated upon the elevation of temperature. Nevertheless, with similar biosorption mechanism, biosorption by *C. krusei* increased from 30°C to 40°C and decreased at 50°C. Since the yeast applied to the sorption system was still living, a possible reason for the increase in biosorption from 30°C to 40°C could be better environment for the biological processes participated in the copper(II) biosorption to be occurred at 40°C. Subsequently, further increase to higher temperature environment gave rise to denaturation of the cell structures which alter the original biosorption ways at 30°C and 40°C, hence the copper(II) uptake was suppressed. The temperature effect on the biosorption by *C. krusei* implied the process was not solely physical, but biological processes also involved.

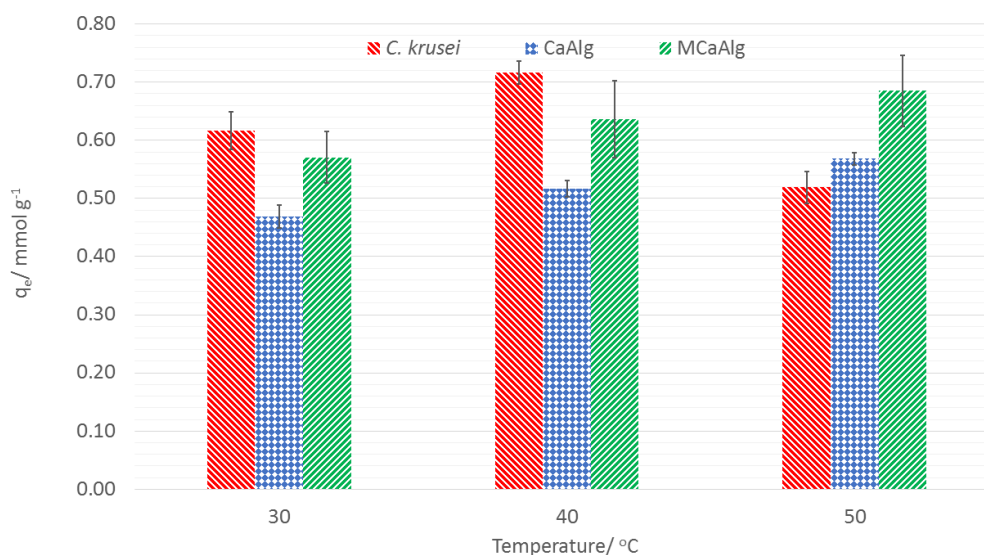


Figure 6.3 Effect of temperature on *C. krusei*, CaAlg and MCaAlg for the biosorption of copper (II).

6.3.3 Kinetics and isotherm modelling

After investigating the effect of pH and temperature, kinetics and isotherm modelling was used to evaluate the biosorption mechanism of a particular pair of biosorbent-biosorbate. Pseudo-first-order(Lagergren, S., 1898), pseudo-second-order (Ho, Y. S. & McKay, G. , 1998), and intraparticle diffusion models(Weber, W. J. & Morris, J. C., 1963)were used to evaluate the biosorption. Table 6.3 summarizes the linear mathematical expressions of the three kinetics models. Figures 6.4(a), 6.4(b), 6.4(c) and 6.4(d) show the plots of the following results: (a) removal kinetics of copper (II) by using *C. krusei*, CaAlg and MCaAlg; (b) intraparticle diffusion fitting; (c) pseudo-first-order fitting and (d) pseudo-second-order fitting. Table 6.4 summarizes the kinetics parameters of the biosorption of copper (II) by using *C. krusei*, CaAlg and MCaAlg. All kinetic experiments were performed as follow: Cu (II): 0.05 mM; 30°C; 20 ml; pH 5.2. Biosorbents: 2 ml of 1.8% (w/v) of CaAlg and MCaAlg; 0.1 gL⁻¹ non-encapsulated and encapsulated *C. krusei*.

Table 6.3 Summary of linear mathematical expressions of three kinetics models. k_1 , k_2 , and k_i are the rate constants of the corresponding kinetic models, respectively; q_e is the amount of adsorbed copper (II) at equilibrium and q_t is the amount of copper (II) adsorbed at time t (mmol g^{-1}).

Kinetic model	Linear form
Pseudo first order model	$\log(q_e - q_t) = \log q_e - \frac{k_1}{2.303} t$
Pseudo second order model	$\frac{t}{q_t} = \frac{1}{k_2 q_e^2} + \frac{1}{q_e} t$
Intraparticle diffusion model	$q_t = k_i \cdot t^{0.5}$

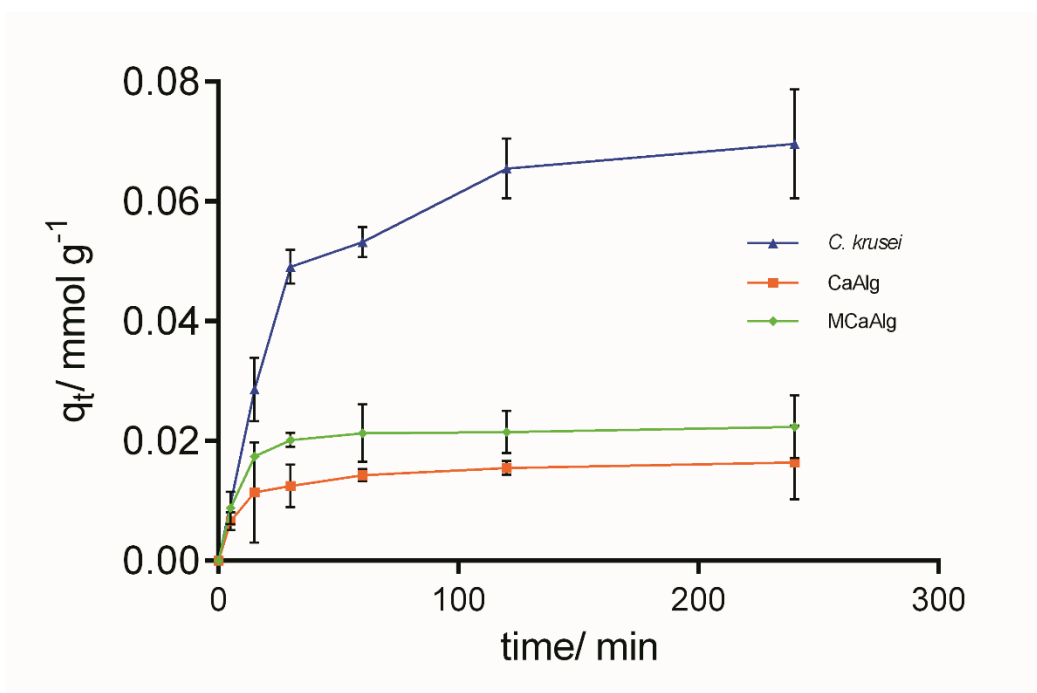


Figure 6.4(a) Removal kinetics of copper(II) by *C. krusei*, CaAlg and MCAAlg.

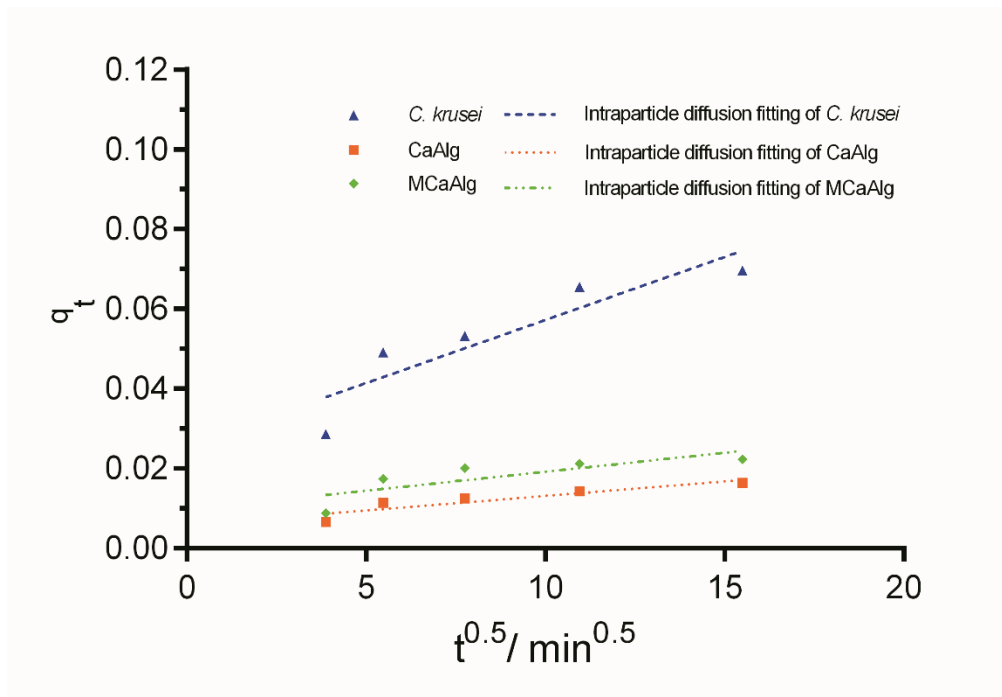


Figure 6.4(b) Intraparticle diffusion fitting of *C. krusei*, CaAlg and MCAAlg.

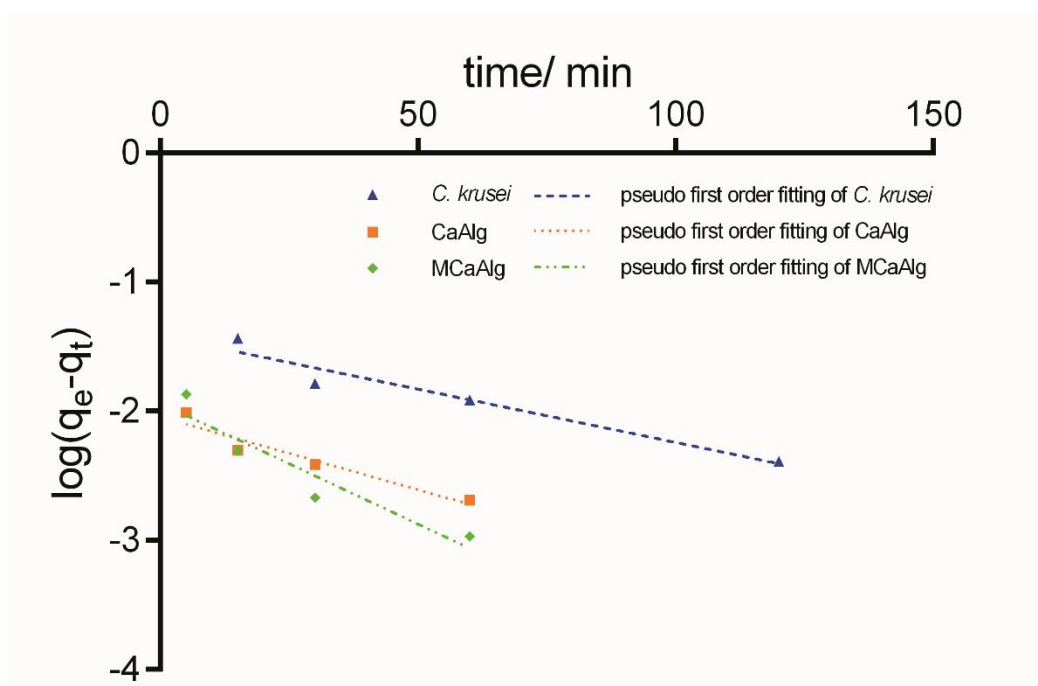


Figure 6.4(c) Pseudo-first order fitting of *C. krusei*, CaAlg and MCAAlg.

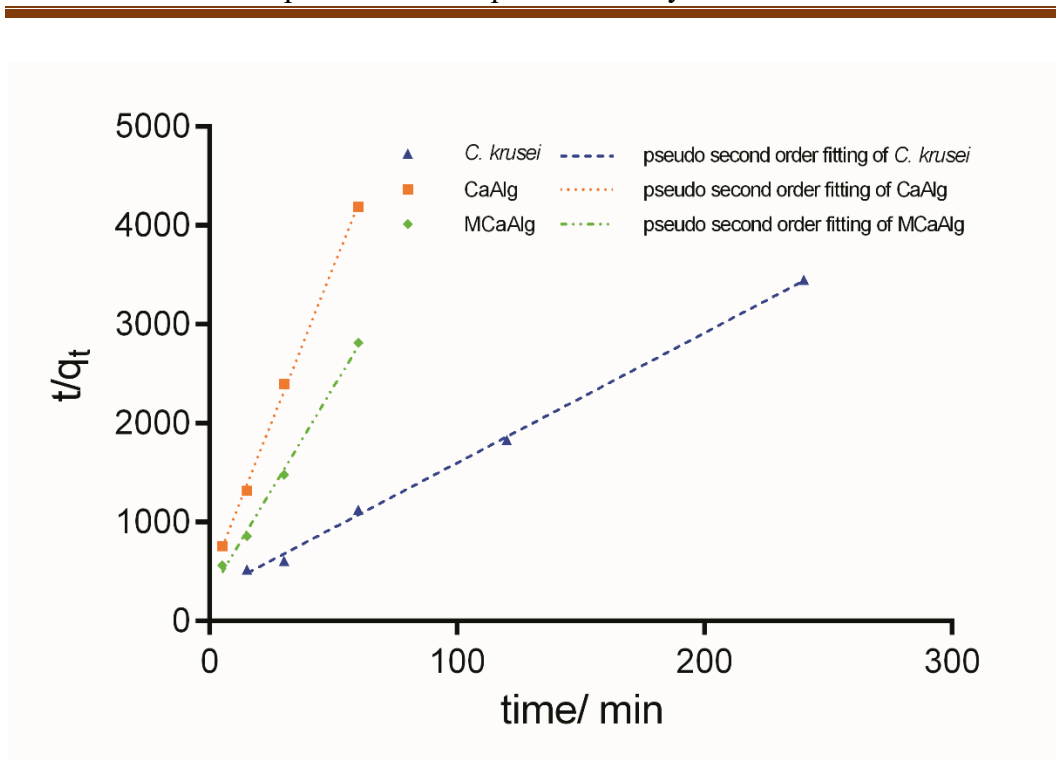


Figure 6.4(d) Pseudo-second order fitting of *C. krusei*, CaAlg and MCAAlg.

Table 6.4 Summary of kinetics parameters of biosorption of copper (II) by using *C. krusei*, CaAlg and MCaAlg.

Intraparticle diffusion				
	<i>C. krusei</i>	CaAlg	MCaAlg	
k_i (mmol g ⁻¹ min ^{-0.5})	0.0031	0.0007	0.0009	
R ²	0.8217	0.8432	0.6457	
Pseudo-first-order				
	q_e (experimental) mmol g ⁻¹	q_e (calculated)	k_1 (min ⁻¹)	R ²
<i>C. krusei</i>	0.0696	0.0384	0.0190	0.9431
CaAlg	0.0164	0.0091	0.0259	0.9248
MCaAlg	0.0224	0.0116	0.0431	0.8950
Pseudo-second-order				
	q_e (experimental) mmol g ⁻¹	q_e (calculated)	k_2 (g mol ⁻¹ min ⁻¹)	R ²
<i>C. krusei</i>	0.0696	0.0760	0.6031	0.9982
CaAlg	0.0164	0.0159	9.1000	0.9986
MCaAlg	0.0224	0.0241	5.9994	0.9962

From the plotting of the removal of copper(II) by using *C. krusei*, CaAlg and MCaAlg, CaAlg and MCaAlg reached equilibrium after 60 minutes after contact while that of *C. krusei* was after 240 minutes. Among the three kinetics models, all three adsorbents show the highest degree of correlation with the pseudo second-order-kinetics (R^2 of *C. krusei* = 0.9982; R^2 of CaAlg = 0.9986; R^2 of MCaAlg = 0.9962) compared to the pseudo-first-order kinetics (R^2 of *C. krusei* = 0.9431; R^2 of CaAlg = 0.9248; R^2 of MCaAlg = 0.8950). The experimental q_e and the calculated q_e obtained from pseudo-second-order kinetics fitting for the three adsorbents were also close in value. The pseudo-second-order kinetics hence best explained the biosorption. This agrees with the research work from Hassan et al. which their research focused on the ionotropic cross-link of metal alginate(Hassan et al. 2012). They illustrated the cross-link of alginates with divalent metal ions in a stoichiometric ratio of 2:1 which correlates with the present pseudo-second-order kinetics fitting result. On the other hand, intraparticle diffusion model describes diffusion-controlled kinetics that any fitting process would pass through the origin when plot and fit. From figure 5(b), all three plots of the biosorption did not pass through the origin. The biosorptions were most like not a diffusion-controlled kinetics but rather a chemical process.

Besides the kinetics fitting, isotherm modelling was also conducted as a function of the initial concentration of copper (II). Figures 6.5(a), 6.5(b) 6.5(c) and 6.5(d) show the equilibrium removal efficiency, Langmuir isotherm fitting, Freundlich isotherm fitting and Temkin isotherm fitting of the three adsorbents on the biosorption of copper (II) at 30°C and pH 5.2 with various initial concentrations. Table 6.5 shows the corresponding isotherm constants. Biosorbents applied in each isotherm experiment were 2 ml of 1.8% (w/v) of CaAlg and MCAAlg, and 0.1 gL⁻¹ non- encapsulated and encapsulated *C. krusei*.

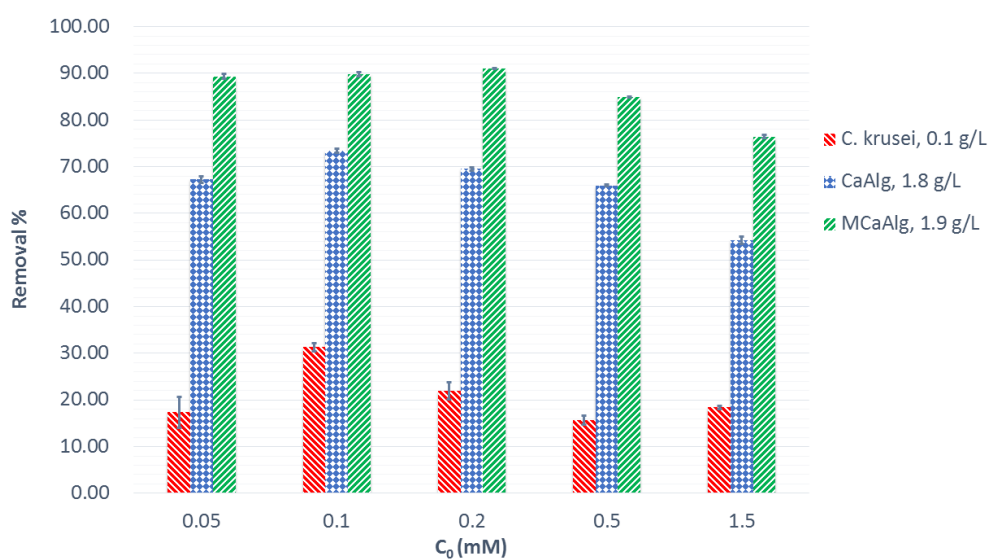


Figure 6.5(a) Equilibrium removal efficiency of *C. krusei*, CaAlg and MCAAlg.

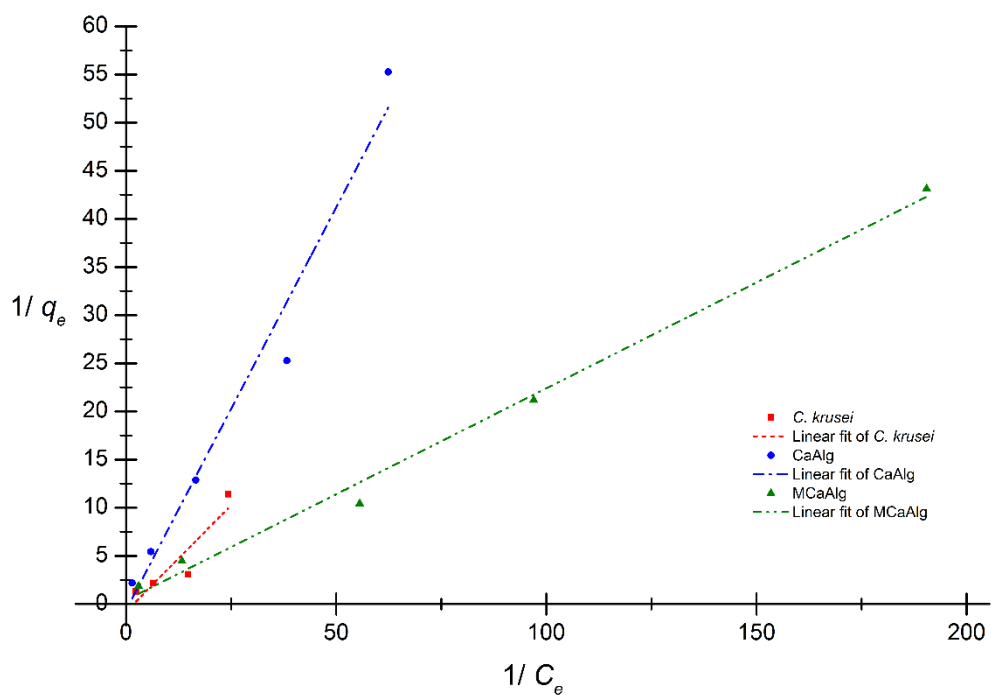


Figure 6.5(b) Langmuir isotherm fitting of *C. krusei*, CaAlg and MCAAlg.

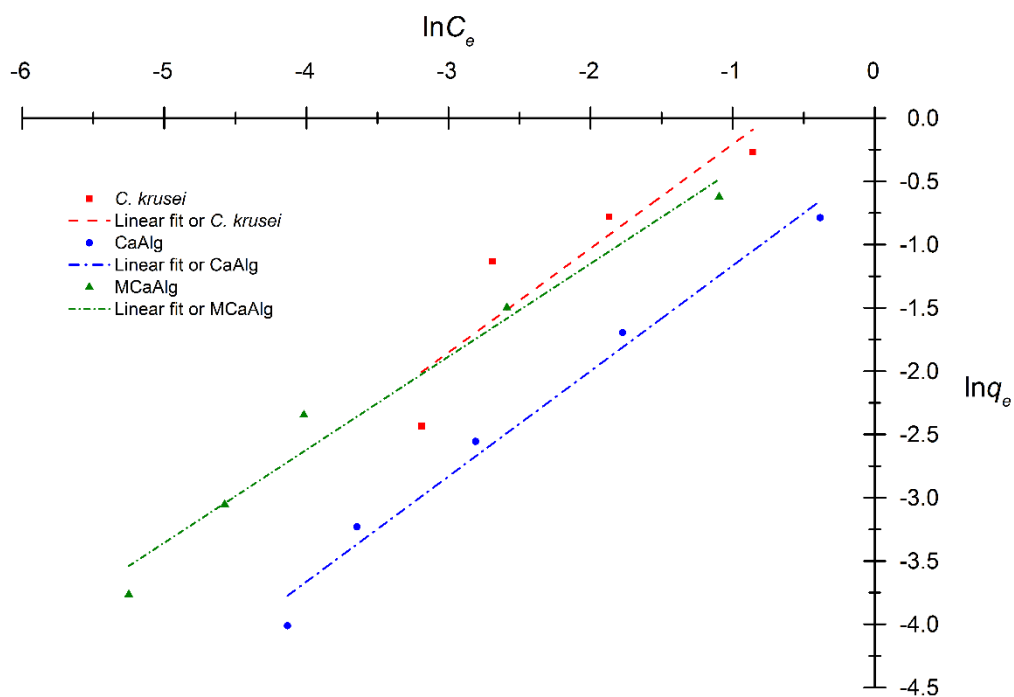


Figure 6.5(c) Freundlich isotherm fitting of *C. krusei*, CaAlg and MCAAlg.

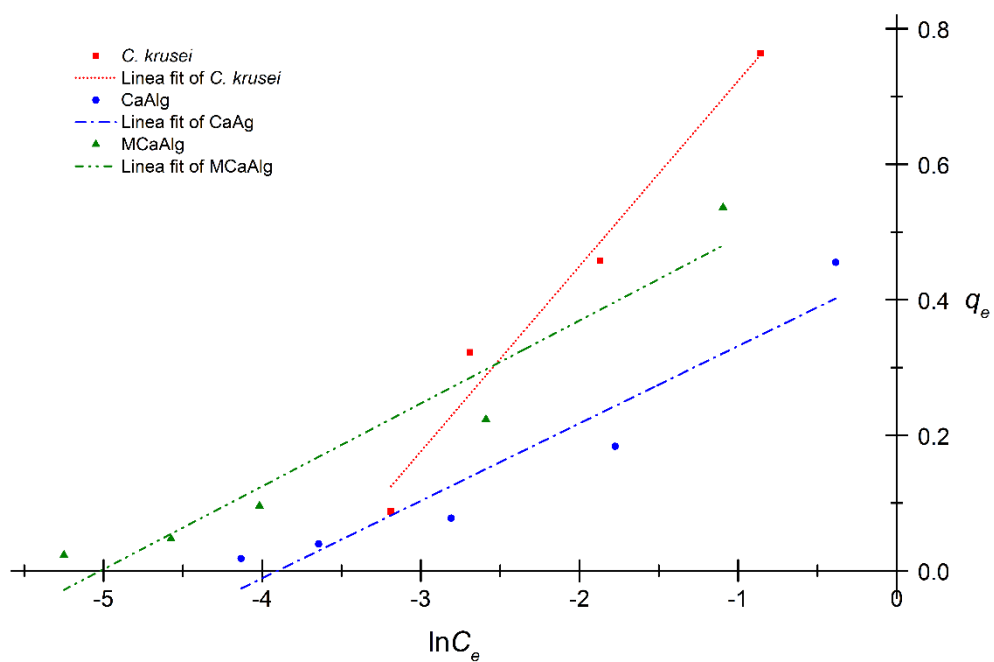


Figure 6.5(d) Temkin isotherm fitting of *C. krusei*, CaAlg and MCAAlg.

Table 6.5 Isotherm modelling constants of *C. krusei*, CaAlg and MCaAlg for removal of copper(II).

	<i>C. krusei</i>	CaAlg	MCaAlg
Langmuir isotherm modelling			
q_{max} (mmol g ⁻¹)	-1.267	-0.645	2.418
K_L (L mmol ⁻¹)	-1.785	-1.550	1.881
R ²	0.76	0.96	0.99
Freundlich isotherm modelling			
n	1.216	1.202	1.396
K_F (L mmol ⁻¹)	1.851	0.7155	1.2588
R ²	0.74	0.98	0.97
Temkin isotherm modelling			
B (J mmol ⁻¹)	0.273	0.114	0.122
b_T	9.213	22.05	20.60
A_T (L g ⁻¹)	38.23	49.59	151.3
R ²	0.96	0.89	0.91

As mentioned in the chapter of the literature review, isotherm modelling provides valuable information of sorption systems. In this study, *C. krusei* ($R^2 = 0.9625$) fitted well with Temkin isotherm. Both MCaAlg and CaAlg fitted Langmuir and Freundlich isotherm with correlation coefficient > 0.96 , where MCaAlg was fitted with a q_{max} of 2.418 mmol g⁻¹. Langmuir isotherm assumes homogeneous and monolayer adsorption while Freundlich assumes heterogeneous adsorption. From previous results and discussions, the biosorptions were revealed as coordination of copper(II) by carboxylate COO⁻ on the biosorbents. At this point,

we could say the monolayer adsorption were regarded as the biosorption by carboxylate groups since all of them share same chemical properties as well as same heat of adsorption. This correlates the good fitting of Langmuir isotherm with CaAlg and MCaAlg. While *C. krusei*, which was also discussed to coordinate copper(II) by carboxylate groups, was having sophisticated surface structures compared to CaAlg and MCaAlg. Therefore, it was given much worse fitting correlation with the two isotherms. The Langmuir isotherm fitting of CaAlg, however, showed negative interception hence negative q_{max} and K_L were interpreted. Nevertheless, the error was statistical that we should rather judge the isotherm fitting with inclusion of previous results and discussions. Therefore, instead of Freundlich isotherm, Langmuir isotherm was chosen to describe the biosorption of CaAlg. On the other hand, MCaAlg was well fitted with Langmuir isotherm and it correlates with the reported results. The good fitting of Temkin isotherm with *C. krusei* indicated the biosorption followed the assumption that the heat of adsorption decreases upon coverage due to adsorbate-adsorbent interactions.

Besides *C. krusei*, CaAlg fitted Temkin isotherm with R^2 of 0.89 and MCaAlg fitted with R^2 of 0.91. This implied biosorption of both of them also shared the Temkin isotherm assumptions. On the other hand, the parameter n in Freundlich isotherm indicates favourable adsorption if it lies between 1 to 10. From the calculations, all three biosorbents were fitted with n around 1 to 2. With high correlation with Freundlich isotherm, the n values indicated favourable sorption of copper(II) on CaAlg and MCaAlg.

6.4 Chapter Summary

The biosorption of heavy metal ions by alginate-based hydrogel beads have been described and discussed in this chapter. Chromium(VI), nickel(II), lead(II) and copper(II) are used and the preliminary results show poor biosorption of chromium(VI) and nickel(II). Further studies on the biosorption of copper(II) with *C. krusei* encapsulated in alginate hydrogel beads are conducted. It was found that a weak acidic environment facilitates the biosorption of copper(II) with the use of *C. krusei*, CaAlg and MCaAlg, owing to the best metal coordination between the biosorbents and the copper(II) ions. From the experiments that examined the effects of temperature, the biosorption capacity of *C. krusei* is reduced with a higher temperature of 50°C, while biosorption is enhanced for both CaAlg and MCaAlg. Kinetic modelling showed that all three biosorbents fitted well with the pseudo-second order kinetics model in that the biosorptions are mainly chemisorption-based. Further isotherm modelling showed that *C. krusei* followed Temkin isotherm and both CaAlg and MCaAlg followed Langmuir isotherm model. This indicated the biosorptions were homogeneous and monolayer in nature and *C. krusei* biosorbed copper(II) based on the assumption that the heat of sorption decreases with coverage.

Chapter 7 CONCLUSION AND RECOMMENDATIONS

7.1 Conclusion

The aim of this study is to encapsulate microorganisms as biosorbents for the removal of synthetic dyes and heavy metal ions. Since conventional methods in removing pollutants are either not effective at low concentrations or costly to implement, the focus of pollution control is now on biosorption. However, there are still research gaps in the field, which are examined in this study. They include: (1) separation issues brought about by the use of plain microorganisms which have been studied as potentially excellent biosorbents; (2) encapsulation of microorganisms which provide similar biosorption ability as plain encapsulating materials or plain cultures or even reduced biosorption. As a result, different potential cultures were screened prior to the biosorption studies and subsequently encapsulated to evaluate their biosorption of synthetic dyes and heavy metal ions. Afterwards, suitable encapsulation materials, which were chitosan and alginate in this study, were used to encapsulate the culture and therefore, the synthesis of the biosorbents is optimized.

The research methodology followed several steps. Started with the selection of microorganisms for encapsulation and the encapsulating materials, the target synthetic dyes and heavy metal ions were then selected. Synthesis and characterisation of the biosorbents were the next step. Finally, the evaluation and mechanistic study of the biosorption synthetic dyes and heavy metal ions were launched. Species of bacteria and yeasts was screened to observe possible biodegradation of the synthetic dyes. Nevertheless, none of the cultures with their standard inoculation mediums could biodegrade the synthetic dyes.

Afterward, a species of lactic acid bacteria, *L. casei*, which has been studied in-depth for its applications in the pharmaceutical and food industries but rarely in the biosorption of pollutants, was chosen and encapsulated by using two kinds of chitosan hydrogel beads. On the other hand, a *Candida sp.* yeast strain, *Candida krusei* (*C. krusei*), was also encapsulated, but into alginate-based hydrogel beads to evaluate its ability to remove heavy metal ions. This strain has not yet been explored but *Candida sp.* have shown excellent biosorption power in scavenging heavy metals. Therefore, it is worthy to investigate this unexplored strain in terms of its removal ability.

The characterisation of the biosorbents includes the use of FTIR spectroscopy, zeta potential measurement and SEM. The viability of the encapsulated culture was also examined in which live culture encapsulation is successfully achieved. The FTIR analyses provide insights on the functional groups of the biosorbents. The crosslink of CB with glutaraldehyde was clearly shown in the FTIR spectrum of GCB. An absorption band shift from 1640.9 cm^{-1} to 1663.8 cm^{-1} indicated the crosslink of the amino groups on CB with the glutaraldehyde. TPPCB, MTPPCB and *L. casei* were also analyzed with FTIR spectroscopy. Common absorption bands attributed to the presence of *N*-acetylglucosamine and *N*-acetylmuramic acid were found in the spectra of the three biosorbents. Differentiation between TPPCB and MTPPCB with *L. casei* could be observed from the absorption band of primary amino groups possessed on chitosan but not on *L. casei*. The absorption band of P=O could also be observed with difference between *L. casei* to those of TPPCB and MTPPCB. Moreover, the presence of absorption band attributed from carboxylic O-H bending found at *L. casei*

distinguishes the culture from the hydrogel beads. Furthermore, FTIR analyses of alginate hydrogel beads showed addition of the absorption bands of the carboxylate COO^- anion after the copper biosorption. This was due to addition of copper ions coordination to the carboxylate groups on the biosorbents. After FTIR analyses, zeta potential measurements were conducted which revealed the surface charge distributions at particular pH values. A scanning electron microscope was used to observe the biosorbents at the micro scale in which the encapsulated cultures were visualized through imaging.

L. casei was first encapsulated in chitosan hydrogel beads synthesized through coacervation with alkaline neutralization. Further chemical crosslinking of the chitosan beads was also conducted to increase the chemical stability of the beads. Direct Red 80, Reactive Yellow 25 and Acid Blue 25 were used to evaluate the biosorption performance. The effects of pH, temperature, crosslinking, and encapsulating of *L. casei* were taken into consideration to evaluate the biosorption of the combined biosorbents. It was found that the ease of electrostatic interaction as well diffusion of the dye molecules into the hydrogel beads have important roles in biosorption efficiency. The effects of the temperature did not have significant impacts on the biosorption of the three types of synthetic dyes. Crosslinking the hydrogel beads not only strengthens the chemical stability of the biosorbents, but also enhanced the biosorption of Reactive Yellow 25 and Acid Blue 25. No biodegradation was observed as the encapsulated *L. casei* was not a live culture. Nevertheless, *L. casei* had positive effects on the biosorption of Direct Red 80 with satisfactory enhancement. Further kinetic and isotherm modelling reveal that the biosorptions of all three

dyes followed a pseudo second order kinetic equation and also a Freundlich isotherm. This revealed chemisorption occurred between the biosorbents with the three synthetic dyes and the biosorption was heterogeneous and possible to be multi-layer biosorption. Another chitosan-based hydrogel bead synthesized through ionotropic crosslinking is used to encapsulate *L. casei* and the viability was maintained. Further freeze-drying improves the physical and chemical stabilities of the beads as well as the viability of the cultures. It was found that plain beads can remove Reactive Blue 19 with high removal efficiency in both acidic and alkaline environments. The kinetic study revealed that encapsulation of *L. casei* in a chitosan matrix could somewhat enhance the biosorption. Both plain and culture-encapsulated freeze-dried chitosan beads followed the pseudo second order kinetics. Chemisorption is revealed in synthetic dyes biosorption.

C. krusei, a yeast strain, was encapsulated into alginate-based hydrogel beads and the viability of the culture is also maintained. The biosorbents were then subjected to heavy metal ions. It was found that the biosorption of chromium(VI) and nickel(II) was not as satisfactory as anticipated, while copper(II) and lead(II) were well biosorbed. Furthermore, copper(II) biosorption is conducted and the pH and temperature effects are also evaluated. The kinetic study reveals that all three biosorbents follow pseudo second order kinetics. Chemisorption was also revealed in copper(II) biosorption with alginate hydrogel beads. The isotherm modelling showed that *C. krusei* followed Temkin isotherm and both CaAlg and MCaAlg followed Langmuir isotherm model. This indicated the biosorptions were homogeneous and monolayer in nature and *C. krusei* biosorbed copper(II) based on the assumption that the heat of sorption decreases with coverage.

7.2 Recommendations

In this study, chitosan- and alginate-based hydrogel beads have been synthesized. A number of polymeric supports, such as polysulfonate, gelatin, and polyvinyl alcohol are also potential candidates for encapsulating different cultures for biosorption. In the biosorption of RB19, the biosorption enhancement of MTPPCB was not that significant in that plain TPPCB was already a very good biosorbent toward RB19. By utilizing the advantages of the polymeric encapsulation materials, encapsulating the same cultures will give significant differences in the biosorption outcome which is worth exploring.

From the view point of biodegradation, no suitable way is found in this study which would obtain biological reactions from the cultures toward the synthetic dyes. More work to examine the general conditions of dye biodegradation by using microorganisms is vital. Specific conditions to biodegrade specific groups of substrate from particular cultures with their biological metabolisms are not enough to deal with practical pollution control. A general method used to biodegrade different groups of synthetic dyes in one pot by culture is beneficial to the development in this study. Besides, pretreatment of microorganisms has not been studied for possible outcomes. However, it has been reported that pretreatment could bring about significant enhancements to the biosorption of synthetic dyes and heavy metal ions. Pretreatment without deteriorating the viability of the cultures could be one of the ways that combine both biosorption and possible biodegradation toward the pollutants.

In the study of the biosorption of heavy metal ions, lead (II) was also biosorbed

in a satisfactory specific sorption capacity. On the other hand, nickel (II), another divalent metal ion that was screened, is surprisingly not biosorbed well by the biosorbents. Further studies on the selectivity of alginate-based biosorbents as well as *C. krusei* toward heavy metal ions are worth investigating.

Besides the aforementioned benefits of biosorption, adsorption-desorption-cycling is also one of the merits with biosorption in which the biosorbed substrate can be desorbed and collected for further applications while the biosorbents can then be reused for next biosorption. This study reveals the surface biosorption of synthetic dyes and heavy metal ions. Cycling experiments can also be conducted to investigate the cycling ability of the biosorbents as well as further understanding of the removal mechanism.

REFERENCE

- Abdel Hameed, M. S. (2006). Continuous removal and recovery of lead by alginate beads, free and alginate-immobilized *Chlorella vulgaris*. *Afr. J. Biotechnol.*, 5, 1819-1823.
- Abo-Farha, S. A., Abdel-Aal, A. Y., Ashourb, I. A., & Garamon, S. E. (2009). Removal of some heavy metal cations by synthetic resin purolite C100. *J. Hazard. Mater.*, 169(190-194).
- Adnan, L. A., Yusoff, A. R. M., Hadibarata, T., & Khudhair, A. B. (2014). Biodegradation of Bis-Azo Dye Reactive Black 5 by White-Rot Fungus *Trametes gibbosa* sp. WRF 3 and Its Metabolite Characterization. *Water Air Soil Poll.*, 225, 1-11.
- Aghaie-Khouzani, M., Forootanfar, H., Moshfegh, M., Khoshayand, M. R., & Faramarzi, M. A. (2012). Decolorization of some synthetic dyes using optimized culture broth of laccase producing ascomycete *Paraconiothyrium variabile*. *Biochem. Eng. J.*, 60, 9-15.
- Ahemad, M. (2012). Implications of bacterial resistance against heavy metals in bioremediation: a review. *J. Inst. Integ. Omics Appl. Biotechnol.*, 3(3).
- Ahemad, M., & Kibret, M. (2013). Recent trends in microbial biosorption of heavy metals: a review. *biochem. Mole. Biol.*, 1, 19-26.
- Ainane, T., Abourriche, A., Kabbaj, M., Elkouali, M., Bennamara, A., Charrouf, M., et al. (2014). Removal of hexavalent chromium from aqueous solution by raw and chemically modified seaweed *Bifurcaria bifurcata*. *J. Mater. Environ. Sci.*, 5, 975-982.
- Akar, T., Celik, S., Gorgulu Ari, A., & Tunali Akar, S. (2013). Nickel removal characteristics of an immobilized macro fungus: equilibrium, kinetic and mechanism analysis of the biosorption. *J. Chem. Technol. Biotechnol.*, 88, 680-689.
- Alhassani, H. A., Rauf, M. A., & Ashraf, S. S. . (2007). Efficient microbial degradation of Toluidine Blue dye by *Brevibacillus* sp. *Dyes Pigments*, 75(2), 395-400.
- Ali, H. (2010). Biodegradation of synthetic dyes-a review. *Water Air Soil Poll.*, 213, 251-273.
- Ali, H., Ahmad, W., & Haq, T. (2009). Decolorization and degradation of Malachite green by *Aspergillus flavus* and *Alternaria solani*. *Afr. J. Biotechnol.*, 8, 1574-1576.
- Ali, N., Hameed, A., & Ahmed, S. (2010). Role of brown-rot fungi in the

- bioremoval of azo dyes under different conditions. *Braz. J. Microbiol.*, *41*, 907-915.
- Alkan, H., Gul-Guven, R., Guven, K., Erdogan, S., & Dogru, M. (2015). Biosorption of Cd, Cu, and Ni Ions by a Thermophilic Haloalkalitolerant Bacterial Strain (KG9) Immobilized on Amberlite XAD-4. *Pol. J. Environ. Stud.*, *24*, 1903 -1910.
- Almeida, E. J. R., & Corso, C. R. (2014). Comparative study of toxicity of azo dye Procion Red MX-5B following biosorption and biodegradation treatments with the fungi *Aspergillus niger* and *Aspergillus terreus*. *Chemosphere*, *112*, 317-322.
- Alvarenga, N., Birolli, W. G., Seleglim, M. H., & Porto, A. L. (2014). Biodegradation of methyl parathion by whole cells of marine-derived fungi *Aspergillus sydowii* and *Penicillium decaturense*. *Chemosphere*, *117*, 47-52.
- Alvarez, M. T., Crespo, C., & Mattiasson, B. (2007). Precipitation of Zn(II), Cu(II) and Pb(II) at bench-scale using biogenic hydrogen sulfide from the utilization of volatile fatty acids. *Chemosphere*, *66*, 1677-1683.
- Ambrósio, S. T., Vilar Júnior, J. C., da Silva, C. A. A., Okada, K., Nascimento, A. E., Longo, R. L., et al. (2012). A Biosorption Isotherm Model for the Removal of Reactive Azo Dyes by Inactivated Mycelia of *Cunninghamella elegans* UCP542. *Molecules*, *17*, 452-462.
- Anal, A. K., & Singh, H. (2007). Recent advances in microencapsulation of probiotics for industrial applications and targeted delivery. *Trend Food Sci. Tech.*, *18*(5), 240-251.
- Anand, P., Isar, J., Saran, S., & Saxena, R. K. (2006). Bioaccumulation of copper by *Trichoderma viride*. *Bioresour. Technol.*, *97*, 1018-1025.
- Anburaj, J., Kuberan, T., Sundaravadivelan, C., & Kumar, P. (2011). Biodegradation of azo dye by *Listeria* Sp. *Int. J. Environ. Sci.*, *1*, 1760-1769.
- Andleeb, S., Atiq, N., Robson, G. D., & Ahmed, S. (2012). An investigation of anthraquinone dye biodegradation by immobilized *Aspergillus flavus* in fluidized bed bioreactor. *Environ. Sci. Pollut. Res.*, *19*, 1728-1737.
- Anjaneya, O., Souche, S. Y., Santoshkumar, M., & Karegoudar, T. B. (2011). Decolorization of sulfonated azo dye Metanil Yellow by newly isolated bacterial strains: *Bacillus* sp. strain AK1 and *Lysinibacillus* sp. strain AK2. *J. Hazard. Mater.*, *190*, 351-358.
- Apiratikul, R., & Pavasant, P. (2008). Batch and column studies of biosorption of heavy metals by *Caulerpa lentillifera*. *Bioresour. Technol.*, *99*,

2766-2777.

- Arivalagan, P., Singaraj, D., Haridass, V., & Kaliannan, T. (2014). Removal of cadmium from aqueous solution by batch studies using *Bacillus cereus*. *Ecol. Eng.*, *71*, 728–735.
- Asfaram, A., Ghaedi, M., Ghezlbash, G. R., Doil, E. A., Tyagi, I., Agarwal, S., et al. (2016). Biosorption of malachite green by novel biosorbent *Yarrowia lipolytica* isf7: Application of response surface methodology. *214*, 249–258.
- Ayed, L., Achour, S., Khelifi, E., Cheref, A., & Bakhrouf, A. (2010). Use of active consortia of constructed ternary bacterial cultures via mixture design for Congo Red decolorization enhancement. *Chem. Eng. J.*, *162*(2).
- Ayed, L., Mahdhi, A., Cheref, A., & Bakhrouf, A. (2011). Decolorization and degradation of azo dye Methyl Red by an isolated *Sphingomonas paucimobilis*: Biototoxicity and metabolites characterization. *Desalination*, *274*, 272-277.
- Aytar, P., Bozkurt, D., Erol, S., Özdemir, M., & Çabuk, A. (2016). Increased removal of Reactive Blue 72 and 13 acidic textile dyes by *Penicillium ochrochloron* fungus isolated from acidic mine drainage. *Desalination Water Treat.*, 1-11.
- Aytar, P., Gedikli, S., Buruk, Y., Cabuk, A., & Burnak, N. (2014). Lead and nickel biosorption with a fungal biomass isolated from metal mine drainage: Box-Behnken experimental design. *Int. J. Environ. Sci. Technol.*, *11*, 1631-1640.
- Azhar, S. S., Liew, A. G., Suhardy, D., Hafiz, K. F., & Hatim, M. D. I. (2005). Dye removal from aqueous solution by using adsorption on treated sugarcane baggase. *Am. J. App. Sci.*, *2*, 1499.
- Azouaou, N., Sadaoui, Z., Djaafri, A., & Mokaddem, H. (2010). Adsorption of cadmium from aqueous solution onto untreated coffee grounds: Equilibrium, kinetics and thermodynamics. *J. Hazard. Mater.*, *184*, 126–134.
- Bahafid, W., Sayel, H., Joutey, N. T., & Ghachtouli, N. E. (2011). Removal mechanism of hexavalent chromium by a novel strain of *Pichia anomala* isolated from industrial effluents of Fez (Morocco). *J. Environ. Sci. Technol.*, *5*(8).
- Balapure, K. H., Jain, K., Chattaraj, S., Bhatt, N. S., & Madamwar, D. (2014). Co-metabolic degradation of diazo dye—Reactive blue 160 by enriched mixed cultures BDN. *J. Hazard. Mater.*, *279*, 85-95.

- Banerjee, K., Ramesh, S. T., Gandhimathi, R., Nidheesh, P. V., & Bharathi, K. S. (2013). A novel agricultural waste adsorbent, watermelon shell for the removal of copper from aqueous solutions. *Iran. J. Energy Environ.*, 3, 143–156.
- Barakat, M. A., & Schmidt, E. (2010). Polymer-enhanced ultrafiltration process for heavy metals removal from industrial wastewater. *Desalination*, 256, 90-93.
- Batool, R., Qurrat-ul-ain, K., & Naeem, A. (2014). Comparative Study of Cr (VI) Removal by *Exiguobacterium* sp. in Free and Immobilized Forms. *Bioremed. J.*, 18, 317-327.
- Bazrafshan, E., Zarei, A. A., & Mostafapour, F. K. (2015). Biosorption of cadmium from aqueous solutions by *Trichoderma* fungus: kinetic, thermodynamic, and equilibrium study. *Desalination Water Treat.*, 1-11.
- Bhakta, J. N., Munekage, Y., Ohnishi, K., & Jana, B. B. (2012). Isolation and identification of cadmium-and lead-resistant lactic acid bacteria for application as metal removing probiotic. *Int. J. Environ. Sci. Technol.*, 9, 433-440.
- Black, R., Sartaj, M., Mohammadian, A., & Qiblawey, H. A. (2014). Biosorption of Pb and Cu using fixed and suspended bacteria. *J. Environ. Chem. Eng.*, 2, 1663 -1671.
- Brachkova, M. I., Duarte, M. A., & Pinto, J. F. (2010). . (2010). Preservation of viability and antibacterial activity of *Lactobacillus* spp. in calcium alginate beads. *Eur. J. Pharm. Sci.*, 41, 589-596.
- Brouers, F., & Al-Musawi, T. J. (2015). On the optimal use of isotherm models for the characterization of biosorption of lead onto algae. *J. Mol. Liq.*, 212, 46–51.
- Camarillo, R., Llanos, J., García-Fernández, L., Pérez, Á., & Cañizares, P. . (2010). Treatment of copper (II)-loaded aqueous nitrate solutions by polymer enhanced ultrafiltration and electrodeposition. *Sep. Purif. Technol.*, 70, 320-328.
- Celik, L., Ozturk, A., & Abdullah, M. I. (2012). Biodegradation of reactive red 195 azo dye by the bacterium *Rhodopseudomonas palustris* 51ATA. *Afr. J. Microbiol. Res.*, 6, 120-126.
- Chatterjee, S., Chatterjee, S., Chatterjee, B. P., Das, A. R., & Guha, A. K. (2005). Adsorption of a model anionic dye, eosin Y, from aqueous solution by chitosan hydrobeads. *J. Colloid Interf. Sci.*, 288(1), 30-35.
- Chaudhari, A. U., Tapase, S. R., Markad, V. L., & Kodam, K. M. (2013). Simultaneous decolorization of reactive Orange M2R dye and reduction

- of chromate by *Lysinibacillus* sp. KMK-A. *J. Hazard. Mater.*, 262, 580-588.
- Chen, Gang, Huang, Man hong, Chen, Liang, & Chen, Dong hui. (2011). A batch decolorization and kinetic study of Reactive Black 5 by a bacterial strain *Enterobacter* sp. GY-1. *Int. Biodeter. Biodegr.*, 65, 790-796.
- Chen, L., Fang, Y., Jin, Y., Chen, Q., Zhao, Y., Xiao, Y., et al. (2015). Biosorption of Cd^{2+} by untreated dried powder of duckweed *Lemna aequinoctialis*. *Desalination Water Treat.*, 53, 183-194.
- Chen, Q. Y., Luo, Z., Hills, C., Xue, G. , & Tyrer, M. (2009). Precipitation of heavy metals from wastewater using simulated flue gas: sequent additions of fly ash, lime and carbon dioxide. *Water Res.*, 43, 2605-2614.
- Cheung, W. H., Szeto, Y. S., & McKay, G. (2009). Enhancing the adsorption capacities of acid dyes by chitosan nano particles. *Bioresour. Technol.*, 100, 1143-1148.
- Chiou, M. S., Ho, P. Y., & Li, H. Y. (2004). Adsorption of anionic dyes in acid solutions using chemically cross-linked chitosan beads. *Dyes Pigments*, 60(1), 69-84.
- Chiou, M. S., & Li, H. Y. (2003). Adsorption behavior of reactive dye in aqueous solution on chemical cross-linked chitosan beads. *Chemosphere*, 50(8), 1095-1105.
- Ciardelli, G., Corsi, L., & Marcucci, M. (2000). Membrane separation for wastewater reuse in the textile industry. *Resour. Conserv. Recy.*, 31(2), 189-197.
- Cojocar, C., Diaconu, M., Cretescu, I., Savić, J., & Vasić, V. (2009). Biosorption of copper (II) ions from aqua solutions using dried yeast biomass. *Colloid. Surface A*, 335, 181-188.
- Çolak, F., Atar, N., Yazıcıoğlu, D., & Olgun, A. (2011). Biosorption of lead from aqueous solutions by *Bacillus* strains possessing heavy-metal resistance. *Chem. Eng. J.*, 173, 422-428.
- Cook, M. T., Tzortzis, G., Khutoryanskiy, V. V., & Charalampopoulos, D. (2013). Layer-by-layer coating of alginate matrices with chitosan-alginate for the improved survival and targeted delivery of probiotic bacteria after oral administration. *J. Mater. Chem.*, 1, 52-60.
- Copello, G. J., Mebert, A. M., Raineri, M., Pesenti, M. P., & Diaz, L. E. (2011). Removal of dyes from water using chitosan hydrogel/SiO₂ and chitin hydrogel/SiO₂ hybrid materials obtained by the sol-gel method. *J. Hazard. Mater.*, 186(1), 932-939.
- Cotton, F. A., & Wilkinson, G. . (1980). Chromium *Advanced Inorganic*

- Chemistry, a Comprehensive Text* (4th ed., pp. 719-736.). New York: John Wiley.
- Cruz, I., Bashan, Y., Hernández-Carmona, G., & De-Bashan, L. E. (2013). Biological deterioration of alginate beads containing immobilized microalgae and bacteria during tertiary wastewater treatment. *Appl. Microbiol. Biotechnol.*, *97*, 9847-9858.
- Cui, L., Wu, G., & Jeong, T. S. (2010). Adsorption performance of nickel and cadmium ions onto brewer's yeast. *Can. J. Chem. Eng.*, *88*, 109-115.
- Daemi, H., & Barikani, M. . (2012). Synthesis and characterization of calcium alginate nanoparticles, sodium homopolymannuronate salt and its calcium nanoparticles. . *Sci. Iranica.*, *19*, 2023-2028.
- Daneshvar, N., Ayazloo, M., Khatee, A. R., & Pourhassan, M. (2007). Biological decolorization of dye solution containing malachite green by microalgae *Cosmarium* sp. *Bioresour. Technol.*, *98*, 1176–1182.
- Danisa, U., & Aydiner, C. (2009). Investigation of process performance and fouling mechanisms in micellar-enhanced ultrafiltration of nickel-contaminated waters. *J. Hazard. Mater.*, *162*, 577-587.
- Das, D., Charumathi, D., & Das, N. (2011). Bioaccumulation of the synthetic dye Basic Violet 3 and heavy metals in single and binary systems by *Candida tropicalis* grown in a sugarcane bagasse extract medium: Modelling optimal conditions using response surface methodology (RSM) and inhibition kinetics. *J. Hazard. Mater.*, *186*, 1541-1552.
- de Almeida, F. T. R., Ferreira, B. C. S., Moreira, A. L. D. S. L., de Freitas, R. P., Gil, L. F., & Gurgel, L. V. A. (2016). Application of a new bifunctionalized chitosan derivative with zwitterionic characteristics for the adsorption of Cu^{2+} , Co^{2+} , Ni^{2+} , and oxyanions of Cr^{6+} from aqueous solutions: Kinetic and equilibrium aspects. *J. Colloid Interf. Sci.*, *466*, 297–309.
- Deivasigamani, C., & Das, N. (2011). Biodegradation of Basic Violet 3 by *Candida krusei* isolated from textile wastewater. *Biodegradation*, *22*, 1169-1180.
- Dong, Q. Y., Chen, M. Y., Xin, Y., Qin, X. Y., Cheng, Z., Shi, L. E., et al. (2013). Alginate-based and protein-based materials for probiotics encapsulation: a review. *Int. J. Food Sci. Technol.*, *48*, 1339-1351.
- Dotto, G. L., & Pinto, L. A. A. (2012). Analysis of mass transfer kinetics in the biosorption of synthetic dyes onto *Spirulina platensis* nanoparticles. *Biochem. Eng. J.*, *68*, 85-90.
- Dotto, G. L., Vieira, M. L. G., & Pinto, L. A. A. (2012). Kinetics and Mechanism

- of Tartrazine Adsorption onto Chitin and Chitosan. *Ind. Eng. Chem. Res.*, *51*, 6862-6868.
- Doula, M. K. (2009). Simultaneous removal of Cu, Mn and Zn from drinking water with the use of clinoptilolite and its Fe-modified form. *Water Res.*, *43*, 3659-3672.
- Du, L. N., Wang, S., Li, G., Wang, B., Jia, X. M., Zhao, Y. H., et al. (2011). Biodegradation of malachite green by *Pseudomonas* sp. strain DY1 under aerobic condition: characteristics, degradation products, enzyme analysis and phytotoxicity. *Ecotoxicology*, *20*, 438-446.
- Dubey, A., & Shiwani, S. (2012). Adsorption of lead using a new green material obtained from *Portulaca* plant. *Int. J. Environ. Sci. Technol.*, *9*, 15-20.
- Dubinín, M. M., & Radushkevich, L. V. (1947). Equation of the characteristic curve of activated charcoal. *Chem. Zentralbl.*, *1*, 875.
- Ejder-Korucu, M., Gürses, A., Dođar, Ç., Sharma, S. K., & Açıkyıldız, M. (2015). Removal of Organic Dyes from Industrial Effluents: An Overview of Physical and Biotechnological Applications. In S. K. Sharma (Ed.), *Green Chemistry for Dyes Removal from Wastewater: Research Trends and Applications*. Hoboken, NJ, USA.: John Wiley & Sons, Inc.
- El-Reash, Y. A., Otto, M., Kenawy, I. M., & Ouf, A. M. (2011). Adsorption of Cr (VI) and As (V) ions by modified magnetic chitosan chelating resin. *Int. J. Biol. Macromol.*, *49*(4), 513-522.
- El-Sheekh, M. M., Gharieb, M. M., & Abou-El-Souod, G. W. (2009). Biodegradation of dyes by some green algae and cyanobacteria. *Int. Biodeter. Biodegr.*, *63*, 699-704.
- El Hassouni, E., Abdellaoui, D., El Hani, S., & Bengueddour, R. (2014). Biosorption of cadmium (II) and copper (II) from aqueous solution using red alga (*Osmundea pinnatifida*) biomass. *J. Mater. Environ. Sci.*, *5*, 967-974.
- Elangovan, R., Philip, L., & Chandraraj, K. (2010). Hexavalent chromium reduction by free and immobilized cell-free extract of *Arthrobacter rhombi*-RE. *Appl. Biochem. Biotechnol.*, *160*, 81-97.
- Elisangela, F., Andrea, Z., Fabio, D. G., Cristiano, R. M., Regina, D. L., & Artur, C. P. (2009). Biodegradation of textile azo dyes by a facultative *Staphylococcus arlettae* strain VN-11 using a sequential microaerophilic/aerobic process. *Int. Biodeter. Biodegr.*, *63*, 280-288.
- Enayatizamir, N., Tabandeh, F., Rodríguez-Couto, S., Yakhchali, B., Alikhani, H. A., & Mohammadi, L. (2011). Biodegradation pathway and detoxification of the diazo dye Reactive Black 5 by *Phanerochaete chrysosporium*.

- Bioresour. Technol.*, 102, 10359-10362.
- Ennigrou, D. J., Gzara, L., Ben Romdhane, M. R., & Dhahbi, M. (2009). Cadmium removal from aqueous solutions by polyelectrolyte enhanced ultrafiltration. *Desalination*, 246, 363-369.
- Erden, E., Kaymaz, Y., & Pazarlioglu, N. K. (2011). Biosorption kinetics of a direct azo dye Sirius Blue K-CFN by *Trametes versicolor*. *Electron. J. Biotechnol.*, 14, 3-3.
- Ergene, A., Ada, K., Tan, S., & Katırcıoğlu, H. (2009). Removal of Remazol Brilliant Blue R dye from aqueous solutions by adsorption onto immobilized *Scenedesmus quadricauda*: Equilibrium and kinetic modeling studies. *Desalination*, 249, 1308–1314.
- Ertugay, N., & Bayhan, Y. K. (2010). The removal of copper (II) ion by using mushroom biomass (*Agaricus bisporus*) and kinetic modelling. *Desalination*, 255, 137–142.
- Farag, S., & Zaki, S. (2010). Identification of bacterial strains from tannery effluent and reduction of hexavalent chromium. *J. Environ. Biol.*, 31, 877-882.
- Feldmann, H. (2012). Yeast Cell Architecture and Functions *Yeast: Molecular and Cell Biology* (2nd ed.). Weinheim, Germany: Wiley-VCH Verlag GmbH & Co. KGaA.
- Ferella, F., Prisciandaro, M., Michelis, I. D., & Veglio, F. (2007). Removal of heavy metals by surfactant-enhanced ultrafiltration from wastewaters. *Desalination*, 207, 125-133.
- Filho, N. C., Venancio, E. C., Barriquello, M. F., Hechenleitner, A. A., & Pineda, E. A. G. (2007). Methylene blue adsorption onto modified lignin from sugarcane bagasse. *Eclét Quím*, 32, 63.
- Flores-Garnica, J. G., Morales-Barrera, L., Pineda-Camacho, G., & Cristiani-Urbina, E. (2013). Biosorption of Ni (II) from aqueous solutions by Litchi chinensis seeds. *Bioresour. Technol.*, 136, 635–643.
- Flouty, R., & Estephane, G. (2012). Bioaccumulation and biosorption of copper and lead by a unicellular algae *Chlamydomonas reinhardtii* in single and binary metal systems: a comparative study. *J. Environ. Manage.*, 111, 106-114.
- Fomina, M., & Gadd, G. M. (2014). Biosorption: current perspectives on concept, definition and application. *Bioresour. Technol.*, 160, 3-14.
- Fontana, K. B., Chaves, E. S., Sanchez, J. D. S., Watanabe, E. R. L. R., Pietrobelli, J. M. T. A., & Lenzi, G. G. (2016). Textile dye removal from aqueous solutions by malt bagasse: Isotherm, kinetic and thermodynamic

- studies. *Ecotox. Environ. Safe.*, 124, 329–336.
- Forgacs, E., Cserhádi, T., & Oros, G. . (2004). Removal of synthetic dyes from wastewaters: a review. *Environ. Int.*, 30(7), 953-971.
- Freundlich, H. (1907). Ueber die adsorption in Loesungen. *Z. Phy. Chem.*, 57, 385-470.
- Fu, F., Chen, R., & Xiong, Y. (2006). Application of a novel strategy—Coordination polymerization precipitation to the treatment of Cu²⁺-containing wastewaters. *Sep. Purif. Technol.*, 52, 388-393.
- Fu, F., Zeng, H., Cai, Q., Qiu, R., Yu, J., & Xiong, Y. (2007). Effective removal of coordinated copper from wastewater using a new dithiocarbamate-type supramolecular heavy metal precipitant. *Chemosphere*, 69, 1783-1789.
- Fu, Fenglian, & Wang, Qi. (2011). Removal of heavy metal ions from wastewaters: A review. *J. Environ. Manage.*, 92(3), 407-418.
- Gönen, F., & Serin, D. S. (2012). Adsorption study on orange peel: removal of Ni (II) ions from aqueous solution. *Afr. J. Biotechnol.*, 11, 1250-1258.
- Galedar, M., & Younesi, H. (2013). Biosorption of ternary cadmium, nickel and cobalt ions from aqueous solution onto *Saccharomyces cerevisiae* cells: batch and column studies. *Am. J. Biochem. Biotechnol.*, 9, 47-60.
- Geetha, P., Latha, M. S., & Koshy, M. (2016). Biosorption of malachite green dye from aqueous solution by calcium alginate nanoparticles: Equilibrium study. *J. Mol. Liq.*, 212, 723–730.
- Ghaedi, M., Brazesh, B., Karimi, F., & Ghezlbash, G. R. (2014). Equilibrium, thermodynamic, and kinetic studies on some metal ions biosorption using black yeast *Aureobasidium pullulans* biomass. *Environ. Prog. Sustain. Energy*, 33, 769-776.
- Ghasemi, F., Tabandeh, F., Bambai, B., & Sambasiva Rao, K. R. S. (2010). Decolorization of different azo dyes by *Phanerochaete chrysosporium* RP78 under optimal condition. *Int. J. Environ. Sci. Technol.*, 7, 457-464.
- Ghodake, G., Jadhav, U., Tamboli, D., Kagalkar, A., & Govindwar, S. (2011a). Decolorization of Textile Dyes and Degradation of Mono-Azo Dye Amaranth by *Acinetobacter calcoaceticus* NCIM 2890. *Ind. J. Microbiol.*, 51, 501-508.
- Ghodake, G., Jadhav, U., Tamboli, D., Kagalkar, A., & Govindwar, S. (2011b). Decolorization of textile dyes and degradation of mono-azo dye amaranth by *Acinetobacter calcoaceticus* NCIM 2890. *Ind. J. Microbiol.*, 51(4).
- Ghosh, S., Mondal, A., & Paul, A. K. (2015a). Hexavalent chromium biosorption by dried biomass of *Aspergillus niger* NUA101 isolated from Indian ultramafic complex. *Afr. J. Microbiol. Res.*, 9(4), 220-229.

- Ghosh, S., Mondal, A., & Paul, A. K. . (2015b). Hexavalent chromium biosorption by dried biomass of *Aspergillus niger* NUA101 isolated from Indian ultramafic complex. *Afr. J. Microbiol. Res.*, 9(4), 220-229.
- Gimenez, G. G., Ruiz, S. P., Caetano, W., Peralta, R. M., & Matioli, G. (2014). Biosorption potential of synthetic dyes by heat-inactivated and live *Lentinus edodes* CCB-42 immobilized in loofa sponges. *World J. Microb. Biot.*, 30, 3229-3244.
- Gode, F., & Pehlivan, E. (2006). Removal of chromium (III) from aqueous solutions using Lewatit S 100: the effect of pH, time, metal concentration and temperature. *J. Hazard. Mater.*, 136, 330-337.
- Gomes, L. H., Alexandrino, N., Roncato Duarte, K. M., & Andrino, F. G. (2011). Cadmium biosorption by immobilized dead yeast cells from bioethanol industries. *Int. J. Environ. Res.*, 5, 833-836.
- Gong, R., Zhu, S., Zhanga, D., Chen, J., Ni, S., & Guan, R. (2008a). Adsorption behavior of cationic dyes on citric acid esterifying wheat straw: kinetic and thermodynamic profile. *Desalination*, 230, 220.
- Greenwood, N. N., & Earnshaw, A. (1984) *Chemistry of the Elements* (pp. 1187-1200). Oxford: Pergamon Press.
- Gupta, V. K., & Suhas. (2009). Application of low-cost adsorbents for dye removal – A review. *J. Environ. Manage.*, 90, 2313–2342.
- H., Wang, W., Zheng X., Q., Su J., Y., Tian, J., Xiong X., & L., Zheng T. (2009). Biological decolorization of the reactive dyes Reactive Black 5 by a novel isolated bacterial strain *Enterobacter* sp. EC3. *J. Hazard. Mater.*, 171, 654-659.
- Hadiyanto, Pradana, A. B., Buchori, L., & Budiyati, C. S. (2014). Biosorption of heavy metal Cu^{2+} and Cr^{3+} in textile wastewater by using immobilized algae. *Res. J. Appl. Sci. Eng. Technol.*, 7, 3539-3543.
- Hai, F. I., Yamamoto, K., & Fukushi, K. (2006). Development of a submerged membrane fungi reactor for textile wastewater treatment. *Desalination*, 192(1-3), 315-322.
- Hai, F. I., Yamamoto, K., Nakajima, F., & Fukushi, K. (2012). Application of a GAC-coated hollow fiber module to couple enzymatic degradation of dye on membrane to whole cell biodegradation within a membrane bioreactor. *J. Membrane Sci.*, 289, 67–75.
- Han, R., Ding, D., Xu, Y., Zou, W., Wang, W., Li, Y, et al. (2008). Use of rice husk for the adsorption of congo red from aqueous solution in column mode. *Bioresour. Technol.*, 99, 2938.
- Haq, I., Kumar, S., Kumari, V., Singh, S. K., & Raj, A. (2016). Evaluation of

- bioremediation potentiality of ligninolytic *Serratia liquefaciens* for detoxification of pulp and paper mill effluent. *J. Hazard. Mater.*, 305, 190-199.
- Haydar, S., Ahmad, M. F., & Hussain, G. (2015). Evaluation of new biosorbents prepared from immobilized biomass of *Candida* sp. for the removal of nickel ions. *Desalination Water Treat.*, 1-13.
- Ho, Y. S. (2006). Review of second-order models for adsorption systems. *J. Hazard. Mater.*, 136, 681-689.
- Ho, Y. S., & McKay, G. (1998). Sorption of dye from aqueous solution by peat. *Chem. Eng. J.*, 70(2), 115-124.
- Ho, Y. S., & McKay, G. . (1998). A Comparison of Chemisorption Kinetic Models Applied to Pollutant Removal on Various Sorbents. . *Process. Saf. Environ.*, 76, 332-340.
- Hofrichter, M. (2002). Review: lignin conversion by manganese peroxidase (MnP). *Enzyme Microb. Technol.*, 30, 454-466.
- Hołda, A. (2013). Hexavalent Chromium Accumulation by Microscopic Fungi. *Arch. Environ. Prot.*, 39(2), 45-56.
- Hossini, H., Esmaeili Taheri, H., Arab Markadeh, A., Rezaee, A., & Rastegar, S. O. (2015). Optimization of effective parameters in the biosorption of Cr (VI) using acid treated date palm fiber from aqueous solution. *Desalination Water Treat.*, 1-10.
- Hsieh, F. M., Huang, C., Lin, T. F., Chen, Y. M., & Lin, J. C. (2008). Study of sodium tripolyphosphate-crosslinked chitosan beads entrapped with *Pseudomonas putida* for phenol degradation. *Proc. Biochem.*, 43, 83-92.
- Hu, X., Zhao, M., Song, G., & Huang, H. (2011). Modification of pineapple peel fibre with succinic anhydride for Cu²⁺, Cd²⁺ and Pb²⁺ removal from aqueous solutions. *Environ. Techol.*, 32, 739-746.
- Huang, J., Liu, D., Lu, J., Wang, H., Wei, X., & Liu, J. (2016). Biosorption of reactive black 5 by modified *Aspergillus versicolor* biomass: Kinetics, capacity and mechanism studies. *Colloid. Surface A*, 492, 242–248.
- Hui, W., Jian, Q. S., Xiao, W. S., Yun, T., Xiao, J. X., & Tian, L. Z. (2010). Bacterial decolorization and degradation of the reactive dye Reactive Red 180 by *Citrobacter* sp. CK3. *Int. Biodeter. Biodegr.*, 63, 395–399.
- Hunger, Klaus, Berneth, H., Gregory, P., Miederer, P., Heid, C., & Mennicke, W. (2003). Important Chemical Chromophores of Dye Classes. In Klaus Hunger (Ed.), *Industrial Dyes: Chemistry, Properties, Applications*. Weinheim: WILEY-VCH Verlag GmbH & Co. KGaA.
- Huq, T., Khan, A., Khan, R. A., Riedl, B., & Lacroix, M. (2013). Encapsulation

- of probiotic bacteria in biopolymeric system. *Cr. Rev. Food Sci.*, 53, 909-916.
- Husain, Q., & Ulber, R. (2011). Immobilized peroxidase as a valuable tool in the remediation of aromatic pollutants and xenobiotic compounds: a review. *Crit. Rev. Env. Sci. Tec.*, 41(8).
- I., Langmuir. (1918). The adsorption of gases on plane surfaces of glass, mica, and platinum. *J. Am. chem. Soc.*, 40, 1361-1403.
- Infante, J., De Arco, R., & Angulo, M. (2014). Removal of lead, mercury and nickel using the yeast *Saccharomyces cerevisiae*. *Rev. MVZ Córdoba*, 19, 4141-4149.
- Iriel, A., Lagorio, M. G., & Cirelli, A. F. (2015). Biosorption of arsenic from groundwater using *Vallisneria gigantea* plants. Kinetics, equilibrium and photophysical considerations. 138, 383–389.
- Iskandar, N. L., Zainudin, N. A. I. M., & Tan, S. G. (2011). Tolerance and biosorption of copper (Cu) and lead (Pb) by filamentous fungi isolated from a freshwater ecosystem. *J. Environ. Sci.*, 23, 824-830.
- Järup, Lars. (2003). Hazards of heavy metal contamination. *Brit. Med. Bull.*, 68(1), 167. doi:10.1093/bmb/ldg032
- Jadhav, J. P., Phugare, S. S., Dhanve, R. S., & Jadhav, S. B. (2010). Rapid biodegradation and decolorization of Direct Orange 39 (Orange TGLL) by an isolated bacterium *Pseudomonas aeruginosa* strain BCH. *Biodegradation*, 21, 453-463.
- Jadhav, S. B., Phugare, S. S., Patil, P. S., & Jadhav, J. P. (2011). Biochemical degradation pathway of textile dye Remazol red and subsequent toxicological evaluation by cytotoxicity, genotoxicity and oxidative stress studies. *Int. Biodeter. Biodegr.*, 65(6).
- Jadhav, S.U., Kalme, S.D., & Govindwar, S.P. (2008). Biodegradation of methyl red by *Galactomyces geotrichum* MTCC 1360. *Int. Biodeter. Biodegr.*, 62, 135-142.
- Jafari, N., Soudi, M. R., & Kasra-Kermanshahi, R. (2014). Biodecolorization of textile azo dyes by isolated yeast from activated sludge: *Issatchenkia orientalis* JKS6. *Ann. Microbiol.*, 64, 475-482.
- Jain, A. K., Gupta, V. K., Bhatnagar, A., & Suhas. (2003). Utilization of industrial waste products as adsorbents for the removal of dyes. *J. Hazard. Mater., B101*, 31.
- Jain, K., Shah, V., Chapla, D., & Madamwar, D. (2012). Decolorization and degradation of azo dye – Reactive Violet 5R by an acclimatized indigenous bacterial mixed cultures-SB4 isolated from anthropogenic dye

- contaminated soil. *J. Hazard. Mater.*, 213-214, 378-386.
- Jiang, x., Sun, Y., Liu, L., Wang, S., & Tian, X. (2014). Adsorption of C.I. Reactive Blue 19 from aqueous solutions by porous particles of the grafted chitosan. *Chem. Eng. J.*, 235, 151-157.
- Jimenez-Cedillo, M. J., Olguin, M. T., Fall, C., & Colin-Cruz, A. (2013). As(III) and As(V) sorption on iron-modified non-pyrolyzed and pyrolyzed biomass from *Petroselinum crispum* (parsley). *J. Environ. Manage.*, 117, 242-252.
- Jin, X., & Ning, Y. (2013). Laccase production optimization by response surface methodology with *Aspergillus fumigatus* AF1 in unique inexpensive medium and decolorization of different dyes with the crude enzyme or fungal pellets. *J. Hazard. Mater.*, 262, 870-877.
- Joshi, M., & Purwar, r. (2008). Developments in new processes for colour removal from effluent. *Rev. Prog. Color.*, 34, 58-71.
- Kadirvelu, K., Kavipriya, M., Karthika, C., Radhika, M., Vennilamani, N., & Pattabhi, S. (2003). Utilization of various agricultural wastes for activated carbon preparation and application for the removal of dyes and metal ions from aqueous solutions. *Bioresour. Technol.*, 87, 129.
- Kalme, S. D., Parshetti, G. K. , Jadhav, S. U., & Govindwar, S. P. (2007). Biodegradation of benzidine based dye Direct Blue-6 by *Pseudomonas desmolyticum* NCIM 2112. *Bioresour. Technol.*, 98(7), 1405-1410.
- Kalyani, D. C., Telke, A. A., Dhanve, R. S., & Jadhav, J. P. (2009). Ecofriendly biodegradation and detoxification of Reactive Red 2 textile dye by newly isolated *Pseudomonas* sp. SUK1. *J. Hazard. Mater.*, 163, 735-742.
- Kang, S. Y., Lee, J. U., Moon, S. H., & Kim, K. W. (2004). Competitive adsorption characteristics of Co^{2+} , Ni^{2+} , and Cr^{3+} by IRN-77 cation exchange resin in synthesized wastewater. *Chemosphere*, 56, 141-147.
- Karthikeyan, K., Nanthakumar, K., Shanthi, K., & Lakshmanaperumalsamy, P. (2010). Response surface methodology for optimization of culture conditions for dye decolorization by a fungus, *Aspergillus niger* HM11 isolated from dye affected soil. *Iran. J. MicroBiol.*, 2, 213-222.
- Kelewou, H., Merzouki, M., & Lhassani, A. (2014). Biosorption of textile dyes Basic Yellow 2 (BY2) and Basic Green 4 (BG4) by the live yeast *Saccharomyces Cerevisiae*. *J. Mater. Environ. Sci.*, 5, 633-640.
- Kelly-Vargas, K., Cerro-Lopez, M., Reyna-Tellez, S., Bandala, E. R., & Sanchez-Salas, J. L. (2012). Biosorption of heavy metals in polluted water, using different waste fruit cortex. *Phys. Chem. Earth*, 37-39, 26–29.

- Khan, R., Bhawana, P., & Fulekar, M. H. (2013). Microbial decolorization and degradation of synthetic dyes: a review. *Rev. Environ. Sci. Biotechnol.*, *12*, 75-97.
- Khan, S. S., Arunarani, A., & Chandran, P. (2015). Biodegradation of Basic Violet 3 and Acid Blue 93 by *Pseudomonas putida*. *CLEAN - Soil, Air, Water*, *43*, 67-72.
- Khataee, A. R., & Dehghan, G. (2011). Optimization of biological treatment of a dye solution by macroalgae *Cladophora* sp. using response surface methodology. *J. Taiwan. Inst. Chem. E.*, *42*, 26-33.
- Khattri, S., & Singh, M. K. (2000). Colour removal from synthetic dye wastewater using a bioadsorbent. *Water Air Soil Poll.*, *120*, 283.
- Khelifi, E., Touhami, Y., Thabet, O. B. D., Ayed, L., Bouallagui, H., Fardeau, M. L., et al. (2012). Exploring bioaugmentation strategies for the decolourization of textile wastewater using a two species consortium (*Bacillus cereus* and *Bacillus pumilus*) and characterization of produced metabolites. *Desalination Water Treat.*, *45*, 48-54.
- Khosravihaftkhany, S., Morad, N., Abdullah, A. Z., Teng, T. T., & Ismail, N. (2015). Biosorption of Pb (II) and Fe (III) from aqueous co-solutions using chemically pretreated oil palm fronds. *RSC Adv.*, *5*, 106498-106508.
- Kiran, S., Ali, S., Asgher, M., & Anwar, F. (2012). Comparative study on decolorization of reactive dye 222 by white rot fungi *Pleurotus ostreatus* IBL-02 and *Phanerochaete chrysosporium* IBL-03. *Afr. J. Microbiol. Res.*, *6*, 3639-3650.
- Kongsricharoern, N., & Polprasert, C. (1995). Electrochemical precipitation of chromium (Cr⁶⁺) from an electroplating wastewater. *Wat. Sci. Technol.*, *31*, 109-117.
- Kónig-Péter, A., Kocsis, B., Kilár, F., & Pernyeszi, T. (2014). Bioadsorption characteristics of *Pseudomonas aeruginosa* PAOI. *J. Serbian Chem. Soc.*, *79*, 495-508.
- Korus, I., & Loska, K. (2009). Removal of Cr(III) and Cr(VI) ions from aqueous solutions by means of polyelectrolyte-enhanced ultrafiltration. *Desalination*, *247*, 390-395.
- Kousi, P., Remoudaki, E., Hatzikioseyan, A., & Tsezos, M. (2007). *A study of the operating parameters of a sulphate-reducing fixed-bed reactor for the treatment of metal-bearing wastewater*. Paper presented at the 17th International Biohydrometallurgy Symposium, Germany, Frankfurt am Main.

- Krasaekoopt, W., Bhandari, B., & Deeth, H. (2003). Evaluation of encapsulation techniques of probiotics for yoghurt. *Int. Dairy J.*, 13(1), 3-13.
- Ku, Y., & Jung, I. L. (2001). Photocatalytic reduction of Cr(VI) in aqueous solutions by UV irradiation with the presence of titanium dioxide. *Water Res.*, 35, 135-142.
- Kumar, C. G., Mongolla, P., Joseph, J., & Sarma, V. U. M. (2012). Decolorization and biodegradation of triphenylmethane dye, brilliant green, by *Aspergillus* sp. isolated from Ladakh, India. *Proc. Biochem.*, 47, 1388-1394.
- Kumar, P. S., Ramalingam, S., Sathiyaselvabala, V., Kirupha, S. D., Murugesan, A., & Sivanesan, S. . (2012). Removal of cadmium(II) from aqueous solution by agricultural waste cashew nut shell. *Environ. Eng.*, 29, 756-768.
- Kumar, S. S., Kumar, M. S., Siddavattam, D., & Karegoudar, T. B. (2012). Generation of continuous packed bed reactor with PVA-alginate blend immobilized *Ochrobactrum* sp. DGVK1 cells for effective removal of *N,N*-dimethylformamide from industrial effluents. *J. Hazard. Mater.*, 199, 58-63.
- Kurade, M. B., Waghmode, T. R., & Govindwar, S. P. (2011). Preferential biodegradation of structurally dissimilar dyes from a mixture by *Brevibacillus laterosporus*. *J. Mater. Chem.*, 192(3).
- Kurniawan, A., Kosasih, A. N., Febrianto, J., Ju, Y. H., Sunarso, J., Indraswati, N., et al. (2011). Evaluation of cassava peel waste as lowcost biosorbent for Ni-sorption: equilibrium, kinetics, thermodynamics and mechanism. *Chem. Eng. J.*, 172, 158–166.
- Kyzas, G. Z., & Lazaridis, N. K. (2009). Reactive and basic dyes removal by sorption onto chitosan derivatives. *J. Colloid Interf. Sci.*, 331(1), 32-39.
- Lagergren, S. (1898). About the theory of so-called adsorption of soluble substances. *Kungliga Svenska Vetenskapsakademiens Handlingar*, 24, 1-39.
- Lakshmi, U. R., Srivastva, V. C., Mall, I. D., Lataye, & H., D. (2009). Rice husk ash as an effective adsorbent: Evaluation of adsorptive characteristics for indigo Carmine dye. *J. Environ. Manage.*, 90, 710.
- Lamia, A., Chaieb, K., Ceheref, A., & Bakhrouf, A. (2010). Biodegradation and decolorization of triphenylmethane dyes by *Staphylococcus epidermidis*. *Desalination*, 260, 137-146.
- Landaburu-Aguirre, J., Pongrácz, E., Perämäki, P., & Keiski, R. L. (2010). Micellar-enhanced ultrafiltration for the removal of cadmium and zinc:

- Use of response surface methodology to improve understanding of process performance and optimisation. *J. Hazard. Mater.*, 180, 524-534.
- Lang, W., Buakaew, P., Buranaporipan, W., Wongchawalit, J., Sakairi, N., Vanichsriratana, W., et al. (2013). Biosorption of Local Textile Dyes Onto Acid-Tolerant Macro-Beads of Chitosan-Immobilized *Rhizopus arrhizus* Biomass. *Kasetsart J. (Nat. Sci.)*, 47, 101 - 114.
- Largergren, S. (1898). Zur theorie der sogenannten adsorption geloster stoffe. *K. Sven. Vetenskapsakad. Handl.*, 24, 1-39.
- Li, X., Li, Y., Zhang, S., & Ye, Z. (2012). Preparation and characterization of new foam adsorbents of poly (vinyl alcohol)/chitosan composites and their removal for dye and heavy metal from aqueous solution. *Chem. Eng. J.*, 183, 88-97.
- Li, X. Y., Chen, X. G., Sun, Z. W., Park, H. J., & Cha, D. S. (2011). Preparation of alginate/chitosan/carboxymethyl chitosan complex microcapsules and application in *Lactobacillus casei* ATCC 393. *Carbohydr. Polym.*, 83, 1479-1485.
- Lim, S. L., chu, W. L., & Phang, S. M. (2010). Use of *Chlorella vulgaris* for bioremediation of textile wastewater. *Bioresour. Technol.*, 101, 7314-7322.
- Liu, X., Zhang, J., Jiang, J., Li, R., Xie, Z., & Li, S. (2011). Biochemical degradation pathway of Reactive blue 13 by *Candida rugopelliculosa* HXL-2. *Int. Biodeter. Biodegr.*, 65, 135-141.
- Liu, Y. G., Liao, T., He, Z. B., Li, T. T., Wang, H., Hu, X. J., et al. (2013). Biosorption of copper (II) from aqueous solution by *Bacillus subtilis* cells immobilized into chitosan beads. *Trans. Nonferrous Met. Soc. China*, 23, 1804-1814.
- Liu, Y., & Liu, Y. J. (2008). Biosorption isotherms, kinetics and thermodynamics. *Sep. Purif. Technol.*, 61, 229-242.
- Lucas, M.S., Amaral, C., Sampaio, A., Peres, J.A., & Dias, A.A. (2006). Biodegradation of the diazo dye Reactive Black 5 by a wild isolate of *Candida oleophila*. *Enzyme Microb. Technol.*, 39, 51-55.
- Luk, C. H. J., Yip, J., Yuen, C. W. M., Kan, C. W. , & Lam, K. H. (2015). Study of Freeze-dried Chitosan Beads Encapsulating Live Lactic Acid Bacteria for Removal of Reactive Dyes Individuals. . *J. Fiber Bioengine. Infor.*, 8(1), 13-23.
- Luk, C. H. J., Yip, J., Yuen, C. W. M., Kan, C. W., & Lam, K. H. (2014). A comprehensive study on adsorption behaviour of direct, reactive and acid dyes on crosslinked and non-crosslinked chitosan beads. . *J. Fiber*

- Bioengine. Inform.*, 7(1), 35-52.
- Maddela, N. R., Reyes, J. J. M., Viafara, D., & Gooty, J. M. (2015). Biosorption of Copper (II) by the Microorganisms Isolated from the Crude-Oil-Contaminated Soil. *Soil Sediment. contam.*, 24, 898 -908.
- Mahiya, Suresh, Lofrano, Giusy, & Sharma, S. K. (2014). Heavy metals in water, their adverse health effects and Biosorptive removal: A review. *Int. J. Chem.*, 3(1), 132-149.
- Mahmoud, M. E. (2015a). Water treatment of hexavalent chromium by gelatin-impregnated-yeast (Gel-Yst) biosorbent. *J. Environ. Manage.*, 147, 264-270.
- Mahmoud, M. E. (2015b). Water treatment of hexavalent chromium by gelatin-impregnated-yeast (Gel-Yst) biosorbent. *Journal of environmental management. J. Environ. Manage.*, 147, 264-270.
- Majeau, J. A., Brar, S. K., & Tyagi, R. D. . (2010). Laccases for removal of recalcitrant and emerging pollutants. *Bioresour. Technol.*, 101(7).
- Manasi, Rajesh, V., Kumar, A. S. K., & Rajesh, N. (2014). Biosorption of cadmium using a novel bacterium isolated from an electronic industry effluent. *Chem. Eng. J.*, 235, 176–185.
- Mane, V. S., Mall, I. D., & Srivastava, V. C. (2007). Kinetic and equilibrium isotherm studies for the adsorptive removal of brilliant green dye from aqueous solution by rice husk ash. *J. Environ. Manage.*, 84, 390.
- Marandi, R. (2011Marandi). Biosorption of hexavalent chromium from aqueous solution by dead fungal biomass of *Phanerochaete cryosporium*: batch and fixed bed studies. *Can, J. Chem. Eng. Technol.*, 2, 8-22.
- Marin-Rangel, V. M., Cortes-Martinez, R., Villanueva, R. A. C., Garnica-Romo, M. G., & Martinez-Flores, H. E. (2012). As (V) biosorption in an aqueous solution using chemically treated lemon (*Citrus aurantifolia* Swingle) residues. *J. Food Sci.*, 77, T10-T14.
- Markou, G., Mitrogiannis, D., Çelekli, A., Bozkurt, H., Georgakakis, D., & Chrysikopoulos, C. V. (2015). Biosorption of Cu^{2+} and Ni^{2+} by *Arthrospira platensis* with different biochemical compositions. *Chem. Eng. J.*, 259, 806–813.
- Martorell, M.M., Pajot, H.F., & de Figueroa, L.I.C. (2012). Dye decolourizing yeasts isolated from Las Yungas rainforest. Dye assimilation and removal used as selection criteria. *Int. Biodeter. Biodegr.*, 66, 25-32.
- Mazengarb, S., & Roberts, G. A. (2009). Studies on the diffusion of direct dyes in chitosan film. . *Prog. Chem. App Chitin Derivat. Media, Lodz*, 14, 25-32.

- Mirbagheri, S. A., & Hosseini, S. N. (2005). Pilot plant investigation on petrochemical wastewater treatment for the removal of copper and chromium with the objective of reuse. *Desalination*, *171*, 85-93.
- Mirmohseni, A., Seyed Dorraji, M. S., Figoli, A., & Tasselli, F. (2012). Chitosan hollow fibers as effective biosorbent toward dye: Preparation and modeling. *Bioresour. Technol.*, *121*, 212-220.
- Mishra, A., & Malik, A. (2012). Simultaneous bioaccumulation of multiple metals from electroplating effluent using *Aspergillus lentulus*. *Water Res.*, *46*(16).
- Modi, H. A., Rajput, G., & Ambasana, C. (2010). Decolorization of water soluble azo dyes by bacterial cultures, isolated from dye house effluent. *Bioresour. Technol.*, *101*, 6580-6583.
- Mogharabi, M., Nassiri-Koopaei, N., Bozorgi-Koushalshahi, M., Nafissi-Varcheh, N., Bagherzadeh, G., & Faramarzi, M. A. (2012). Immobilization of laccase in alginate-gelatin mixed gel and decolorization of synthetic dyes. *Bioinorg. Chem. Appl.*
- Mohan, S. V., Ramanaiah, S. V., & Sarma, P. N. (2008). Biosorption of direct azo dye from aqueous phase onto *Spirogyra* sp. *I02*: Evaluation of kinetics and mechanistic aspects. *Biochem. Eng. J.*, *38*, 61-69.
- Mohsenzadeh, F., & Shahrokhi, F. (2013). Biological Removing and Isothermal Absorption Studies of Copper by Fungal Biomass of *Trichoderma*. *Int. J. Environ. Pollut. Solution.*, *1*, 98.
- Motsi, T., Rowson, N. A., & Simmons, M. J. H. (2009). Adsorption of heavy metals from acid mine drainage by natural zeolite. *Int. J. Miner. Process*, *92*, 42-48.
- Murugavelh, S., & Mohanty, K. (2012). Bioreduction of hexavalent chromium by live and active *Phanerochaete chrysosporium*: Kinetics and modeling. *CLEAN - Soil, Air, Water*, *40*, 746-751.
- Muxel, A. A., Gimenez, S. M. N., de Souza Almeida, F. A., da Silva Alfaya, R. V., & da Silva Alfaya, A. A. (2011). Cotton fiber/ZrO₂, a new material for adsorption of Cr(VI) ions in water. *CLEAN - Soil, Air, Water*, *39*, 289-295.
- Nagy, B., Tonk, S., Indolean, C., Maicaneanu, A., & Majdik, C. (2013). Biosorption of Cadmium Ions by Unmodified, Microwave and Ultrasound Modified Brewery and Pure Strain Yeast Biomass. *Am. J. Anal. Chem.*, *4*, 63-71.
- Nasreen, Z., Bajwa, R., & Kusar, T. (2007). Decolorization of textile dyes and their effluents using white red fungi. *Afr. J. Biotechnol.*, *6*, 424.
- Naydenova, V., Badova, M., Vassilev, S., Iliev, V., Kaneva, M., & Kostov, G.

- (2014). Encapsulation of brewing yeast in alginate/chitosan matrix: lab-scale optimization of lager beer fermentation. *Biotechnol. Biotec. Eq.*, 28, 277-284.
- Netzahuatl-Muñoz, A. R., de María Guillén-Jiménez, F., Chávez-Gómez, B., Villegas-Garrido, T. L., & Cristiani-Urbina, E. (2012). Kinetic Study of the Effect of pH on Hexavalent and Trivalent Chromium Removal from Aqueous Solution by *Cupressus lusitanica* Bark. *Water Air Soil Poll.*, 223, 625-641.
- Noreen, R., Asgher, M., Bhatti, H. N., Batool, S., & Asad, M. J. (2011). *Phanerochaete chrysosporium* IBL-03 secretes high titers of manganese peroxidase during decolorization of Drimarine Blue K2RL textile dye. *Environ. Techol.*, 32, 1239-1246.
- Noroozi, B., Sorial, G. A., Bahrami, H., & Arami, M. (2008). Adsorption of binary mixtures of cationic dyes. *Dyes Pigments*, 76, 784.
- Ofomaja, A. E., Naidoo, E. B., & Modise, S. J. (2010). Biosorption of copper(II) and lead(II) onto potassium hydroxide treated pine cone powder. *J. Environ. Manage.*, 91, 1674-1685.
- Okur, M., Saracoglu, N., & Aksu, Z. (2014). Use of response surface methodology for the bioaccumulation of Violet 90 metal-complex dye by *Candida tropicalis*. *Turkish J. Eng. Env. Sci.*, 38, 217-230.
- Ola, I. O., Akintokun, A. K., Akpan, I., Omomowo, I. O., & Areo, V. O. (2010a). Aerobic decolourization of two reactive azo dyes under varying carbon and nitrogen source by *Bacillus cereus*. *Afr. J. Biotechnol.*, 9, 672-677.
- Ola, I. O., Akintokun, A. K., Akpan, I., Omomowo, I. O., & Areo, V. O. (2010b). Aerobic decolourization of two reactive azo dyes under varying carbon and nitrogen source by *Bacillus cereus*. *Afr. J. Biotechnol.*, 9(5), 672-677.
- Omar, H. H. (2008). Algal decolorization and degradation of monoazo and diazo dyes. *Pak. J. Biol. Sci.*, 11, 1310-1316.
- Ostroski, I. C., Barros, M. A. S. D., Silvab, E. A., Dantas, J. H., Arroyo, P. A., & Lima, O. C. M. (2009). A comparative study for the ion exchange of Fe(III) and Zn(II) on zeolite NaY. *J. Hazard. Mater.*, 161, 1404-1412.
- Özverdi, A., & Erdem, M. (2006). Cu²⁺, Cd²⁺ and Pb²⁺ adsorption from aqueous solutions by pyrite and synthetic iron sulphide. *J. Hazard. Mater.*, 137, 626-632.
- Pérez-Marín, A. B., Zapata, V. M., Ortuno, J. F., Aguilar, M., Sáez, J., & Lloréns, M. (2007). Removal of cadmium from aqueous solutions by adsorption onto orange waste. *J. Hazard. Mater.*, 139, 122-131.
- Pajot, H. F., Farina, J. I., & Castellanos de Figueroa, L. I. (2011). Evidence on

- manganese peroxidase and tyrosinase expression during decolorization of textile industry dyes by *Trichosporon akiyoshidainum*. *Int. Biodeter. Biodegr.*, *65*, 1199-1207.
- Pajot, H. F., Figueroa, L. I. C. , Spencer, J. F. T., & Fariña, J. I. (2008). Phenotypical and genetic characterization of *Trichosporon* sp. HP 2023 a yeast isolate from Las Yungas rainforest (Tucumán, Argentina) with azo dye decolorizing ability. *Antonie. Van. Leeuwenhoek*, *94*, 233-244.
- pan, H., Cerniglia, J., Cerniglia, C. E., & Chen, H. (2011). Effects of Orange II and Sudan III azo dyes and their metabolites on *Staphylococcus aureus*. *J. Ind. Microbiol. Biotechnol.*, *38*, 1729-1738.
- Pang, Y., Zeng, G. M., Tang, L., Zhang, Y., Liu, Y. Y., Lei, X. X., et al. (2011). Cr (VI) reduction by *Pseudomonas aeruginosa* immobilized in a polyvinyl alcohol/sodium alginate matrix containing multi-walled carbon nanotubes. *Bioresour. Technol.*, *102*, 10733–10736.
- Park, D., Yun, Y. S., & Park, J. M. (2010). The past, present, and future trends of biosorption. *Biotechnol. Bioproc. Eng.*, *15*, 86-102.
- Peniche, C., Argüelles-Monal, W., Peniche, H., & Acosta, N. . (2003). Chitosan: an attractive biocompatible polymer for microencapsulation. . *Macromol. Biosci.*, *3*(10), 511-520.
- Pereira, L., & Alves, M. (2012). Dyes-Environmental Impact and Remediation. In A. Mailk & E. Grohmann (Eds.), *Environmental Protection Strategies for Sustainable Development* (1 ed., pp. 111-162): Springer Netherlands.
- Pereira, M. F. R., Soares, S. F., Órfão, J. J. M., & Figueiredo, J. L. (2003). Adsorption of dyes on activated carbons: influence of surface chemical groups. *Carbon*, *41*(4), 811-821.
- Petrinić, I., Andersen, N. P. R., Šostar-Turk, S., & Le Marechal, A. M. (2007). The removal of reactive dye printing compounds using nanofiltration. *Dyes Pigments*, *74*, 512-518.
- Picot, A., & Lacroix, C. (2004). Encapsulation of bifidobacteria in whey protein-based microcapsules and survival in simulated gastrointestinal conditions and in yoghurt. *Int. Dairy J.*, *14*(6), 505-515.
- Prado, A. G., Macedo, J. L., Dias, S. C., & Dias, J. A. (2004). Calorimetric studies of the association of chitin and chitosan with sodium dodecyl sulfate. *Colloid. Surface B*, *35*(1), 23-27.
- Prithviraj, D., Deboleena, K., Neelu, N., Noor, N., Aminur, R., Balasaheb, K., et al. (2014). Biosorption of nickel by *Lysinibacillus* sp. BA2 native to bauxite mine. *Ecotox. Environ. Safe.*, *107*, 260–268.
- Priya, B., Uma, L., Ahamed, A. K., Subramanian, G., & Prabakaran, D. (2011).

- Ability to use the diazo dye, CI Acid Black 1 as a nitrogen source by the marine cyanobacterium *Oscillatoria curviceps* BDU92191. *Bioresour. Technol.*, 102, 7218-7223.
- Rajee, O., & Patterson, J. (2011). Decolorization of Azo Dye (Orange MR) by an Autochthonous Bacterium, *Micrococcus* sp. DBS 2. *Ind. J. Microbiol.*, 51, 159-163.
- Reddy, D. H. K., Ramana, D. K. V., Seshaiyah, K., & Reddy, A. V. R. (2011). Biosorption of Ni(II) from aqueous phase by *Moringa oleifera* bark, a low cost biosorbent. *Desalination*, 268, 150–157.
- Redlich, O., & Peterson, D. L. (1959). A useful adsorption isotherm. *J. Phy. Chem.*, 63, 1024-1024.
- Rehman, A., & Anjum, M. S. (2010). Cadmium uptake by yeast, *Candida tropicalis*, isolated from industrial effluents and its potential use in wastewater clean-up operations. *Water Air Soil Poll.*, 205, 149-159.
- Robinson, T., Chandran, B., & Nigam, P. (2002a). Removal of dyes from a synthetic textile dye effluent by biosorption on apple pomace and wheat straw. *Water Res.*, 36, 2824.
- Robinson, T., Chandran, B., & Nigam, P. (2002b). Removal of dyes from a synthetic textile dye effluent by biosorption on apple pomace and wheat straw. *Water Res.*, 36(11).
- Royer, B, Cardoso, N. F., Lima, E. C., Vagheti, J. C. P., Simon, N. M., Calvete, T., et al. (2009). Applications of Brazilian pine-fruit shell in natural and carbonized forms as adsorbents to removal of methylene blue from aqueous solutions—Kinetic and equilibrium study. *J. Hazard. Mater.*, 164, 1213.
- Ruthven, D. M. (1984). *Principles of Adsorption and Adsorption Processes* (1 ed.): Wiley & Sons Ltd.
- Saeed, A., Iqbal, M., & Zafar, S. I. (2009). Immobilization of *Trichoderma viride* for enhanced methylene blue biosorption: batch and column studies. *J. Hazard. Mater.*, 168, 406-415.
- Saleem, M., Pirzada, T., & Qadeer, R. (2007). Sorption of acid violet 17 and direct red 80 dyes on cotton fiber from aqueous solutions. . *Colloid. Surface A*, 292(2), 246-250.
- Salvadori, M. R., Ando, R. A., do Nascimento, C. A. O., & Corrêa, B. (2014). Intracellular biosynthesis and removal of copper nanoparticles by dead biomass of yeast isolated from the wastewater of a mine in the Brazilian Amazonia. *PloS One*, 9.
- Samuel, J., Pulimi, M., Paul, M. L., Maurya, A., Chandrasekaran, N., &

- Mukherjee, A. (2013). Batch and continuous flow studies of adsorptive removal of Cr (VI) by adapted bacterial consortia immobilized in alginate beads. *Bioresour. Technol.*, 128, 423-430.
- San Keskin, N. O., Celebioglu, A., Sarioglu, O. F., Ozkan, A. D., Uyar, T., & Tekinay, T. (2015a). Removal of a reactive dye and hexavalent chromium by a reusable bacteria attached electrospun nanofibrous web. *RSC Adv.*, 5, 86867-86874.
- San Keskin, N. O., Celebioglu, A., Sarioglu, O. F., Ozkan, A. D., Uyar, T., & Tekinay, T. (2015b). Removal of a reactive dye and hexavalent chromium by a reusable bacteria attached electrospun nanofibrous web. *RSC Adv.*, 5(106), 86867-86874.
- Sanlier, S. H., Ak, G., Yilmaz, H., Ozbakir, G., & Cagliyan, O. (2013). Removal of textile dye, direct red 23, with glutaraldehyde cross-linked magnetic chitosan beads. *Prep. Biochem. Biotech.*, 43, 163-176.
- Saranraj, P., Sumathi, V., Reetha, D., & Stella, D. . (2010). Decolourization and Degradation of Direct Azo Dyes and Biodegradation of Textile Dye Effluent by using Bacteria Isolated from Textile Dye Effluent. *KJ. Ecobiotechnol.*, 2(7).
- Sarkar, D., & Paul, G. (2015). Bioremediation of nickel ions from aqueous system by dry cells of *Pseudomonas aeruginosa* DSGPM4 species. *Int. J. Pharm. Life Sci.*, 6.
- Schär-Zammaretti, P., & Ubbink, J. (2003). The cell wall of lactic acid bacteria: surface constituents and macromolecular conformations. *Biophys. J.*, 85(6), 4076-4092.
- Sen, K., Pakshirajan, K., & Santra, S. B. (2012). Modelling the Biomass Growth and Enzyme Secretion by the White Rot Fungus *Phanerochaete chrysosporium* in Presence of a Toxic Pollutant *J. Environ. Prot.*, 3, 114-119.
- Sen, T. K., Mohammad, M., Maitra, S., & Dutta, B. K. (2010). Removal of cadmium from aqueous solution using castor seed hull: a kinetic and equilibrium study. *CLEAN - Soil, Air, Water*, 38, 850-858.
- Senthilkumar, S., Perumalsamy, M., & Prabhu, H. J. (2014). Decolourization potential of white-rot fungus *Phanerochaete chrysosporium* on synthetic dye bath effluent containing Amido black 10B. *J. Saudi Chem. Soc.*, 18, 845-853.
- Shafique, U., Ijaz, A., Salman, M., Zaman, W., Jamil, N., Rehman, R., et al. (2012). Removal of arsenic from water using pine leaves. *J. Taiwan. Inst. Chem. E.*, 43, 256–263.

- Shah, M. P., Patel, K. A., Nair, S. S., & Darji, A. M. (2013a). Bioremoval of azo dye Reactive Red by *Bacillus* spp. ETL-1982. *J. Bioremed. Biodeg.*, 4.
- Shah, M. P., Patel, K. A., Nair, S. S., & Darji, A. M. (2013b). Microbial Decolorization of Methyl Orange Dye by *Pseudomonas* spp. ETL-M. *Int. J. Environ. Bioremed. biodeg.*, 1, 54-59.
- Shah, M. P., Patel, K. A., Nair, S. S., & Darji, A. M. (2014). Microbial degradation and decolorization of reactive dyes by *Bacillus* Spp. ETL-1979. *Am. J. Microbiol. Res.*, 2, 16-23.
- Shahverdi, F., Ahmadi, M., & Avazmoghadam, S. (2015). Isotherm models for the nickel (II) biosorption using dead fungal biomass of *Aspergillus awamori*: comparison of various error functions. *Desalination Water Treat.*, 1-11.
- Shaker, M. A. (2015). Thermodynamics and kinetics of bivalent cadmium biosorption onto nanoparticles of chitosan-based biopolymers. *J. Taiwan. Inst. Chem. E.*, 47, 79–90.
- Shankar, A. M., Henciya, S., & Malliga, P. (2013). Bioremediation of tannery effluent using fresh water cyanobacterium *Oscillatoria annae* with coir pith. *Int. J. Environ. Sci.*, 3, 1881-1890.
- Shankar, P., Gomathi, T., Vijayalakshmi, K., & Sudha, P. N. (2014). Comparative studies on the removal of heavy metals ions onto cross linked chitosan-g-acrylonitrile copolymer. *Int. J. Biol. Macromol.*, 67, 180-188.
- Sharma, S., & Adholeya, A. (2012). Hexavalent chromium reduction in tannery effluent by bacterial species isolated from tannery effluent contaminated soil. *J. Environ. Sci. Technol.*, 5(3), 142.
- Sharma, S. K., Mahiya, S., & Lofrano, G. (2015). Removal of divalent nickel from aqueous solutions using *Carissa carandas* and *Syzygium aromaticum*: isothermal studies and kinetic modelling. *Appl. Water Sci.*, 1-14.
- Shin, W. S., & Kim, Y. K. (2014). Biosorption characteristics of heavy metals (Ni^{2+} , Zn^{2+} , Cd^{2+} , Pb^{2+}) from aqueous solution by *Hizikia fusiformis*. *Environ. Earth Sci.*, 71, 4107-4114.
- Shinde, N. R., Bankar, A. V., Kumar, A. R., & Zinjarde, S. S. (2012). Removal of Ni (II) ions from aqueous solutions by biosorption onto two strains of *Yarrowia lipolytica*. *J. Environ. Manage.*, 102, 115–124.
- Shokri Khoubestani, R., Mirghaffari, N., & Farhadian, O. (2015). Removal of three and hexavalent chromium from aqueous solutions using a microalgae biomass-derived biosorbent. *Environ. Prog. Sustain. Energy*, 34, 949-956.

- Silva-Stenico, M. E., Vieira, F. D. P., Genuário, D. B., Silva, E. S. P., Moraes, A. B., & Fiore, M. F. (2012). Decolorization of textile dyes by cyanobacteria. *J. Braz. Chem. Soc.*, *23*, 1863-1870.
- Singh, K., & Arora, S. (2011). Removal of Synthetic Textile Dyes From Wastewaters: A Critical Review on Present Treatment Technologies. *Crit. Rev. Env. Sci. Tec.*, *41*(9), 807-878.
- Sips, R. (1948). On the structure of a catalyst surface. *J. chem. Phys.*, *16*, 490-495.
- Soares, E. V., & Soares, H. M. (2012). Bioremediation of industrial effluents containing heavy metals using brewing cells of *Saccharomyces cerevisiae* as a green technology: a review. *Environ. Sci. Pollut. Res.*, *19*, 1066-1083.
- Solís, M., Solís, A., Pérez, H. I., Manjarrez, N., & Flores, M. (2012). Microbial decolouration of azo dyes: a review. *Proc. Biochem.*, *47*(12).
- Somasundaram, V., Philip, L., & Bhallamudi, S. M. (2009). Experimental and mathematical modeling studies on Cr (VI) reduction by CRB, SRB and IRB, individually and in combination. *J. Hazard. Mater.*, *172*, 606-617.
- Stolz, A. (2001). Basic and applied aspects in the microbial degradation of azo dyes. *Appl. Microbiol. Biotechnol.*, *56*, 69-80.
- Subbaiah, M. V., & Yun, Y. S. (2013). Biosorption of Nickel (II) from aqueous solution by the fungal mat of *Trametes versicolor* (rainbow) biomass: equilibrium, kinetics, and thermodynamic studies. *Biotechno. Bioproc. E.*, *18*, 280-288.
- Tálos, K., Pernyeszi, T., Majdik, C., Hegedúsova, A., & Páger, C. (2012). Cadmium biosorption by baker's yeast in aqueous suspension. *J. Serb. Chem. Soc.*, *77*, 549-561.
- Taffarel, S. R., & Rubio, J. (2009). On the removal of Mn^{2+} ions by adsorption onto natural and activated Chilean zeolites. *Miner. Eng.*, *22*, 336-343.
- Tamboli, D. P., Kagalkar, A. N., Jadhav, M. U., Jadhav, J. P., & Govindwar, S. P. (2010). Production of polyhydroxyhexadecanoic acid by using waste biomass of *Sphingobacterium sp.* ATM generated after degradation of textile dye Direct Red 5B. *Bioresour. Technol.*, *101*(7).
- Tan, L., Ning, S., Zhang, X., & Shi, S. (2013). Aerobic decolorization and degradation of azo dyes by growing cells of a newly isolated yeast *Candida tropicalis* TL-F1. *Bioresour. Technol.*, *138*, 307-313.
- Tan, W. S., & Ting, A. S. Y. (2012). Efficacy and reusability of alginate-immobilized live and heat-inactivated *Trichoderma asperellum* cells for Cu (II) removal from aqueous solution. *Bioresour. Technol.*, *123*, 290-295.

- Telke, A. A., Kadam, A. A., Jagtap, S. S., Jadhav, J. P., & Govindwar, S. P. (2010). Biochemical characterization and potential for textile dye degradation of blue laccase from *Aspergillus ochraceus* NCIM-1146. *Biotechno. Bioproc. E.*, 15, 696-703.
- Temkin, D. (1934). Die gas adsorption under nernstsche wärmesatz. *Acta. Physicochim. URSS*, 1, 36-52.
- Tham, C. S. C., Peh, K. K. , & Liong, M. T. (2015). Survivability of encapsulated lactobacilli in high acid foods. *Acta. Aliment.*, 44, 374-382.
- Tharannum, S., Krishnamurthy, V., & Mahmood, R. (2012). Characterization of chromium remediating bacterium *Bacillus subtilis* isolated from electroplating effluent. *Inter. J. Engin. Res. Appl.*, 2, 961-966.
- Ting, A. S. Y., Rahman, N. H. A., Isa, M. I. H. M., & Tan, W. S. (2013). Investigating metal removal potential by Effective Microorganisms (EM) in alginate-immobilized and free-cell forms. *Bioresour. Technol.*, 147, 636-639.
- Tsekova, K., Todorova, D., Dencheva, V., & Ganeva, S. (2010). Biosorption of copper (II) and cadmium (II) from aqueous solutions by free and immobilized biomass of *Aspergillus niger*. *Bioresour. Technol.*, 101, 1727-1731.
- Tuttolomondo, M. V., Alvarez, G. S., Desimone, M. F., & Diaz, L. E. (2014). Removal of azo dyes from water by sol-gel immobilized *Pseudomonas* sp. *J. Environ. Chem. Eng.*, 2, 1321-1136.
- Vemmer, M., & Patel, A. V. (2013). Review of encapsulation methods suitable for microbial biological control agents. *Biol. Control*, 67, 380-389.
- Vijayaraghavan, K., Han, M. H., Choi, S. B., & Yun, Y. S. (2007). Biosorption of Reactive black 5 by *Corynebacterium glutamicum* biomass immobilized in alginate and polysulfone matrices. *Chemosphere*, 68, 1838-1845.
- Vishnu, G., & Joseph, K. (2007). Nanofiltration and ozonation for decolorisation and salt recovery from reactive dyebath. *Color. Technol.*, 123, 260-266.
- Vitor, V., & Corso, C.R. (2008). Decolorization of textile dye by *Candida albicans* isolated from industrial effluents. *J. Ind. Microbiol. Biotechnol.*, 35, 1357.
- Vodnar, D. C., Socaciu, C., Rotar, A. M., & Stanila, A. (2010). Morphology, FTIR fingerprint and survivability of encapsulated lactic bacteria (*Streptococcus thermophilus* and *Lactobacillus delbrueckii* subsp. *bulgaricus*) in simulated gastric juice and intestinal juice. *Int. J. Food Sci. Technol.*, 45(11), 2345-2351.
- Waghmode, T.R., Kurade, M.B., & Govindwar, S.P. (2011). Time dependent

- degradation of mixture of structurally different azo and non azo dyes by using *Galactomyces geotrichum* MTCC 1360. *Int. Biodeter. Biodegr.*, *65*, 479-486.
- Wang, H., Su, J. Q., Zheng, X. W., Tian, Y., Xiong, X. J., & Zheng, T. L. (2009). Bacterial decolorization and degradation of the reactive dye Reactive Red 180 by *Citrobacter* sp. CK3. *Int. Biodeter. Biodegr.*, *63*, 395-399.
- Wang, J., Liu, G. F., Lu, H., Jin, R. F., Zhou, J. T., & Lei, T. M. (2012). Biodegradation of Acid Orange 7 and its auto-oxidative decolorization product in membrane-aerated biofilm reactor. *Int. Biodeter. Biodegr.*, *67*, 73-77.
- Weber, W. J., & Morris, J. C. (1963). Kinetics of adsorption on carbon from solution. *J. Sanit. Eng. Div. Am. Soc. Civ. Eng.*, *89*, 31-59.
- Wong, Y. C., Szeto, Y. S., Cheung, W. H., & McKay, G. (2004). Adsorption of acid dyes on chitosan—equilibrium isotherm analyses. *Process Biochemistry*, *39*, 695-704.
- Wu, F. C., Tseng, R. L., & Juang, R. S. (2000). Comparative adsorption of metal and dye on flake-and bead-types of chitosans prepared from fishery wastes. *J. Hazard. Mater.*, *73*, 63-75.
- Wu, J., Eiteman, M., & Law, S. (1998). Evaluation of Membrane Filtration and Ozonation Processes for Treatment of Reactive-Dye Wastewater. *J. Environ. Eng.*, *124*(3), 272-277.
- Wu, J., Kim, K. S., Sung, N. C., Kim, c. H., & Lee, Y. C. (2009). Isolation and characterization of *Shewanella oneidensis* WL-7 capable of decolorizing azo dye Reactive Black 5. *J. Gen. Appl. Microbiol.*, *55*, 51-55.
- Xiao, X., Luo, S., Zeng, G., Wei, W., Wan, Y., Chen, L., et al. (2010). Biosorption of cadmium by endophytic fungus (EF) *Microsphaeropsis* sp. LSE10 isolated from cadmium hyperaccumulator *Solanum nigrum* L. *Bioresour. Technol.*, *101*, 1668–1674.
- Xie, Y., Li, H., Wang, X., Ng, I. S., Lu, Y., & Jing, K. (2014). Kinetic simulating of Cr (VI) removal by the waste *Chlorella vulgaris* biomass. *J. Taiwan. Inst. Chem. E.*, *45*, 1773–1782.
- Xu, J., Song, X. C., Zhang, Q., Pan, H., Liang, Y., Fan, X. W., et al. (2011). Characterization of metal removal of immobilized *Bacillus* strain CR-7 biomass from aqueous solutions. *J. Hazard. Mater.*, *187*, 450-458.
- Yang, Q., Yang, M., Pritsch, K., Yediler, A., Hagn, A., Schloter, M., et al. (2003). Decolorization of synthetic dyes and production of manganese dependent peroxidase by new fungal isolates. *Biotechnol. Lett.*, *25*, 709-713.
- Yang, X. Q., Zhao, X. X., Liu, C. Y., Zheng, Y., & Qian, S. J. (2009).

- Decolorization of azo, triphenylmethane and anthraquinone dyes by a newly isolated *Trametes* sp. SQ01 and its laccase. *Proc. Biochem.*, *44*, 1185-1189.
- Ying, X., & Fang, Z. (2006). Experimental research on heavy metal wastewater treatment with dipropyl dithiophosphate. *J. Hazard. Mater.*, *137*, 1636-1642.
- Yu, Ming-Ho. (2005). Soil and Water Pollution – Environmental Metals and Metalloids *Environmental Toxicology: Biological and Health Effects of Pollutants* (2nd ed.). Boca Raton, London, New York, Washington, D.C., USA: CRC Press LLC.
- Yu, Z., & Wen, X. (2005a). Screening and identification of yeasts for decolorizing synthetic dyes in industrial wastewater. *Int. Biodeter. Biodegr.*, *56*, 109-114.
- Zahoor, A., & Rehman, A. (2009). . (2009). Isolation of Cr (VI) reducing bacteria from industrial effluents and their potential use in bioremediation of chromium containing wastewater. *J. Environ. Sci.*, *21*(6), 814-820.
- Zeldowitsch, J. (1934). Über den mechanismus der katalytischen oxydation von CO an MnO₂. *Acta. Physicochim. URSS*, *1*, 364-449.
- Zeng, X., Tang, J., Yin, H., Liu, X., Jiang, P., & Liu, H. (2010). Isolation, identification and cadmium adsorption of a high cadmium-resistant *Paecilomyces lilacinus*. *Afr. J. Biotechnol.*, *9*, 6525-6533.
- Zhang, B., Fan, R., Bai, Z., Wang, S., Wang, L., & Shi, J. (2013). Biosorption characteristics of *Bacillus gibsonii* S-2 waste biomass for removal of lead (II) from aqueous solution. *Environ. Sci. Pollut. Res.*, *20*, 1367–1373.
- Zhao, F., Yu, B., Yue, Z., Wang, T., Wen, X., Liu, Z., et al. (2007). Preparation of porous chitosan gel beads for copper (II) ion adsorption. *J. Hazard. Mater.*, *147*(1), 67-73.
- Zheng, X., & Liu, J. (2006). Dyeing and printing wastewater treatment using membrane bioreactor with gravity drain. *Desalination*, *190*(1-3), 277-286.
- Zhou, L., Liu, Z., Liu, J., & Huang, Q. (2010). Adsorption of Hg (II) from aqueous solution by ethylenediamine-modified magnetic crosslinking chitosan microspheres. *Desalination*, *258*(1), 41-47.